Using Accelerometers to Quantify Infant General Movements as a Tool for Assessing Motility to Assist in Making a Diagnosis of Cerebral Palsy

Mark S. Conover

Thesis submitted to the Faculty of the
Virginia Polytechnic Institute and State University
in partial fulfillment of the requirements of the degree of

Master of Science
in
Mechanical Engineering

Dr. Alfred L. Wicks, Chair
Dr. Harry H. Robertshaw
Dr. Dawn H. Peck

September 19, 2003
Blacksburg, Virginia

Keywords: general movement, cerebral palsy, motility, signal processing, accelerometer

Using Accelerometers to Quantify Infant General Movements as a Tool for Assessing Motility to Assist in Making a Diagnosis of Cerebral Palsy

Mark S. Conover

Abstract

Quantitative approaches to directly measure infant movement have not utilized miniature electronics technology, nor been used effectively in evaluating neurological dysfunctions' affect on movement. This thesis presents a new quantitative technique for measuring infant general movements (GMs) using micro-electromechanical accelerometers, while discussing future improvements for this technology and possible benefits to present methods of diagnosing cerebral palsy.

For decades, GMs have interested neurologists because characteristics can indicate neurological dysfunctions. Motions over the entire body that show fluency, variation, and complexity characterize normal GMs. Analyzing these movements can accurately predict neurological dysfunction – cerebral palsy, in particular.

This research describes a technique to make consistent, quantitative measurements of GMs using accelerometers on infant limbs. Signal processing techniques can find patterns, later determined characteristic of neurological dysfunctions. Such analyses complement the current technique of video footage review. Additionally, data could be reanalyzed using updated signal processing algorithms. An accurate collection of data allows physicians to quickly review an infant's entire history of motion studies.

Physical information can be inferred from the data. Correlation techniques have compared motions from different limbs to examine coordination. Evidence suggests this may help indicate dysfunction. High-speed data acquisition enables the study of high-frequency motions, possibly undetectable with the human eye.

This research has successfully recorded acceleration and video during GMs from four limbs on multiple infants. Signal processing techniques have been applied to create various graphical representations. The direct measurement of movement makes this work unique, enabling a graphical analysis tool for physicians based on physical performance.

Acknowledgements

Support from many individuals has made this work possible; it is to them that I will be forever indebted. Without funding for this project, I have relied on the advise, assistance, and time of people who receive little to no benefit for helping me and my research.

First off, Dr. Harry Robertshaw's support of my Master's studies through employment as a Graduate Teaching Assistant for the undergraduate Mechanical Engineering Labs has been instrumental in sustaining my livelihood through the stipend and tuition it provided. Without this help, I would not have been able to physically survive during my time in graduate school. Fortunately, it was as a Teaching Assistant that I learned so much about working with laboratory equipment, teaching and instructing fellow engineers, and reading, writing, and presenting technical research. Much of my gains as an engineer have come through my experiences working with and for Dr. Robertshaw, and for that opportunity and experience I am very grateful.

Dr. Dawn Peck has been instrumental in aiding my understanding of the medical side of my research. Her detailed descriptions and insights on current cerebral palsy diagnosis techniques was imperative in the linking of the medical and engineering disciplines required for this research. My enthusiasm was always fueled by her eagerness to help and support me during the past year. I hope that in the near future this work will continue with her help and she will get the recognition deserved for her knowledge and expertise.

The continual help from the Infant Perception Lab in the Psychology Department at Virginia Tech enabled me to conduct trials on human subjects. Without the enthusiasm, advice, and assistance from both Dr. Robin Cooper and Megan McIlvreavy, my research would not have progressed as far as it has. Their help in providing test space and subjects, along with assisting me in getting IRB approval for testing on human subjects, was extremely valuable and appreciated, despite the lack of benefit for themselves.

My lab colleagues, Dave Szakelyhidi and Eric Slominski have made working in the Experimental Modal Analysis lab much more enjoyable, but have also been active in helping me get oriented to my current project, as well as future iterations of the research involving miniaturized printed circuit board, wireless data transmission, and efficient battery-power

supplies. Their help and friendship have been invaluable.

The administrative departments of the Mechanical Engineering Department have always been available to help me during my time here and their help is often unappreciated. Cathy Hill and Eloise McCoy in the administrative office were always helpful when I had problems with schedules and paperwork. Ben Poe, Jamie Archual, and Randy Smith were always pleasant and helpful with my computer and electronics questions and needs. Also, Peggy Caldwell and Mike Harness were very patient and supportive during my grant submission process.

Finally, I sincerely appreciate the guidance and support provided to me by my advisor, Dr. Al Wicks. After posing the initial concept for the work, he did a fantastic job allowing me to explore and research on my own, with little oversight. Without this freedom to choose the paths for this research, I do not feel my educational benefit would be as great. His expertise in signal processing and electronics provided me with valuable help when needed, but he never dictated the paths my research should take. While I wish we could have secured some form of funding for future work before I finished my work, I feel that he helped present me with opportunities to learn about the process of writing proposals for grants, an overlooked aspect of research for most graduate students. Dr. Wicks also empowered me to present my information and research to interested parties in search of funding ideas and support.

Table of Contents

List of Figures

List of Tables

List of Videos

1 Introduction

The purpose of this chapter is to introduce the reader to general movements (GMs) in infants and detail how these GMs are used to qualitatively assess the motility of infants when diagnosing cerebral palsy and other neurological dysfunctions. From here, the motivation for quantifying infant motion during GMs will be discussed and the advantage of utilizing new microelectronic technology for this purpose will be shown. Finally, the long-term work required for extension of this research is introduced.

1.1 Motivation of Research

Cerebral palsy (CP) is a disorder in the motor control areas of the brain and currently affects over 500,000 persons in the United States. Based on information from genetics, brain imaging, neurodevelopmental assessment, and motion analysis, physicians make qualitative evaluations on the likelihood that a child has some form of CP. Currently, neurodevelopmental assessment is the "standard-of-care" in diagnosing CP. Further diagnosis of CP is traditionally done in a clinical setting, where one aspect includes the recording of an infant's motions, which are later reviewed by trained physicians. However, this motion analysis is not yet the "standard-of-care" method, rather it is an additional tool for the overall process.

An early detection is paramount in enacting early treatment and therapy that can help the child to maximize their developmental potential. The United Cerebral Palsy Research Foundation (UCP), has described the need for this type research in their September 2002 publication, *Diagnosis of Cerebral Palsy – A Research Status Report* by stating a need for [UCP, 2002]:

1. an increased ability to quantitatively evaluate the resulting neuro-muscular impairment(s) and functional disabilities [in infants];
2. the development and evaluation of improved methods to measure the functional performance of the infant, child and adult with a motor dysfunction.

While current clinical evaluations are very accurate, it has been noted that more detailed studies of an infant's movements would be helpful in the diagnosis process. Although an infant may be at high risk for CP based on genetics or brain imagining, the extent to the impairment cannot be fully understood without studying the motor function of the infant. Qualitative measurements that are currently taken from infant motion do not take full advantage of the current state of miniature and wireless electronics technology, or low-cost, high-speed data acquisition systems.

This research is motivated by the desire to incorporate new technologies like miniature electronics, wireless data transmission, transportable data acquisition, and high-speed data analysis into the diagnosis of cerebral palsy in infants. While improved motion analysis will not fully replace the current clinical diagnosis procedures, it opens another window into the understanding of how infant movement changes during maturation and how the motion of individuals with various motor dysfunctions differs. A final motivation is the addition of data and graphs based on physical measurement to the diagnostic process. While measurements made using Gestalt perception techniques are valuable, they make inter-institutional studies difficult and hard to compare [Einspieler, et al, 1997].

1.2 Objectives of Research

The primary objective of this research was to develop a method to directly record quantitative data from infant movement, while not disturbing the spontaneity of an infant's general movements and limiting the infant's motility. The data needed to be reproducible between devices and testing locations, while the measurement devices were to be limited in size, weight, and cost. A significant assumption of this work is that any such device would not alter the types of movements an infant produces during GMs.

With this improvement in measurement, studies could be conducted at different institutions and their data could be more easily compared because it was not recorded qualitatively using Gestalt principles. Additionally, it enables physicians to understand even more about the relationship between neurological impairment of the brain and its affects of on the physical movement. Work with direct measurement of physical motion has not been studied in much depth due to limitations on the size of measurement devices and the speed

of data acquisition and analysis.

Taking recorded data, an effective method for analyzing the numbers to point out characteristics about the human movement needed to be shown. Pediatricians have expressed an interest in seeing graphical representations of data from human movement, which has not previously been produced from clinical tests. This is clear in a quote from a paper by Dr. Susan Harris entitled "Movement Analysis – An Aid to Early Diagnosis of Cerebral Palsy" [Harris, 1991]:

> Fortunately, data based studies conducted during the past two decades have begun to identify important clinical signs that can be used in the early identification of CP. Unfortunately, there has been little attempt to summarize or consolidate these findings in order to identify commonalities across these studies.

Cleary she is noting the need for a uniform method of measuring movement to produce analyzable data. Essentially, the graphs presented in this work and their analysis could represent another valuable tool in the medicine bag for pediatricians and neurological physicians to use during the diagnosis of cerebral palsy. As mentioned by Dr. Harris, this could be crucial in helping identify commonalities among larger patient populations.

1.3 Future Work Required for Extension of Research

The primary objective of proving the feasibility of using a wired device to record data from infant motion has been accomplished. The long-term goal of this research is to implement this technology into the diagnostic process. This implementation requires additional research in both the electronics and signal processing.

To further improve the electronics, the wired devices must be miniaturized and placed onto printed circuit board (PCB). Additionally, some form of wireless data transmission must be implemented to reduce the constraining nature of the wired devices. A much more comprehensive study on a larger field of test subjects is also required. While this work did use multiple healthy infants, the subject pool was limited in age and lacked any motor impairment. Future studies will need to be done using both healthy infants as well as

infants at a high risk for developing cerebral palsy, as determined by present clinical diagnosis. Such a comprehensive study will require coordination of efforts with pediatricians and physicians in a neonatal intensive care unit (NICU) that often works with high-risk infants.

Upon collecting additional data that is paired with simultaneous video recordings and clinical evaluations, various signal processing techniques must be evaluated to determine measurement levels that indicate the presence of normalcy in the motor function of infants. This work will require multiple iterations of various techniques along with consultation from the medical community to help determine what characteristics in the motion data can be accentuated in graphical form. It is hoped that an efficient graphical or visual method for viewing test data and analysis can be developed that is easier for physicians to decipher during the diagnosis of CP, when compared to the tedious task of video footage review.

An additional goal of future work should be to maximize the ease of data collection and review. By constructing the measurement devices and data acquisition system in a robust fashion, while minimizing testing variables, this technique could be used as a screening by nurses during regular infant check-ups. When the variability is taken out of the testing procedure and data becomes comparable between institutions, nurses would be able to conduct the same test as an experienced physician, thus enabling a broader screening and understanding of CP.

2 Background Information and Literature Review

This chapter introduces the reader to cerebral palsy (CP) and its affects on the motor function of those impaired with the disease. General movements (GMs) are introduced and the research pertaining to their value in the diagnosis of CP is discussed. Most importantly, previous methods of both qualitatively and quantitatively assessing GMs will be detailed, along with professional criticism of these methods.

2.1 Introduction to Cerebral Palsy

Cerebral palsy (CP) is a disorder affecting the motor control area of the human brain and it is not progressive. CP can arise from defects in an infant's brain due to some form of shock or to poor development prior to birth. Additionally, one can acquire CP at a later time due to some traumatic experience to the motor control area of the brain, but the vast majority of cases are seen in underdeveloped infants. In the United States alone, nearly 10,000 new cases of CP are reported every year and this number has increased 25% in the past decade, primarily due to improved techniques for caring for prematurely born infants [UCP, 2002].

The term cerebral palsy comes from the two terms, cerebral, meaning brain, and palsy, which describes a disorder affecting the control of bodily movement. It is important to note that motor problems associated with cerebral palsy are due to the brain and not to the muscle tissue. Rather the control center for muscles is disrupted, as opposed to the muscles operating improperly.

2.1.1 Symptoms of Cerebral Palsy

Symptoms of CP vary between individuals and can even change over time within an individual. Fine motor skills are often difficult for an individual with cerebral palsy to perform, such as cutting things scissors, writing, walking, and maintaining balance. Some

individuals are affected with involuntary movements such as writhing or fidgety motions across some or all of the body. CP is not however always a debilitating disorder. In cases of only mild CP, a child may only appear slightly awkward in conducting activities requiring fine motor skills. In cases with more severe CP, an individual may require extensive care throughout their life, while never being able to walk [NINDS].

2.1.2 Classifications of Cerebral Palsy

There exist a number of categories in which doctors classify CP. These forms are classified based on the type of disturbance in the movement of the individual and include: spastic, athetoid, ataxic, and mixed forms.

Over 70 percent of CP patients are inflicted with spastic CP, where the muscles are permanently contracted, making the individual very stiff and awkward. Spastic CP is further categorized base on the limbs affected by the disorder. An individual will often have one half of the body affected with spastic CP due to damage in one region of the motor control area of the brain. These halves can be vertical (right or left side of the body) or horizontal (arms or legs). Occasionally, two types can overlap causing three limbs to be affected by the disorder.

Slow, writhing movements across the body of the individual characterize athetoid CP. These motions can appear in the hands, feet, arms, legs, and even in smaller muscle groups. Some cases of athetoid CP even prevent the individual from speaking due to lack of control of face and tongue muscles; this is known as dysarthria. Overall, athetoid CP affects between 10 and 20 percent of individuals with CP.

Ataxic CP is a rare form affecting the muscles groups requiring coordination for activities such as walking. Due to the decreased sense of balance and depth perception, individuals typically walk with a wide gait and cannot react quickly with precision movements. Some affected individuals also experience tremors that are triggered by voluntary acts such as reaching, which increases as finer and finer motor skills are required. This form of CP affects around 5 to 10 percent of patients.

A final classification involves multiple types of CP can appear in one individual.

This is referred to as mixed forms. The most common combination involves spastic and athetoid CP [NINDS].

The research presented in this paper believes that coordination between hemispheres of the body will be detectable with this new technology. Specifically, paired writhing motions that seem uncontrollable may be distinguishable, while conscious coordinated efforts between limbs will also be detectable. Patterns between two specific limbs may be detectable and point to specific types of spastic CP. Writhing motions are characteristic of both spastic and athetoid CP and may also be easily detected, although they develop over time, as the infant ages. Finally, tremors, which also develop over time, due to ataxic CP may be recognizable by the frequency at which they occur. This is something easily seen using signal processing, but often unnoticed by the human eye. By understanding the various manifestations and characteristics of CP in the motion of an individual, the process of analysis and processing of data becomes easier.

2.1.3 Diagnosis and Treatment of Cerebral Palsy

By viewing and testing an infant's motor skills, a doctor can diagnose CP. Typically, other factors such as genetics, imbalanced hand use, and other possible disorders play into the final diagnosis. In older children, testing is much easier because they are more capable of interacting and reacting to their environment. The difficult task is testing and understanding the movements of younger infants, typically less than 52-week postmenstrual age.

Currently, CP has no known cure, but through research, various institutions are attempting to develop methods of prevention as well as early-intervention and treatment to lessen the severity of the disorder on the daily activities of the individual. It is the detection of CP characteristics that can help with early-intervention and treatment. Technologies such as the one presented in this thesis are one method to detect characteristics to flag an individual as possibly needing further study or treatment.

2.2 Abnormal General Movements as an Indicator of Neurological Dysfunction

Dr. Mijna Hadders-Algra of the Department of Medical Physiology – Developmental Neurology at the University of Groningen in the Netherlands has published papers over the past decade describing work which has found that the quality of general movements during infancy is highly related to neurological dysfunction [Hadders-Algra, 1999]. Specifically, the fidgety stage of GM development in infants represents the most sensitive period for GM analysis for accurately predicting neurological development. This stage occurs around two to three months of age in the infant. Dr. Hadders-Algra's opinion is that physiotherapeutic intervention at this point in the infant's development is crucial to future improvement of motor function abilities in later life.

While CP cannot be prevented at this point, intervention is the only method for lifestyle improvements. Mildly abnormal GMs in the fidgety stage have even pointed to increased risk of ADHD and aggressive behavior. Her strategy is to use such information to inform parents of at-risk infants, that the development of their brain makes them less tolerant of environmental adversities.

The study of GMs is an important step in the diagnosis procedure. Brain imaging as shown in Figure 2.2.1 can be used to determine if an infant has any neurological damage, but it is not until the movements are studied that physicians can understand the impact of such impairment on the livelihood of the infant.

Figure 2.2.1. Typical image of the brain used in determine neurological impairments [UCP, 2002].

2.3 Present Methodology of General Movement Assessment with Video Footage

The present methodology for assessing general movements is to track qualitative assessments of movement during the maturation of an infant. Techniques have evolved in the past few decades, but the method presented by Prechtl and Hadders-Algra remains today's standard. This section will outline that method, as well as touch on a few other techniques.

2.3.1 Present Qualitative Evaluation of General Movements with Video

The present qualitative method for analyzing GMs calls for a trained physician to review hours of video footage from movement studies from the first few months of an infant's life [Hadders-Algra and Prechtl, 1992]. This is not currently the "standard-of-care" method for officially diagnosing CP, but is one tool commonly implemented to understand the impact from suspected neurological disorders on motor function. Based on this review, the physician grades the infant's movements qualitatively using Gestalt perception principles. These qualitative grades are tracked during the infant's maturation and aid in eventual diagnosis at about two years in age. During this evaluation process, it is important for the infant to remain in a supine position and not be distracted by any outside events or observers. This isolation helps to ensure that their movements are spontaneous, and not a reaction to outside stimuli.

In their paper, Prechtl and Hadders-Algra use a number of designations to classify infant movements. Specifically, these movement classifications include writhing quality, fidgety quality, wiggling-oscillating movements, saccadic movements, swiping movements, and swatting movements. Of all these characteristics, writhing and fidgety movements are the most common and easily recognizable. In their paper, a number of infant videos are analyzed and such classifications are applied to portions of the video and tracked graphically in various types of charts. There is little to tell from such charts outside of changes in type simply due to the complicated nature of plotting various patterns in time to describe each

movement classification. This study was more to track the evolution of these movement types through development. The movements are judged on their fluency, variation, and complexity.

During this study, Hadders-Algra kept a record of a number of the videos used and has published them to aid in understanding the qualitative diagnosis of CP. A sample from one such video study is shown in Video 2.3.1.1 (video2311.mpg) and is from the film entitled *The Assessment of the Quality of General Movements* [Hadders-Algra, 2002]. This film shows samples of various GMs from infants with varying degrees of neurological impairment during different stages of development. One can see that a mirror is used to supply the reviewer with multiple viewing angles of the infant in these videos. The video sample in Video 2.3.1.1 is from an infant approximately one month in age during typical writhing GMs.

Video 2.3.1.1. Sample 10-second video of normal writhing GMs (see vide file **video2311.mpg**) [Hadders-Algra, 2002].

As second video clip contained in Video 2.3.1.2 is also from Dr. Hadders-Algra's film and is of an infant during normal fidgety movements. These movements become prominent after about two months of age. In the video, paired leg motions, trunk movements, and arm extensions can be seen. It should be noted that the infant in the video appears to be reacting to the reflection seen in the mirror, which negates the scenario required for GMs as described in Prechtl's method.

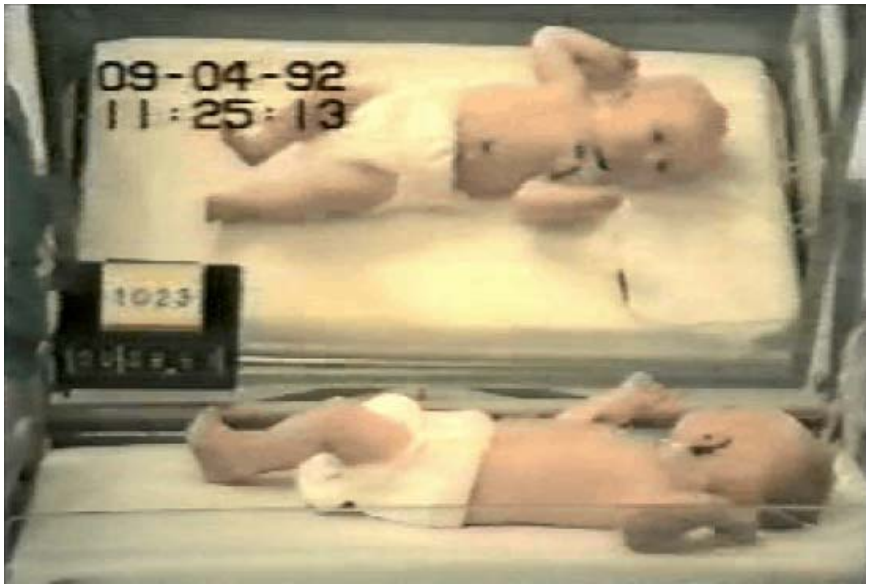

Video 2.3.1.2. Sample 35-second video of normal fidgety GMs (see vide file **video2312.mpg**) [Hadders-Algra, 2002].

Finally, a third video sample from Dr. Hadders-Algra's film is contained in Video 2.3.1.3. This sample represents abnormal fidgety motions, in contrast to those seen in Video 2.3.1.2. There are obvious kicking patterns that are quite abrupt and lack good fluency. Additionally, this infant's motion is quite repetitive, lacking complexity and variation.

Video 2.3.1.3. Sample 22-second video of abnormal fidgety GMs (see vide file **video2313.mpg**) [Hadders-Algra, 2002].

Many articles have been written on the inaccuracy within a single physician's scale, as well as across the span of scales of several reviewers. An example of the classification trajectories of multiple infants is shown in Figure 2.3.1.1. Here, at various points throughout the development of the child (birth being designated by the asterisk), a physician has evaluated the child's movements and classified the child's GMs with a degree of abnormality using a letter abbreviation (explained within the figure title). These evaluations are shown along a horizontal path for each infant. Over the course of 24 weeks, the physician tracks the infant's classifications and makes an estimate pertaining to the future normality of the child's motor skills.

	Postmenstrual Age (weeks)																								
Case	32	33	34	35	36	37	38	39	40	41	42	43	44	45	46	47	48	49	50	51	52	53	54	55	≥ 56	Outcome 2 years
1			*		N	N	N		N			N					N				N			N		N
2					*	PR		PR		PR			PR		N			N			N					N
3			*		CS		PR		PR			PR			PR			AF			AF					DR
4	*	PR	Ch		Ch		Ch		PR		PR			PR				AF		AF						CP
5			*	PR	PR	CS	CS		CS			CS			CS			F-			F-		F-			CP
6		*		CS	CS	CS	CS		CS			CS			CS		CS		F-		F-			F-		CP

Figure 2.3.1.1. Examples of different individual development trajectories from a qualitative study: N, normal GM or outcome; PR, poor repertoire of GMs; CS, cramped-synchronized GMs, AF, abnormal fidgety GMs; DR, developmental retardation; CP, cerebral palsy; Ch, chaotic GMs; F-, absent fidgety GMs [Einspieler, et al, 1997].

Figure 2.3.1.1 shows that the tracking of these qualitative measurements appears to result in consistent, correct diagnoses of the infants, as seen in the outcome column. The difficulty with this process is that every single classification for a child represents hours of an experienced physician's time. Figure 2.3.1.1 shows at least eight individual classifications per infant over the first few months of their life. All this time is spent watching video footage and evaluating the infants GMs using Gestalt principles, which is neither easily performed nor easily repeated with consistent results. The proposed study searches to determine if each of those classifications could represent a series of data files taken from an infant's motion, which could later be reanalyzed by different processing methods to determine patterns indicative of certain types of cerebral palsy.

2.3.2 Previous Clinical Qualitative Assessment Tools

Dr. Susan Harris and Dr. Carolyn Heriza state norm-referenced developmental assessment tools as being an important component of infant movement evaluation in a paper on *Measuring Infant Movement* [Harris and Heriza, 1987]. They do state a need for a standardized qualitative assessment tool as well, which Prechtl developed in the early 1990's and has been incorporated into diagnosis. Prior to that, there existed three different assessment scales. All three were described in Harris and Heriza's paper and are quite involved. They are referred to as the Movement Assessment of Infants (MAI), the Bayley Motor Scale, and the Peabody Developmental Motor Scales, and will not be detailed here because of their outdated nature.

2.4 Present Methodologies for Quantitatively Measuring Infant Movement

The quantification of human movement data has been limited by the technology available to physicians and physical therapists. To date, few studies have actually collected data points based on some sort of physical motion. A group of physicians in the Netherlands [Bos et al., 1997] did try to quantify spontaneous motility by reviewing video footage in a manner described earlier, but simply noting occurrence and duration of periods of motion classifiable in such categories as: GMs, isolated leg movements, startles, and twitches. While this may be valuable, the time spent by a physician is costly and could be replaced if accurately monitored with advanced electronic equipment. This section will further describe more quantitative methods for recording infant movements.

2.4.1 Present Quantitative Evaluation of General Movement with Video

The idea of measuring an infant's physical movement is not new. Current analysis procedures use quantitative methods for tracking frequency and amplitude of spontaneous movements of infants, but these still required the trained eyes of physicians to monitor

motion [Harris, 1991]. These methods involve analyzing joint angles of the limbs of infants from video footage recorded at 60 frames per second. An example of one frame from such video footage is shown in Figure 2.4.1.1, with the joint angles *a*, *b*, and *c* labeled.

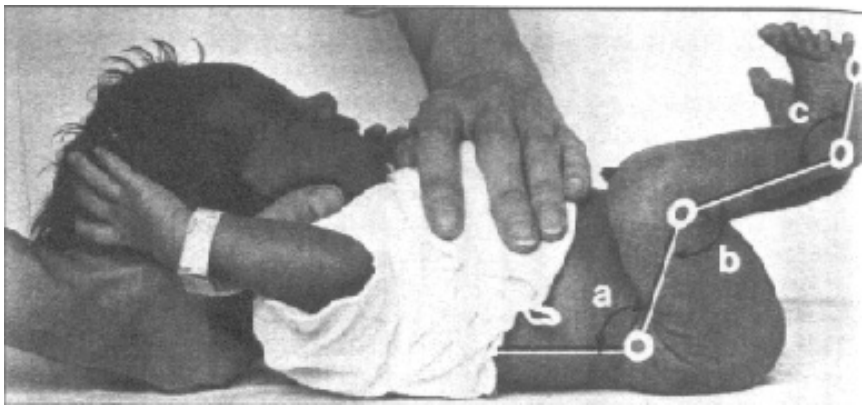

Figure 2.4.1.1. Sample frame from movement video showing recorded joint angles [Heriza, 1991].

This process still involves the monitoring of video footage to record joint angles from each frame of video. The data is effectively taken at 60 Hz for this study, because of the frame speed of the video. What results is quite an interesting plot of joint angles over time. Figure 2.4.1.2 shows plots of joint angles and knee velocity for two different infants over a period of 10 seconds. The velocity is shown for the hip, knee, and ankle, and is labeled *a*, *b*, and *c* in Figure 2.4.1.1, respectively. Comparison the data from these two infants shows a difference in the frequency and velocity with which they flex their knee. Also shown is how their range of motion may be limited by investigating the limits to which they extend their joints. While this test does produce worthwhile data, the time and effort involved with its recording is quite extensive. Using computers, the rate, accuracy, and efficiency of the acquisition and analysis of such motion could be increased greatly.

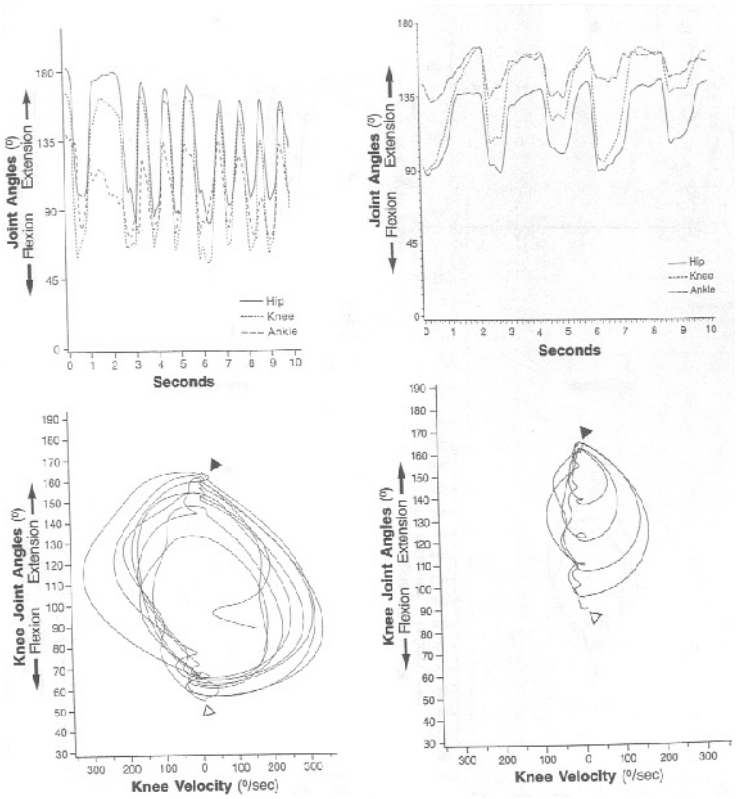

Figure 2.4.1.2. Knee joint angle and velocity for two different infants [Heriza, 1991].

Since its first use twenty years ago, this qualitative method has had many opponents. According to Dr. Jan Piek [Piek, 2001],

> Several recent papers have been critical of the quantitative approach, arguing that it fails to detect differences in movement patterns between brain-damaged and low-risk infants, unlike the qualitative approach, which has been successful in identifying infants with cerebral palsy through the observation of early motor patterns.

Because of this criticism, a quantitative procedure that involves more detailed recording for later grading and tracking of the progress of an infant's GMs could improve the cost, time, accuracy, and repeatability of motion analysis. Specifically, new electronic components, wireless data transmissions techniques, and data acquisition systems offer advantages unavailable when this method was first devised.

2.4.2 Automated Quantitative Evaluation of General Movements

Dr. Jan Piek has used one advanced quantitative technique to monitor spontaneous kicking in two-month-old infants [Piek, 1996]. In this work, Dr. Piek uses a MacReflex motion analysis system to track two dimensions of position data from the joints on infant's legs during spontaneous kicking. This work involves infrared cameras positioned to record the positions of the joints in time. Specifically, the x-y coordinates were sampled at 25 Hz in 60-second windows, 10 separate times. From this information, joint angles were calculated and tracked, but neither position nor acceleration. These angles are similar to those shown in Figure 2.4.1.1.

In Dr. Piek's reported findings, cross-correlation functions (CCF) were conducted on three-second samples of data determined to be from spontaneous movement. Previous investigators had studied 10-second bursts, but according to Dr. Piek, these longer samples often included spurious movement components that would affect results of analysis. The CCFs were conducted both between angle data on the same limb and on different limbs. Intralimb coupling of spontaneous kicking found high correlation with zero lag across all angles. Interlimb coupling did not find any significant pairing or coordinated movement. As a general comment about the reported findings, the detailed tables of data were very hard to interpret and a more graphical or visual method would be useful.

2.4.3 Use of EMG Readings From Major Muscle Groups

In studying spontaneous leg movements in infants Ester Thelen and Donna Fisher used not only video footage to quantify leg angles, but also EMG data [Thelen and Fisher, 1983]. An EMG, or electromyograph, is a graphic record of the electrical muscle activity. In this method, electrodes are placed on the skin of the infant in specific locations to measure when muscles contract. This research studied the following muscles on the right leg: tibialis anterior (ankle dorsiflexor), medial gastrocnemius (planar ankle flexor), rectus-femoris (hip flexor and knee extendor), and the medial hamstrings (knee flexor and hip extensor).

While many data files were recorded through this method, it becomes complicated to

understand the relationship of all the data because a single physical motion requires the use of so many muscles at one time. This complexity is probably one reason why this has not shown prominence in the field of infant motion analysis in the past twenty years.

2.5 Present Signal Processing Techniques for Analysis of Human Movement Data

This section will discuss some methods of signal processing and data analysis that pertain the stated research project. All examples are from processes conducted on data from human movement information. Some examples relating to frequency content and cross-correlations have already been discussed in the previous section, such as cross-correlation [Piek, 1996].

2.5.1 Analysis of Oscillation and Complexity in Infant Motion

Dr. Steven Robertson has viewed infant cyclic motor activity (CM) with a more dynamic systems approach and often relating it to chaos theory [Roberston, 1993]. In his research, Dr. Robertson chose similar groups of infants to test and used the same methods of preparing the infant to increase spontaneity. The research he conducted did not however take complicated direct movement data. Rather, two piezoelectric sensors were placed in the seat and back of the chair an infant was placed in during testing. His record of movement was related simply a Boolean variable of presence or lack of movement.

What is of interest in Dr. Robertson's methods is the way he analyzed the data. In particular, he looked for nonlinear forecasting of patterns. He states that the limited data collected limits this type of analysis.

Data reduction techniques are used in his research to obtain a movement time series. The sensor output is tracked so that movement is quantified as a percentage of movement recorded within a 5-second window. What results is a plot of movement where the vertical axis has the units of seconds per 5 seconds, which could also be viewed as a percentage. This method could be used to grossly study the periods and burst frequency of acceleration data, but may difficult to apply to the work presented here.

2.5.2 Sequence Comparison for Analysis of Infant Movement Patterns

Another method for analyzing infant movement patterns has been presented by Dr. Lucy Miller and Dr. Gale Roid [Miller and Roid, 1993]. Their work details studies on toddlers with and without motor delays to analyze the patterns in which movement occur. This research differs from other types already discussed because they classify specific movement types such as rolling over, turning the head, and lifting the upper body. These are all much more mature movements than would be seen during GM motion.

Having classified each type of motion, they studied the patterns in which they occurred. Each unit of motion is grouped in a greater set of motions and compared for toddlers with different motor delays. The results are described as being helpful in planning intervention. In general, this does not apply to the data oriented nature of GM analysis, but the technique of tracking patterns of motion units could be applicable in future research with data files.

3 Development of Accelerometer Devices

This chapter will outline a number of methods for recording data from movement and touch on the devices available to do this task. Once it has been established that acceleration measurement is the most appropriate for this work, background on the existing technology will be discussed. From here, the decision to use the Analog Devices ADXL202 will be justified.

Having explained the rationale behind the decision to use the ADXL202, the implementation of this device will be outlined for this research project. Within this discussion, aspects such as power requirements, circuit design, and device housing for the complete acceleration measurement device will be explained.

3.1 Methods for Recording Human Movement Data

Data from human movement has been recorded using many methods over the past twenty years. The method used for different projects are selected based on the limitations related to cost and precision. Three-dimensional imaging of the body is a very accurate method for recording all joints and related movements. The tradeoff is that this technology is very expensive and requires a system setup that takes up a considerable amount of space and is not easily transported. Other less precise methods involve video footage as previously discussed for cerebral palsy applications, but these methods are more subjective, but can be transported and cost far less to complete. Another technology just records times of gross movement in the seat or back of an infant's chair. This method does not give detailed information on the movements.

Systems such as those produced by Vicon [Vicon] are capable of recording motion in three dimensions. These require the use of tracking devices placed on the points to be recorded by the system, typically rotation points like hips, elbows, and knees. An instrumented child is shown in Figure 3.1.1. From this figure, we can see that the tracking

devices read by the imaging system of the Vicon are quite large and intrusive. This size would most likely cause motility problems with infants and should be minimized in design of a new device.

Figure 3.1.1. A child in a gait lab instrumented with a Vicon system [Vicon].

Vicon systems are typically used in gait applications to study dysfunctions in motor ability of children and adults. The information gained can help in the treatment of such disorders and track the progress of patients. Another common use for such technology is to record data related to human movement to make computer graphics for movies and video games appear more lifelike. The computer used to process the data is able to determine the velocity and acceleration of all points after data has been recorded, so in many cases the amount of data allows almost any bit of information to be extracted. This may be overkill for use on infants as only a few degrees of freedom in their motion are controllable. Figure 3.1.2 illustrates a computer image generated from data recorded by a system similar to a Vicon.

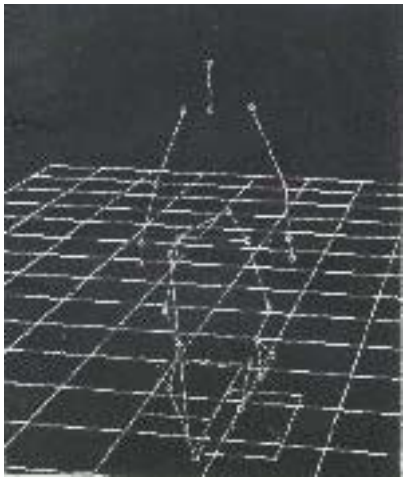

Figure 3.1.2. Computer generated graphic based on Vicon-type data [UCP, 2002].

Systems like the Vicon exist in many laboratories around the country. While these may not be ideal for clinical use in NICU facilities, they offer a valuable tool in helping to calibrate any future devices. An infant instrumented with both an existing technology such as a Vicon and a new measurement device could be recorded and the data later compared to ensure accuracy of the new device.

3.2 Background Information on Acceleration Measurement

This section will briefly introduce the idea of acceleration and some of its uses in engineering and science. Acceleration will also be related to the physical world and more easily understood measurements such as velocity and position. Finally, a discussion of various technologies to measure acceleration will conclude this section.

3.2.1 Understanding Acceleration

Acceleration is a measurement of how rapidly velocity changes in time. Velocity is in turn a measurement of how rapidly position changes in time. Gravity is the cause of any freefall acceleration towards earth and it measures at about 9.81 meters/second^2 (32.2 feet/second^2), commonly called one unit of gravity. Acceleration is also commonly measured to

understand a force (F) produced because force is directly related to the acceleration of a mass by the equation:

$$F = m \cdot a ,$$

where m is mass and a is acceleration. Common units are F in Newtons (N), mass in grams, and acceleration in meters/second^2, as mentioned previously. Acceleration measurement devices are often used to estimate the force produced in various engineering applications, using a known mass.

Another way to look at acceleration is that it is a measurement of a change in velocity over a certain change in time. Acceleration (a) can be seen in the equation:

$$a = \frac{\Delta v}{\Delta t} ,$$

where Δ represents a change in, v is velocity, and t is time. Velocity (v) can be thought of in a similar manner related to a change in position over a certain change in time as shown in:

$$v = \frac{\Delta p}{\Delta t} ,$$

where p is position. Using the mathematic techniques of integration and differentiation, we can extract position from acceleration, or vise versa, respectively.

For the current research, we are relying on acceleration dictating the presence of movement because in all cases of motion (unless there is no change in velocity), acceleration will be measured. Actual position in this research is not as important as the presence of motion, so the sole measurement and use of acceleration data will suffice. In engineering applications, acceleration is typically thought of as a vector because there is a direction associated with the measured acceleration. Due to this vector notation, acceleration can be measured, as positive or negative depending on the direction of application relative to the direction the positive axis of the vector measurement is oriented. Likewise, vectors can be

summed to form a total acceleration vector, even if the two measurements are not along the same axis. This will apply to any pair of measurements made on orthogonal axis, such as found on the accelerometer mentioned later in this chapter.

3.2.2 Technology Used to Measure Acceleration

Two primary types of accelerometers are currently used in various engineering applications: capacitive and piezoelectric. The capacitive accelerometers use two electrodes, one fixed and one moveable. As the device moves, the capacitance detected between the two electrodes is related to the acceleration seen by the device. Manufacturers calibrate the devices such that they know the capacitance reading between the electrodes for known accelerations and incorporate this into the algorithm used to decipher the actual acceleration measured. An example of different motions is shown in Figure 3.2.2.1, where the affects of accelerations in different directions can be seen on the interior mass and electrodes of the accelerometer. It should be noted that capacitive accelerometers are capable of measuring static accelerations, including gravity, as shown on the left of Figure 3.2.2.1. This can be used to measure tilt in some cases, but can be an added problem in other designs.

Figure 3.2.2.1. Capacitive accelerometer interior during static vertical gravity (left) and an XY acceleration (right).

The second technology, piezoelectric measurement, uses piezoelectric (piezo-ceramic) materials to measure displacement of a fixed mass within the accelerometer. The piezo material works to produce a voltage when deformed. As the piezo attached to a known mass are deformed and voltages around the mass are created, algorithms can determine the exact acceleration produced and direction in which it is moving by relating all

the voltage readings. Figure 3.2.2.2 illustrates these scenarios. Notice that on the left, the static force of gravity has no effect on a piezo-based accelerometer. On the right, a vertical acceleration (other than gravity) is applied and can be measured. This means that static forces cannot be measured and only dynamic (moving or changing) readings are recognizable. One downfall of such devices is that they require a large amplification of the very small voltages to allow for recognizable differences in measurement of acceleration, especially when accelerations in the range of a fraction of one unit of gravity are sought.

Figure 3.2.2.2. Piezoelectric accelerometer interior during static vertical gravity (left), an XY acceleration (middle), and a vertical acceleration (right).

Factors such as size, power consumption, amplification needed, cost, and static versus dynamic measurement must be weighed in the final design process. These technologies are constantly evolving and electronic circuits are shrinking in size such that older, large methods are now small enough to enable new applications.

3.3 Existing Microelectronic Devices for Acceleration Measurement

A survey of existing microelectronic devices available for measurement was completed in the fall of 2002 and a decision was made on which device to use for acceleration measurement in this project. Since that time, newer, smaller devices have arrived on the market and may be more suitable in future designs. This research is presented based on work completed using the device selected in the fall of 2002.

Table 3.3.1 lists a number of accelerometers available on the market. Both two and three-dimensional options are listed, while single axis devices were considered to be too simple for use in this project. Key specifications are also listed for each device along with the reference.

Table 3.3.1. Specifications for various two and three-dimensional accelerometers.

Parameter	**Analog Devices ADXL202**	**Analog Devices ADXL250**	**Kistler 8305A2**	**Star APA300**	**Star ACA302**	**MEMSIC MXA2312U**	**Crossbow CXL04LP3**
Measurement Range (±g)	2	5	2	50	2	2	4
Axis	2	2	2	3	3	2	3
Sensitivity (mV/g)	167	38	500	4.6	300	312	500
Power Supply (V)	2.7	4-6	7-16	5	2.7-5.5	2.7	5
Frequency Response (kHz)	6	1	250	1000	15	25	100
Type	Capacitive	Capacitive	Capacitive	Piezo	Capacitive	Thermal	Capacitive
Size (mm)	5x5x2	10x9x5.5	25x25x9	9.6x7.6x3.9	16x16x7.3	5x5x2	20x45x27
Mass (g)	1	3	6.5	1	3.5	1	46
Reference	[AD]	[AD]	[Kistler]	[Star Micronics]	[Star Micronics]	[MEMSIC]	[Crossbow]

Upon reviewing the various specifications compiled in Table 3.3.1, the Analog Devices ADXL 202 was chosen. It was not until the spring of 2003 that the ADXL311 was released, which offers the same performance as the ADXL202, but with direct analog measurements, as opposed to the direct digital pulse width modulated (PWM) measurements. The primary reason for this choice was the availability of Analog Device components via their sampling program. Due to the limitations on research expenditures, the free sample nature made these the most attractive component. Other factors will be discussed in the next subsection.

3.3.1 Performance Requirements for the Accelerometer

Performance requirements for use on infants were estimated prior to design choice. First, a maximum acceleration reading of around 2 units of gravity (g) was chosen. Most devices

come in 2, 5, or 10 g options and the 2 g option was the most logical choice. If a capacitive model were chosen, that limit would surely be pushed if the acceleration were to occur in the direction of earth's gravity. This was considered, but deemed unimportant.

While three axis of measurement seems more powerful, extra data acquisition and storage would make this a more costly process. Additionally, studies of infant motion point to a limited amount of movement of higher degree of freedom joints such as wrists and ankles. In fact, at an age of about two months, most infants really only have gross motor function in the hips and shoulders, while the elbows and knees are only starting to become disassociated with the larger muscle groups. It is because of this expected limitation on fine movement that only two axes were deemed important for study. In particular, the planes on the side of the ankle is of most interest on the leg because side to side swaying of the leg is not as prominent as kicking up and out away from the body. For the wrist, the top plane, even with the back of the hand, was chosen because rotation of the shoulder or elbow does not seem as active as the other two dimensions in infants.

Sensitivity was of interest in that a maximum voltage for minimal acceleration measurement would allow finer measurement of accelerations. Related to sensitivity is the power supply required. With a larger power supply from which to divide the range of acceleration measurement, sensitivity could be increased. The tradeoffs here are to maximize the window of useable measurement range, while minimizing the power required. The most difficult part of the design process is minimizing the weight of the device, and while the mass of the accelerometer may be small, the battery to power it can severely cripple the use of the final device. Therefore, to minimize weight and size of the battery, power supply is therefore limited, as is sensitivity. This will be discussed further in the section of this chapter pertaining to battery choice.

Frequency response of the device is important in that we would like to be able to resolve the highest frequency possible we would expect to see from the movements of the infant. Here too we find quite a few important tradeoffs. First, frequencies much over 10 Hz (10 oscillations per second) are thought to be extremely unlikely, although we cannot view these fine movements easily with the naked eye. In recording this type of data, we would be required to sample it at a rate about ten times the greatest frequency we want to resolve. Therefore, a sample rate of 100 Hz would be required for this frequency, which

would create more data to be stored, possibly slowing down the data acquisition system or limiting the number of channels we could record simultaneously. With these considerations in mind, all devices exceed 1000 Hz (1 kHz) in frequency response, so this is not an issue for this design.

The decision to use capacitive or piezo-ceramic comes down to what type of data is to be recorded. As previously described, capacitive accelerometers will measure static accelerations such as gravity, which can complicate the reading taken if measurements are made while the axis is even partially in the plane of earth's gravity. Piezo-ceramic accelerometers do not have the capability to measure such static accelerations, and therefore only measure a change. Here there is a much lower voltage outputted from the device (less sensitive) so they require amplification and often times a larger power supply. Based on these options, capacitive accelerometers seem to the best choice at this time for this project.

Finally, as mentioned, mass and size are a consideration. To minimize the overall impact of the device on an infant and their motility, these should both be minimized. Looking at Table 3.3.1, we can see that most devices only have a few grams of mass and are only a few cubic millimeters. One consideration that should be handled is the mounting of many of these devices. Due to their small size, many can only be mounted on printed circuit board (PCB) and this requires specially manufactured PCB and very fine detail soldering. During prototyping, both PCB and fine soldering are very difficult to manage, but complications are reduced when and final design and production have commenced.

3.3.2 Final Accelerometer Choice Based on Criteria and Specifications

After reviewing all the available specs in Table 3.3.1, the Analog Devices (AD) ADXL202 was chosen. Many models exist for various temperature applications, but all are suitable for the working range of 15-25 degrees Celsius. These devices stood out not only for the minimum size and power supply requirements, but also because of the ideal range and acceptable sensitivity. The frequency response is lower than others, but will be fine for this application.

A major plus for this product was the sampling policy of Analog Devices, which

allows for free samples of all versions of this chip in small quantities. For this research, approximately fifteen of the accelerometers in various temperature ratings were obtained at no cost. A hidden issue that was later resolved was the mounting of these devices. No standard pin-out options exist for this model, so prototyping on normal circuit board is very difficult. This means that metal pins do not exist on the device, thus requiring an exact matching footprint on PCB must be found to properly mount the device. The footprint and size of the ADXL202 or ADXL311 can be seen in Figure 3.3.2.1.

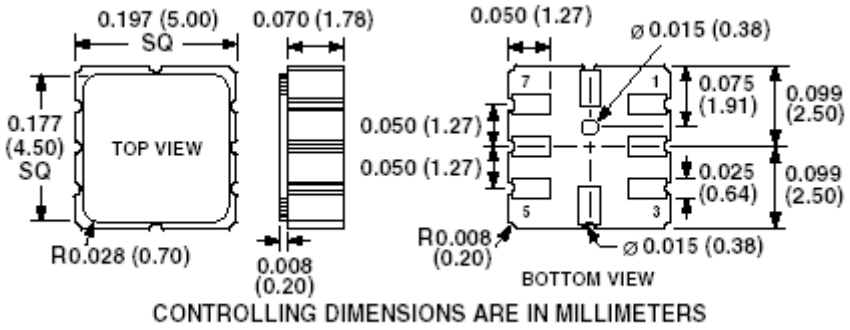

Figure 3.3.2.1. Diagram of ADXL202 of ADXL311 Footprint with Terminals [AD].

In the spring of 2003, Analog Devices introduced another model of the ADXL202, the ADXL311, which offers the same performance, but outputs the signal in only an analog option. The ADXL202 can be outputted either as a pulse-width modulated (PWM) digital signal (where varying periods of 0 volts and a high voltage are outputted to describe the acceleration reading) or a straight analog signal from 0 to a high voltage with intermediate voltages in between. The PWM option could be helpful in later designs using micro controllers to buffer and transmit data, but for directly wired devices, the analog was an easier option. Designs for this research did use the ADXL202, but the ADXL311 could be used directly in its place, with only basic wiring modifications.

3.4 Power Requirements for Acceleration Measurement Device

Having chosen the ADXL202 as the accelerometer for the measurement device, a power supply of at least 2.7 volts needed to be found to power the instrument. It was desired to put the supply on board with the device in the housing rather than running from an external source, due to additional lines required for transmission, as well as issues relating to increased opportunity for contact with the infant. Additionally, future designs are hoped to be wireless, so all power will eventually have to be on board the device, so it only makes sense to include that consideration in this design.

A survey of various battery options was conducted. There exist two shapes of batteries available in the 2.7-volt range: coin and cylinder. Coin-type batteries are like those found in watches, while cylinder-type batteries are various diameters and lengths of standard AA batteries used in common electronic devices. An additional plus to coin-type batteries is the availability of designs with positive and negative leads being parallel to each other from the same surface for computer board applications. Cylinder-shaped batteries that have their poles on opposite ends are much more difficult to wire due to the often large distance between poles and awkward shape of the battery. Being that the final housing design is intended to look similar to a wristwatch, the coin-type makes the most sense for this use.

A survey of options available from electronics suppliers indicated that a 3.0-volt battery is very standard. With this power, capacities up to 1000 mAh (milli-amp hour) are available, as well as sizes from 15 mm in diameter and 5 mm thick to 28 mm in diameter and 10 mm thick. These options were all lithium-ion batteries and are not rechargeable. Rechargeable options do exist, but have a much smaller capacity than single-use batteries, so they were not considered during prototyping.

Consultation with other research projects related to the use of micro-controllers and wireless transmitters point to issues relating to minimum power requirements from 3.0 to 3.3 volts for micro-controllers. With this increase at a future time, a 3.0-volt battery may be insufficient. For this reason, the smaller market of 3.6-volt coin-cell batteries was explored. Within this domain, a 400-mAh capacity coin-type battery was found from Tadiran. The TL-5186 is similar in size to other 3.0-volt lithium-ion batteries, as well as weight at only 5.3 grams [Tadiran]. The two terminals located on one side, isolated from each other by a

plastic backing made this option even more attractive. While the power consumption of the final device was unknown prior to battery selection, it was estimated to be less than 1 mA. This value will increase with the use of micro-controllers and wireless transmitters, but for a wired design, this was a safe estimate. With this estimate, 400 mAh in capacity should last for 400 hours of operation. Figure 3.4.1 details the size and shape of the battery chosen for use in prototyping.

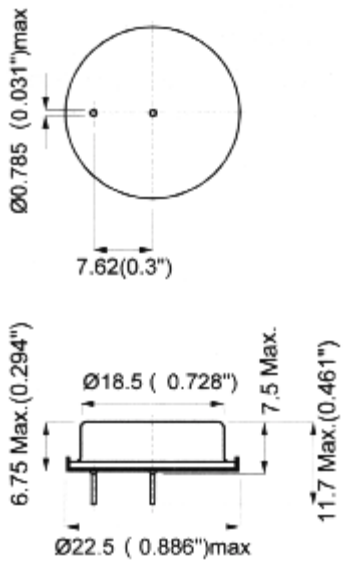

Figure 3.4.1. Diagram of Tadiran TL-5186 3.6V lithium-ion coin-cell battery [Tadiran].

Table 3.4.1 outlines the specifications for the battery. As mentioned previously in this section, this device meets all the criteria to power the ADXL202 chosen as the accelerometer.

Table 3.4.1. Specifications of the Tadiran TL-5186 [Tadiran].

Nominal capacity @ 0.3mA TO 2V	0.4Ah
Rated voltage	3.6V
Weight	5.3g (0.187 oz.)
Volume	1.2 cc
Operating temperature range	-55'C to +75'C

3.5 Circuit Design for Acceleration Measurement Device

This section will outline how the ADXL202 was incorporated into a built circuit for placement in a housing for use in testing. After explaining the electrical circuit diagram required for the device, a description of the capacitor selection to enable proper frequency response will be presented. Because the ADXL202 is intended for mass-produced PCB, the method for converting the PCB design to an 8-pin-out design will be explained. Finally, a brief introduction to the final assembly of the circuit will be presented.

3.5.1 Circuit Diagram and Layout

The ADXL202 has 8 pin-outs. Figure 3.5.1.1 diagrams some of the interior circuitry of the device and notes all the required external terminals that must be connected for proper operation of the device. Of key importance are the power supply from 3.0 to 5.25 volts, for which a supply of 3.6 volts has been chosen. Additionally, there are two capacitors, a self-test (unused for this application), a PWM resistor set, a ground, and two PWM outputs. To receive an analog signal, a voltage reading is taken across the corresponding frequency response capacitor, as indicated by C_x and C_y in Figure 3.5.1.1, so the X_{out} and Y_{out} are unused for our application. R_{set}, the resistor to set the PWM width is set to a nominal value of around 1 MΩ, but this is unimportant because the PWM signal is not used. The selection process is outlined further in the data sheet for the ADXL202 as supplied by Analog Devices [AD].

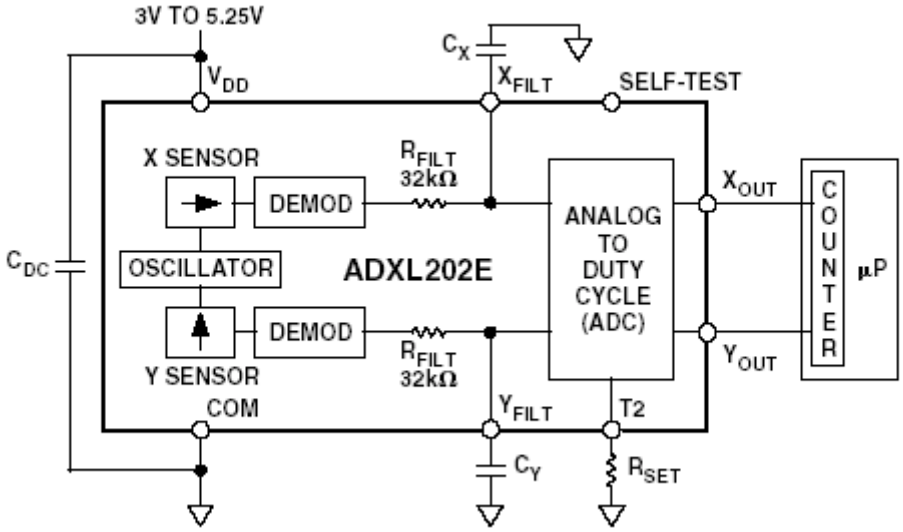

Figure 3.5.1.1. Function block diagram of ADXL202 [AD].

3.5.2 Capacitor Selection for Proper Frequency Response

In selecting the capacitor values, the data sheet for the ADXL202 was used as a reference [AD]. Table 3.5.2.1 is from that data sheet and outlines the capacitor values to be used for various frequency ranges. The bandwidth listed refers to the –3 dB point on the magnitude plot, where the magnitude drops below half its strength at lower frequency (as in a Bode plot). For our application, it has been determined that no information above 10 Hz is of interest. This is because infants are not predicted move at a frequency greater than that and additional bandwidth requires a higher sampling rate and ultimately larger data storage files. The capacitor value determined was 0.47 µF, which as described in the data sheet, reduces the overall noise in the recorded data to 8 mg (milli-unit of gravity) of RMS noise.

Table 3.5.2.1. Capacitor selection table to determine frequency response [AD].

Bandwidth	Capacitor Value
10 Hz	0.47 µF
50 Hz	0.10 µF
100 Hz	0.05 µF
200 Hz	0.027 µF
500 Hz	0.01 µF
5 kHz	0.001 µF

3.5.3 Connection of ADXL202 to Printed Circuit Board Adapter

The ADXL202 is only available in a PCB-style component package, making connecting the accelerometer to prototyping board very difficult. A search was done for a method to create pin outs on the device rather than standard flat PCB terminals. The pin configuration on the accelerometer is shown in Figure 3.5.3.1, which is not a standard shape.

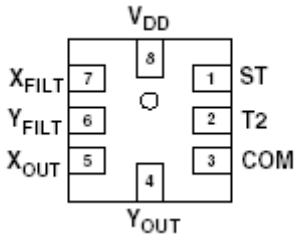

Figure 3.5.3.1. Pin configuration on bottom view of ADXL202 [AD].

After searching for a matching design to mate with the terminals, a circular design produced by BrownDog Component Adapters [BrownDog]. The device is called their *DIP8 to TO-99 adapter* and is shown in Figure 3.5.3.2.

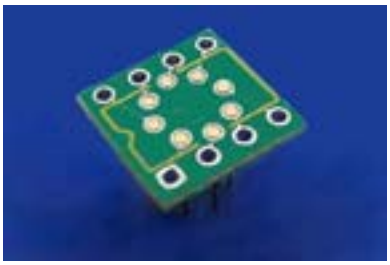

Figure 3.5.3.2. BrownDog DIP8 to TO-99 adapter used with ADXL202 [BrownDog].

As can be seen from comparing the terminals of the ADXL202 to the gold tabs on the BrownDog adapter, their configurations are not a perfect match. To connect the two a few modifications had to be made. First, the gold pins in the circular layout on the BrownDog adapter were removed by pulling them through from below, using pliers. Once removed, the sockets in the circular arrangement and the terminals on the ADXL202 were tinged using solder to get a base to connect the two pieces. Having done this, a generous amount of flux was lathered on the adapter surface over the tinged sockets and the ADXL202 was essentially glued to the adapter with that flux.

After positing the terminals on the midpoint of the sides of the accelerometer directly over the points in the circle closet to the straight edges of the adapter, a light amount of solder was applied with a soldering iron to connect the two pieces at all four points. The remaining four connections had to be done very carefully using a fine-tipped soldering iron inserted just under the corners of the accelerometer. Only a small amount of solder could be used in any connection, as too much would separate the two planes. Notice that it is very important to try and maintain a parallel nature between the top face of the adapter and the accelerometer. In addition, it is important to keep the sides of the two as parallel as possible. Any misalignment will cause slight errors later in the use of the device.

The final step was to create pin-outs on the 8 sockets lining the sides of the adapter. To do this, small strips of sturdy copper wire were placed in the sockets and soldered in place such that they stuck out the bottom of the adapter. The finished combination was an ADXL202 with 8 pin-outs in the standard prototyping configuration to use in sample designs. The final layout of pin-outs from the ADXL202 to the adapter is shown in Figure 3.5.3.3 and will be explained later in this section.

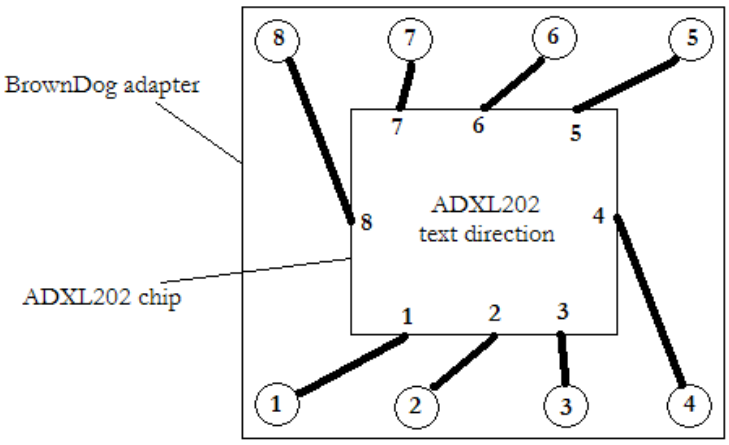

Figure 3.5.3.3. Final pin-out diagram of the ADXL202 with the adapter.

3.5.4 Final Circuit Assembly

Referring back to Figures 3.3.2.1 and 3.5.3.1, we can see the pin number corresponding to those shown in Table 3.5.4.1. Using these as a reference, the accelerometers were connected to prototyping board. Special attention was paid during this process to ensure that the final board would fit within a plastic housing. The housing design is outlined in the next section, but the interior surface area for a board was known to be about 1.8 inches by 1.1 inches, with a screw hole in the center.

Table 3.5.4.1. Pin function descriptions for ADXL202 [AD].

Pin No.	Mnemonic	Description
1	ST	Self-Test
2	T2	Connect R_{SET} to Set T2 Period
3	COM	Common
4	Y_{OUT}	Y-Channel Duty Cycle Output
5	X_{OUT}	X-Channel Duty Cycle Output
6	Y_{FILT}	Y-Channel Filter Pin
7	X_{FILT}	X-Channel Filter Pin
8	V_{DD}	3 V to 5.25 V

In designing and assembling the circuit, two ports were left open so that battery drain could be limited while the device was not in use. To do this, the battery port (integrating the battery into the circuit) was made to be two female ports located four pinholes apart on a standard electronics socket as shown in Figure 3.5.4.1. The ports on top were used to plug the battery into, as well as run wires back to the circuit. On the bottom, the terminal pins from the adjacent ports were crossed and soldered, as shown in the bottom view. The advantage of this design was to place the entire port at a point away from the circuit board, while allowing removal of the battery. By having the entire port unattached to the board, placement in the house was easier and minimized the total height of the circuit to allow it to fit within the housing.

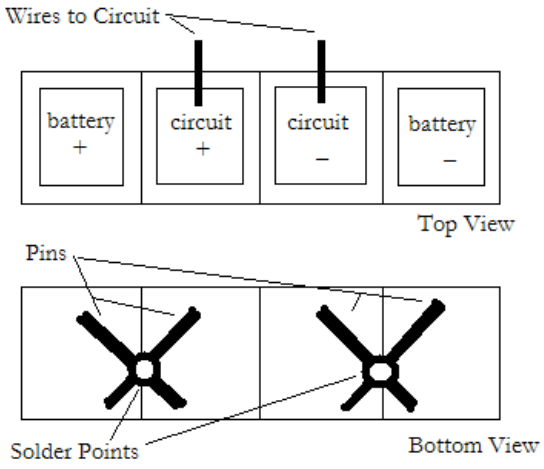

Figure 3.5.4.1. Design for connecting the battery to the circuit.

Figure 3.5.4.2 shows a picture of the battery connection terminal as diagramed in Figure 3.5.4.1. Here you can see the top view with the open ports for the positive and negative battery terminals as well as the positive and negative wires running to the circuit. Note that the wires have been soldered into the terminal sockets.

Figure 3.5.4.2. Battery connection terminal.

As a final design option, a breaker was placed between the battery and the circuit. This breaker had external terminals, so when connected, the circuit was complete. This feature minimizes drain on the battery when not in use. Even when data is not being recorded, the battery powered nature of the device means that the accelerometer will constantly measure acceleration and drain the battery. By placing the breaker in the circuit, there exists an on/off switch. An actual switch was not used because of limitations on parts in the prototyping lab, in addition to the small size and weight required of the switch. The jumper used to complete the circuit can be seen in Figure 3.5.4.3, where the open terminals are shown in the left picture and the connected terminals using the jumper are shown in the right picture.

Figure 3.5.4.3. Zoomed view of break in circuit to minimize battery drain.

The final circuit layout is shown in Figure 3.5.4.4. On this diagram, the direction of orientation of the X- and Y-axes is shown; these will later be related to the outside of the device housing. The pin-out numbers can be referenced with Table 3.5.4.1. Also notice the jumper pins and battery ports described in the previous part of this subsection. Pins 4 and 5 are left unused because they are the PWM X- and Y-axis outputs, but we are reading the analog signal from parallel lines across their corresponding capacitors, Cx and C_y.

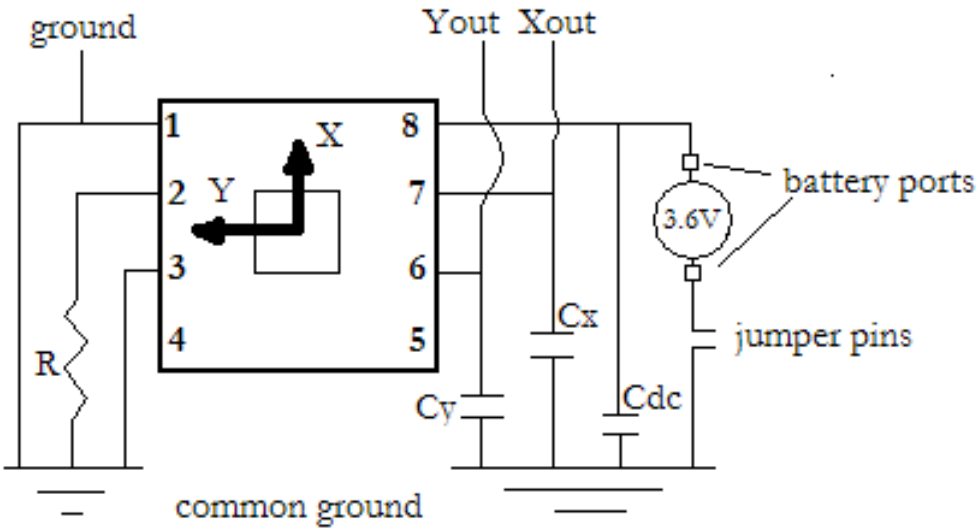

Figure 3.5.4.4. Circuit design for use of ADXL202 to output analog accelerations.

An annotated picture of the circuit layout is shown in Figure 3.5.4.5. In this figure you can see the different components discussed earlier in this section. Additionally, the three output terminals are labeled, but slightly covered by the wire socket connecting the device to the central data acquisition system. The X_{out} and Y_{out} terminals as well as the common ground are all sent via the connecting wire to the data acquisition system. Note that the white wire on the cable is unused. The orientation of the positive measurement axes is also labeled in the photo.

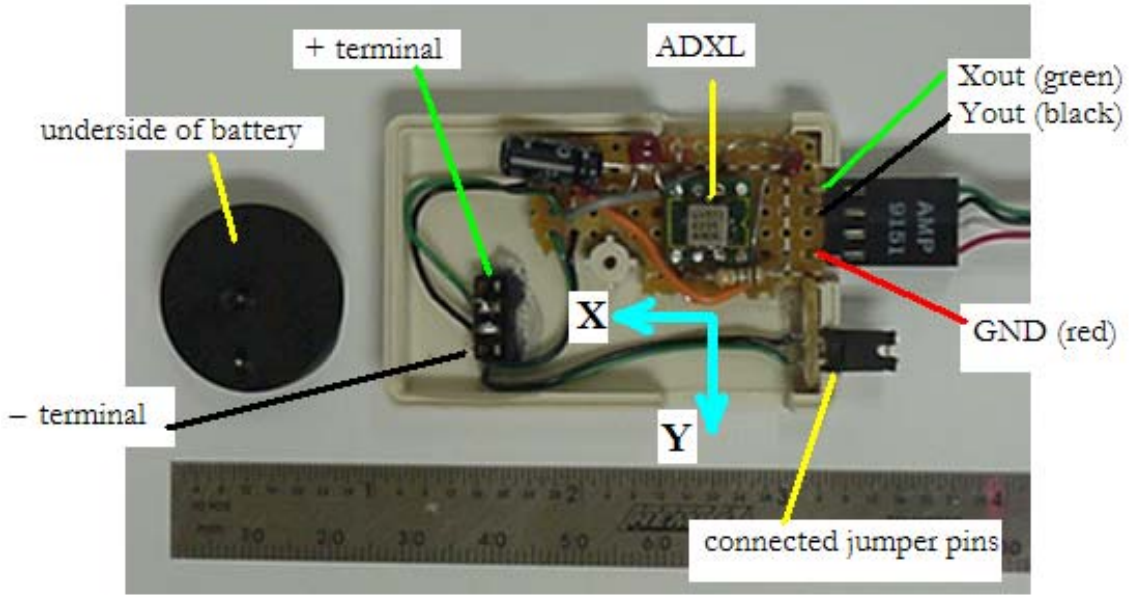

Figure 3.5.4.5. Annotated photo of circuitry for the acceleration measurement device.

3.6 Housing Design for Acceleration Measurement Device

The next step in the design of the acceleration measurement devices was to design a method to house the electronics, while connecting the package to the wrist or ankle of an infant. Based on the size of the prototype electronics, a common plastic prototyping housing was selected, measuring 2 1/8 inches by 1 3/8 inches by 9/16 inches. The internal dimensions available in the housing for electronic components measure approximately 1.8 inches by 1.1 inches by 0.4 inches. These dimensions were known prior to building the circuit and were therefore factored into the design of the electronics. Ports on the housing were required for the output terminals, jumper terminals, and a Velcro® strap used to attach the device to an infant. A screw hole is also located in the center of the device that must be isolated from the circuitry.

Figure 3.6.1 shows a picture of the inside of the final housing design with the circuitry in place. In this photo, the battery is in place and ovals have been drawn to indicate places where the housing had to be altered to allow fitting of the entire device. Red ovals indicate where entire parts of the side of the housing were removed to allow components to

pass through the wall such as terminals plugs or Velcro® straps. Green ovals indicate areas where the interior had to be shaved slightly to allow full closure of the house due to the size of the battery. The top of the housing is shown on the right and has been flipped open, so would simply be replaced on the base by rotating it as if a hinge existed between the two halves.

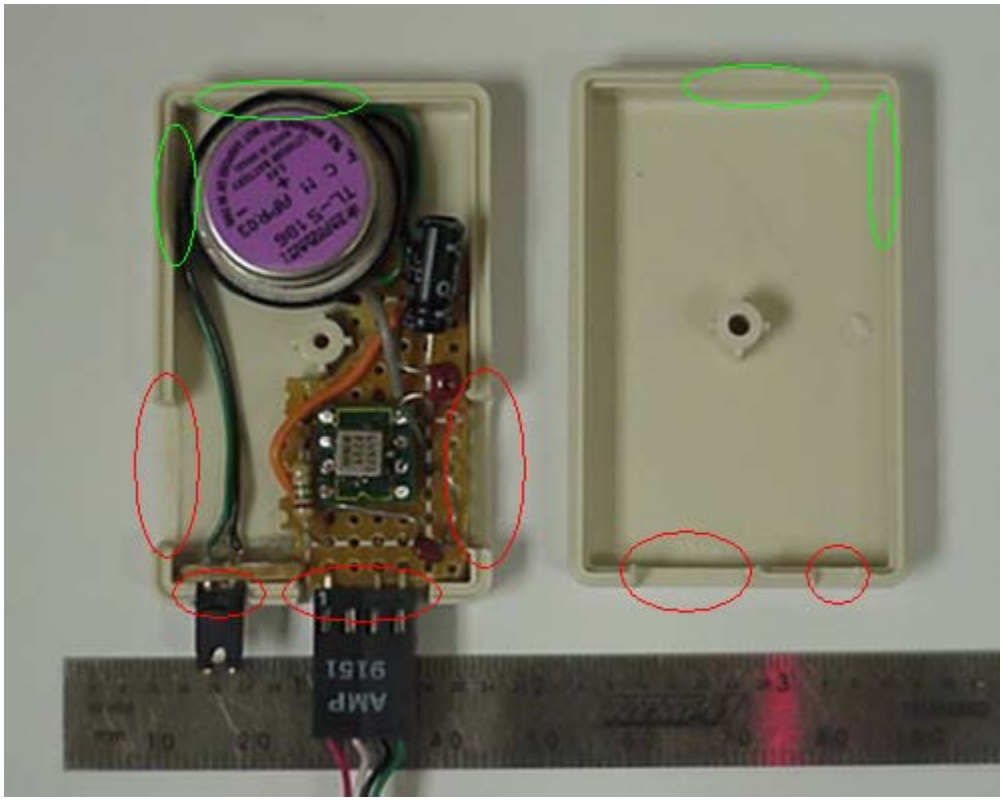

Figure 3.6.1. Interior design of acceleration measurement device housing.

Figure 3.6.2 shows a top view of the device with the housing closed using the securing screw. The positive measurement axes are shown in the picture. It should be noted that these are not the exact axes as small variations in the parallel nature of the chip (the base axes) to the adapter board, prototype circuit board, and the housing could slightly alter the actual measurement axes relative to the exterior of the device. A discussion of how these slight misalignments were accounted for is located in the description of the data acquisition code in a later chapter. Annotated on the figure are the individual output terminals, the jumper terminal pair, and the Velcro® strap used to attach the device to a human subject.

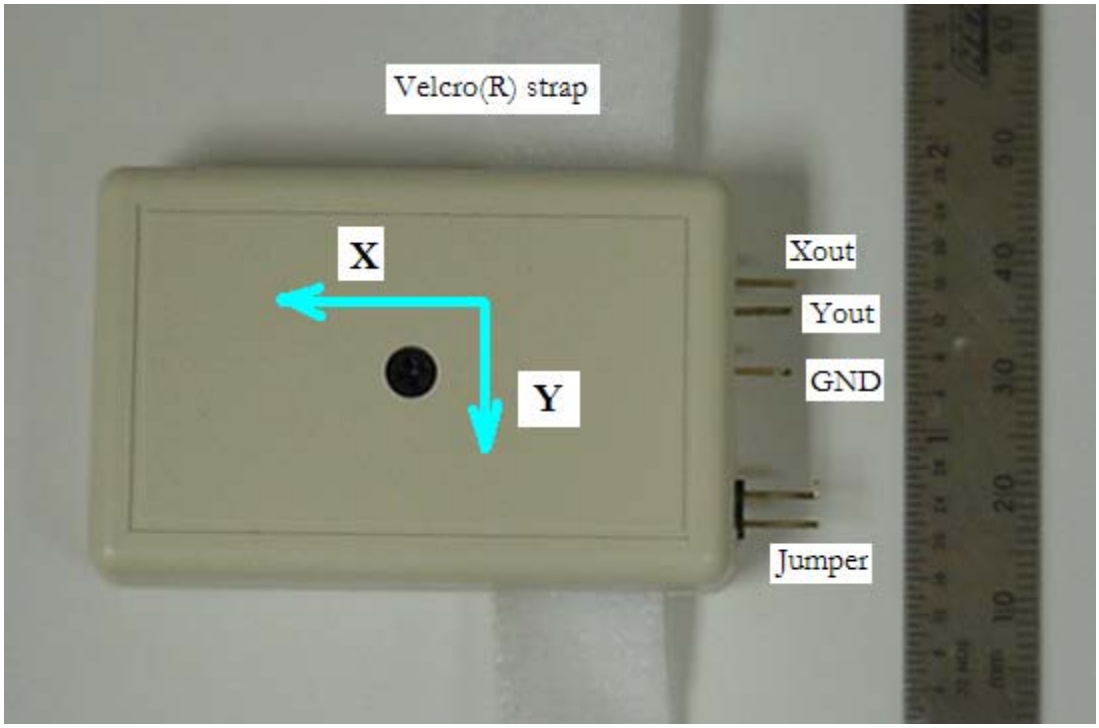

Figure 3.6.2. Top view of the outside of acceleration measurement device housing.

To make room for the entire battery and terminal, the vertical room within the housing had to be slightly altered. As described in previous sections of this paper, to allow for easy removal of the battery from the circuit, the base terminal was placed in a rectangular hole in the base of the housing. In Figure 3.6.3, the bottom of the housing can be seen with a piece of electrical tape covering the bottom hole. This hole was placed to allow enough room for the battery inside the housing. Precautions were taken to isolate the positive and negative terminals on the underside of the connection terminal from the outside of the housing using electrical tape and clear caulk. This negates the possibility of the terminals being shorted across the infant's skin, which would not present a danger to the infant, but has been considered.

Figure 3.6.3. Bottom view of the outside of the acceleration measurement device housing.

A final view of the front side of the device housing is shown in Figure 3.6.4. This illustrates the space allotted in the walls of the housing for the jumper terminal (right side of figure) and the three output terminal pins (left side of figure). Also, the strap used for attaching the device to a human subject is seen. Note that the "loop" side of the Velcro® strap makes up enough length to traverse the circumference of an infant's wrist or ankle, and only a small section of the "hook" side of the Velcro® strap is used. This is intended to minimize the discomfort an infant might experience if contact with the "hook" side of the strap were contacted.

Figure 3.6.4. Front face view of the outside of the acceleration measurement device housing.

3.7 Final Specifications for Acceleration Measurement Device

A full description of the design and construction of the acceleration measurement device has now been discussed. This section will explain final specifications of the device while showing some of its performance characteristics. Plots shown in this section were made after recording data using the data acquisition software and hardware outlined in the next chapter.

3.7.1 Final Device Size and Performance

The final device, as shown in previous figures, has a total mass of 25 grams (approximately 2/3 of an ounce). The outside dimensions are 2 1/8 inches by 1 3/8 inches by 9/16 inches and a Velcro® strap of about 5 inches is attached to the inside of the housing, routed under the electronic circuitry. This mass and size were not anticipated to disturb an infant of normal size at an age of 1-3 months. The current size of the prototype device is believed to be too large for a prematurely born infant. Later total packages should be designed to weigh less and be placed in smaller housings, utilizing PCB.

The output from the internal sensor is a voltage proportional to the measured acceleration, which is reported from two orthogonal channels. This output is also proportional to the supply voltage, which is approximately 3.6 volts. As the voltage changes slightly, the voltage output and conversion factor will also change slightly. An acceleration reading of zero units will measure exactly half of the supply voltage, which should be about 1.8 volts. Again, this will drop slightly as the supply voltage drops. The drop in static voltage is only noticeable during the first few minutes of operation once the battery has been connected into the circuit via the closing of the jumper terminals.

The sensitivity of the accelerometer is related to the supply voltage, so as the supply drops, so does the sensitivity. No information is given in the data sheet about linearity of this calibration, but because any voltage changes would be small, a linear relationship was assumed. The calibration constant (C) can be calculated from the following relationship:

$$C = 56 \cdot Vs,$$

where Vs is the supply voltage in volts (assumed to be around 3.6 V) and the units on the constant, 56, are $\frac{mV}{g \cdot V}$. This calibration constant is then used to relate a voltage output to the measured acceleration (a) by the following equation:

$$a = \frac{\left(v - \frac{Vs}{2}\right)}{C},$$

where v is the output voltage reading in millivolts, Vs is the source voltage in millivolts, and C is the calibration constant with units $\frac{mV}{g}$. The acceleration vector now can have a positive or negative value because the zero acceleration value has been offset from the mid-voltage value on the voltage output. The orientation of such positive and negative directions can be related back to the positive axes illustrated in Figures 3.5.4.5 and 3.6.2.

Due to the capacitors placed in the circuit, the frequency cutoff is at 10 Hz, so any frequency content above this has been attenuated to much less than half of its value. This will help in reducing high-frequency noise, making a cleaner signal. Capacitors of 0.47 μF in value were used at the C_x and C_y positions, as shown in previous diagrams. A resistor value around 1 MΩ was used at the R_{set} position in the circuit, but this was unimportant because the PWM signals were not taken from the accelerometer, just the analog values at the C_x and C_y pins. A capacitor (C_{DD}) with a value of 0.1 μF was placed in parallel with the power source, as recommended in the data sheet for the ADXL202, supplied by Analog Devices [AD].

3.7.2 Impact of Rotation and High-Frequency Vibrations on Measurements

This subsection outlines how the tilt sensing ability of the ADXL202 affects measurements taken. Additionally, figures will be shown that illustrate the ability of the device to measure

high-frequency components.

A simple test was conducted to show the impact of rotating the two axis of the acceleration measurement device into a plane parallel with earth's gravity. Without regard to time, a single device was taken and rotated such that the positive Y-axis (labeled lateral acceleration) and positive X-axis (labeled forward acceleration) were rotated into the plane of gravity, respectively. The negative axes were then rotated into the plane of gravity in the same sequence. The results of this test are shown in Figure 3.7.2.1, where we can see that they both approach positive and negative one units of gravity, after the data was processed to change the data to units of gravity from volts (as mentioned in the previous subsection). The maximum acceleration appears to be around 0.8 g while the minimum is about -1.2 g. Measurements of 1.0 and –1.0 g are expected due to the nature of 1.0 g equaling earth's gravity, so the initial calibration before this test was done improperly. The range does remain at 2.0 g, as expected.

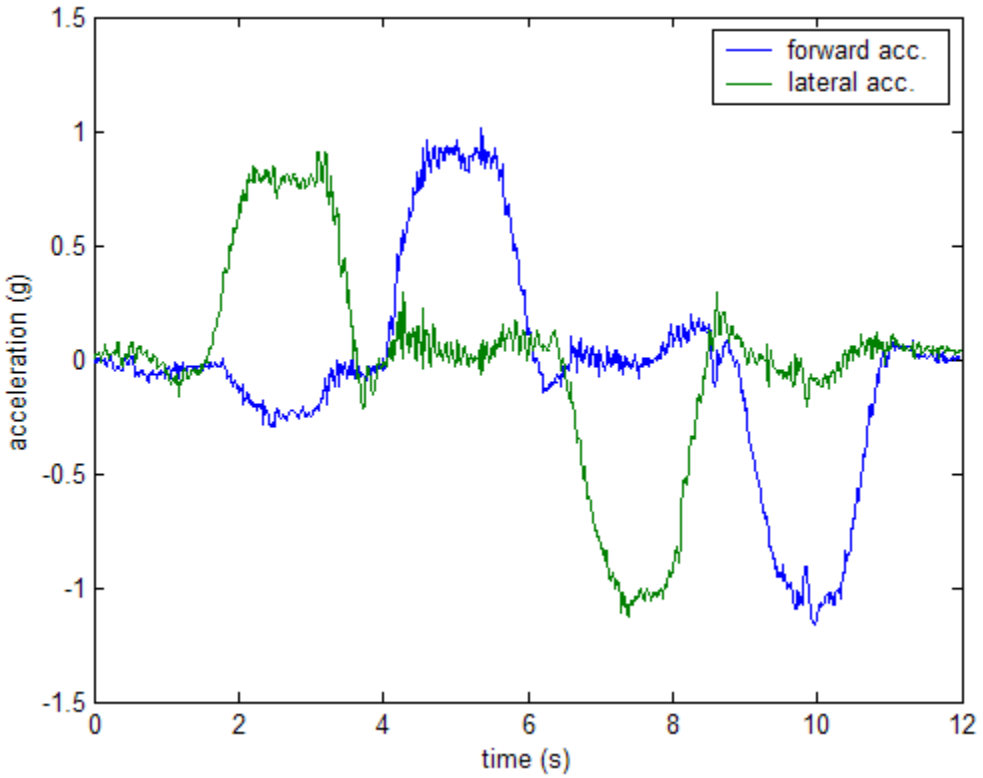

Figure 3.7.2.1. Acceleration measured during unsteadied device rotation (+Y, +X, -Y, -X).

This first figure represents data taken when accelerations were measured having the device held freely by the experimenter's hand. A later test shows a difference when the device was steadied on a table during the test and high-frequency vibrations were not transmitted to the accelerometer, resulting in a signal with less noise.

The data previously presented can also be viewed completely independent of time in an X-Y plot, where each point in time is plotted by its accelerations in both the X and Y directions. Figure 3.7.2.2 shows this type of plot for the previous data. We can see the straight nature of the total accelerations in only one dimension of the plot. This one-dimensional nature of the plot indicates that the device was only moving in one dimension during the time. Note that again, lateral acceleration refers to the Y-axis, while forward acceleration refers to the X-axis of the accelerometer, but they have been oriented as seen on the external housing of the device.

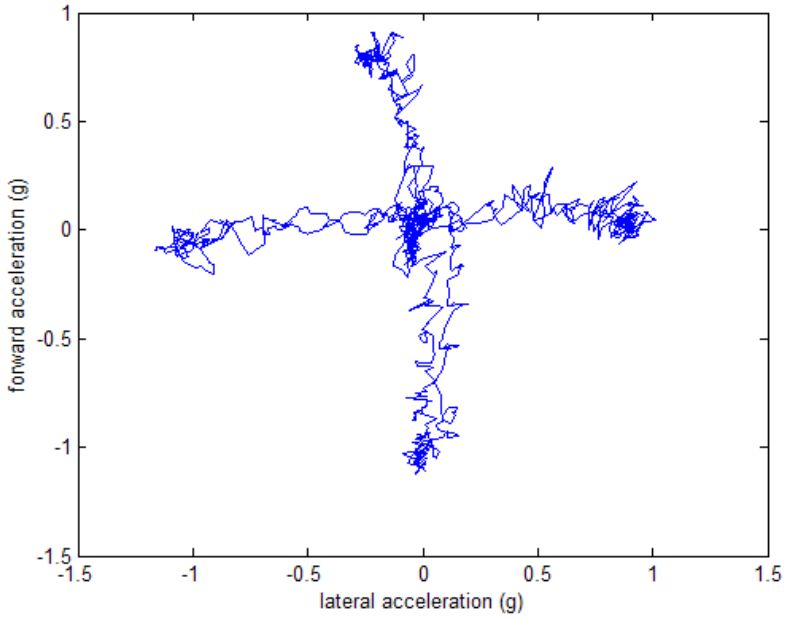

Figure 3.7.2.2. X-Y plot of acceleration during unsteadied rotation test.

A second tilt test was conducted where the device was steadied on a table and free vibration from the experimenter's hand did not affect the readings. A plot from this test can been seen in Figure 3.7.2.3. In comparing this to Figure 3.7.2.1, which was completed in the same progression of axes, we can see much more stable data. There is far less noise due to

vibrations of the device. The spikes in the data most likely represent the stop of rotated acceleration when the housing made contact with the table it was rotated on. Again, we see the total range of about 2.0 g, but the maximum is only 0.8 g while the minimum acceleration is –1.2 g.

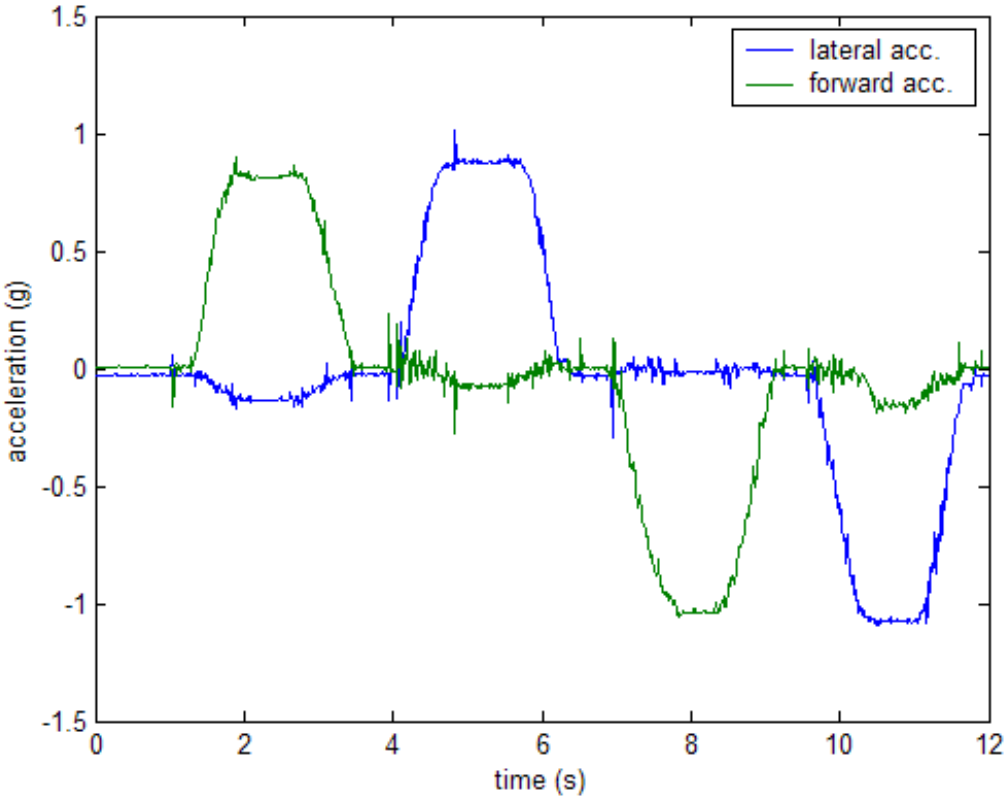

Figure 3.7.2.3. Acceleration measured during steadied device rotation (+Y, +X, -Y, -X).

Figure 3.7.3.4 shows an X-Y plot of this data. Again we see the one-dimensional nature, but there is far less noise due to the steadied nature of the device during measurement. Time is once again not shown in this plot.

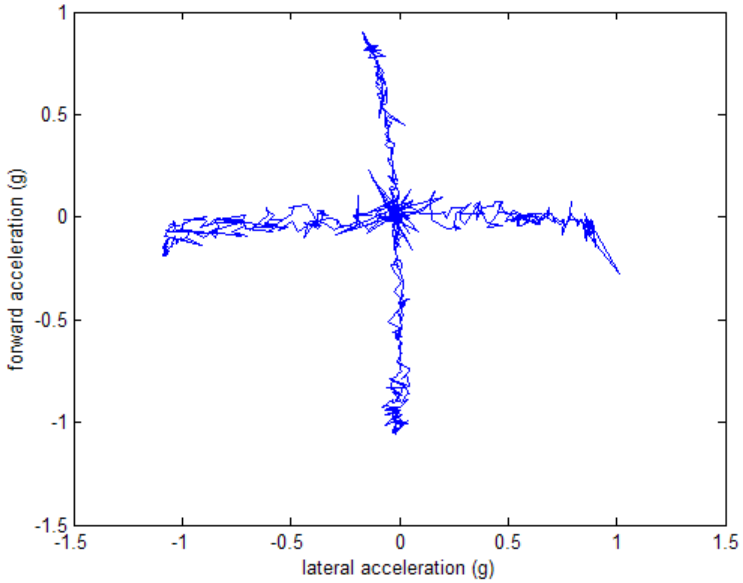

Figure 3.7.2.4. X-Y Plot of acceleration during steadied rotation test.

3.7.3 Measurement Signals from a Cross-Shaped Movement Pattern

As a test to see what data was produced during some basic shapes traced by the device, a cross was mimicked while the device was recording acceleration. During this test, the device was steadied on a flat table to which the device had been calibrated (to be explained in the next chapter). From a central point, the device (with the output wires positioned toward the experimenter) was moved a few inches to the right and then left back to the start. This was followed by similar, smooth, out and back movements, towards, to the left of, and away from the experimenter; all in succession. The total pattern traced was in the shape of a cross or addition-sign.

Figure 3.7.3.1 shows the data recorded from this test. We can see that each movement was pretty well isolated to one channel, but there was some motion in the orthogonal direction. With each motion there was a component accelerating in the direction of motion, then decelerating in that direction, and finally accelerating back again. This notion of acceleration can be difficult to grasp because it is the change in velocity. A smooth motion in one direction will experience an initial acceleration to start motion and then a negative acceleration as the velocity slows to a stop and the device turns around. At

the turning point, the acceleration will peak in the negative direction as the velocity is turned back towards the starting position of motion. Again, we will see the velocity increase in the opposing direction and the acceleration will once again become positive as the velocity in the negative direction is actually slowing. This can be thought of as accelerating in the original positive direction, or decelerating in the negative direction, where the double negative makes it a positive. This progression is viewed four times in Figure 3.7.3.1. Again, the lateral acceleration refers the Y-axis and forward acceleration refers to the X-axis.

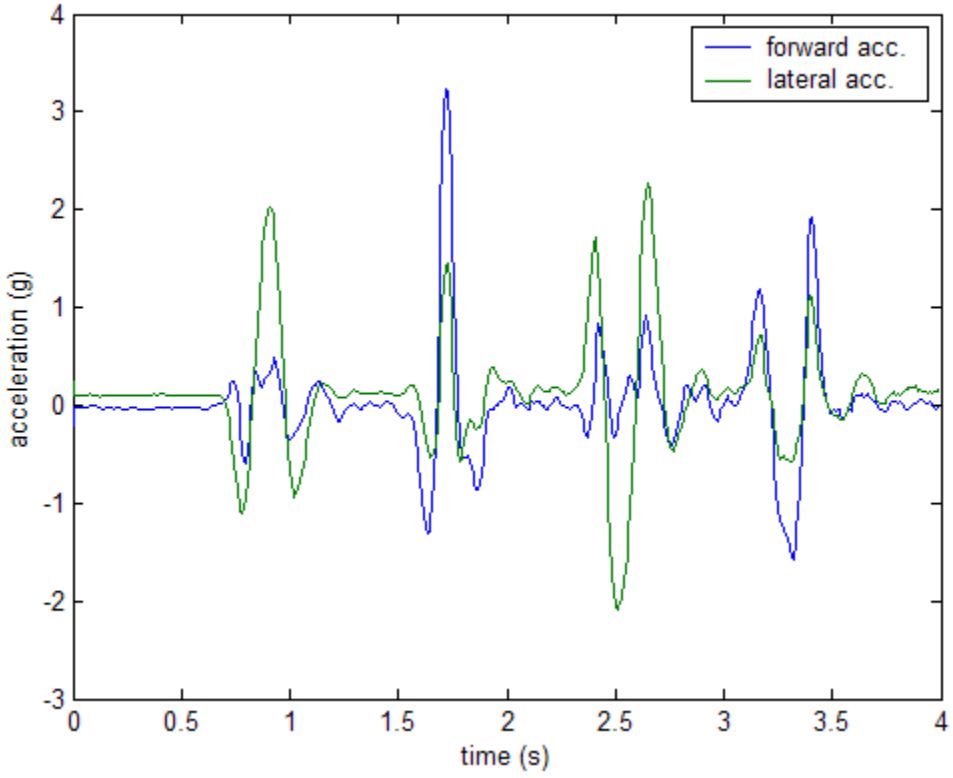

Figure 3.7.3.1. Accelerations produced during the tracing of a cross-shape.

An X-Y plot of the previous data is shown in Figure 3.7.3.2. Compared to previous X-Y plots we can see much smoother data and loops at the transitions. The data also tends to have components from both dimensions incorporated into it, as the data does not lie solely on the X- and Y-axes. Close inspection of the plot will show three loops in both the positive and negative directions of both axes. This is related to the shape produced.

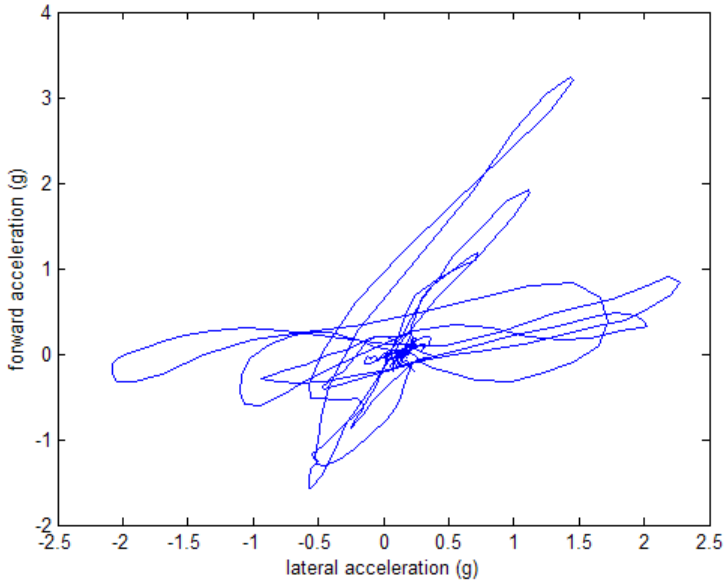

Figure 3.7.3.2. X-Y Plot of accelerations produced during the tracing of a cross-shape.

3.7.4 Measurement Signals from a Square-Shaped Movement Pattern

The second shape traced was a square. This is quite similar to the cross-shape, but each motion ended as opposed to return to the original starting point. Figure 3.7.4.1 shows the data from this test. The movement progression was made relative to the experimenter: right, forward, left, and back. Each side of the square was about three inches long. Clearly each movement only creates half the oscillations as in the out and back nature of the cross-shaped trace.

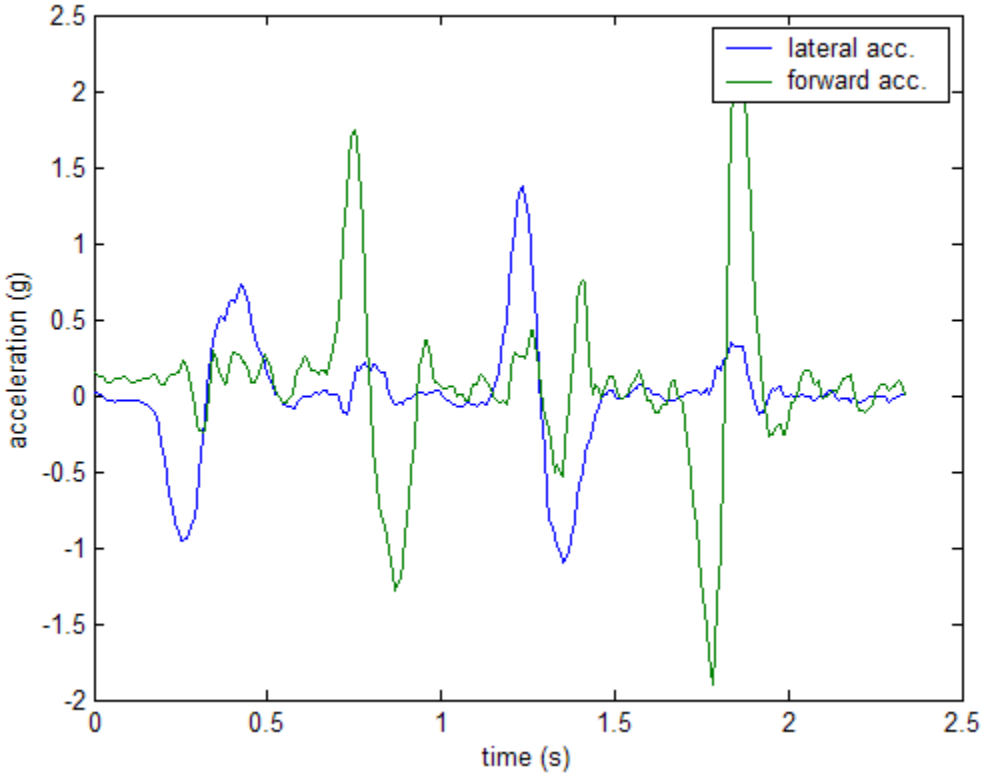

Figure 3.7.4.1. Accelerations produced during the tracing of a square.

In Figure 3.7.4.2 we can see an X-Y plot of the data from the previous experiment. Here the data still bleeds outside of a single dimension during each movement, but there is less of looped nature at each transition because the ends of the motion were more abrupt. Two loops are seen in both the positive and negative directions of the two axes because of the acceleration measured during one movement and the deceleration measured in the opposing direction.

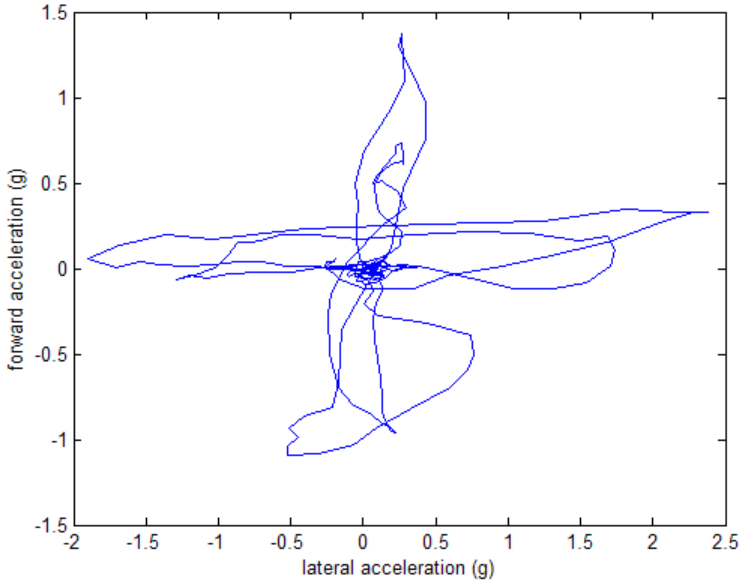

Figure 3.7.4.2. X-Y plot of accelerations produced during the tracing of a square.

3.7.5 Measurement Signals from Circular Movement Pattern

The final shape tested was that of a circle. With the device steadied in the plane of a flat table's surface, a counterclockwise (CCW) circle with a radius of about 3 inches was traced on the table. The data from this experiment is shown in Figure 3.7.5.1 and both the lateral (Y-axis) and forward (X-axis) accelerations are shown. Assuming that the circle was made at a constant angular velocity, we can expect the accelerations from the orthogonal axes of the measurement device to record sine-shaped waves that are 90 degrees out of phase. Clearly shown are two signals that are 90 degrees out of phase. Because it is a CCW circle, the positive X-axis will (forward acceleration) will lead the positive Y-axis (lateral acceleration, where left is positive). While the radial and tangential accelerations are constant during constant angular velocity, these two dimensions are not the same as the measurement axes. The result is a splitting of these two values between the measurement axes. As these measurement axes rotate, they also trade the components of the constant tangential and radial accelerations (relative to the circle traced) between the outputted signals.

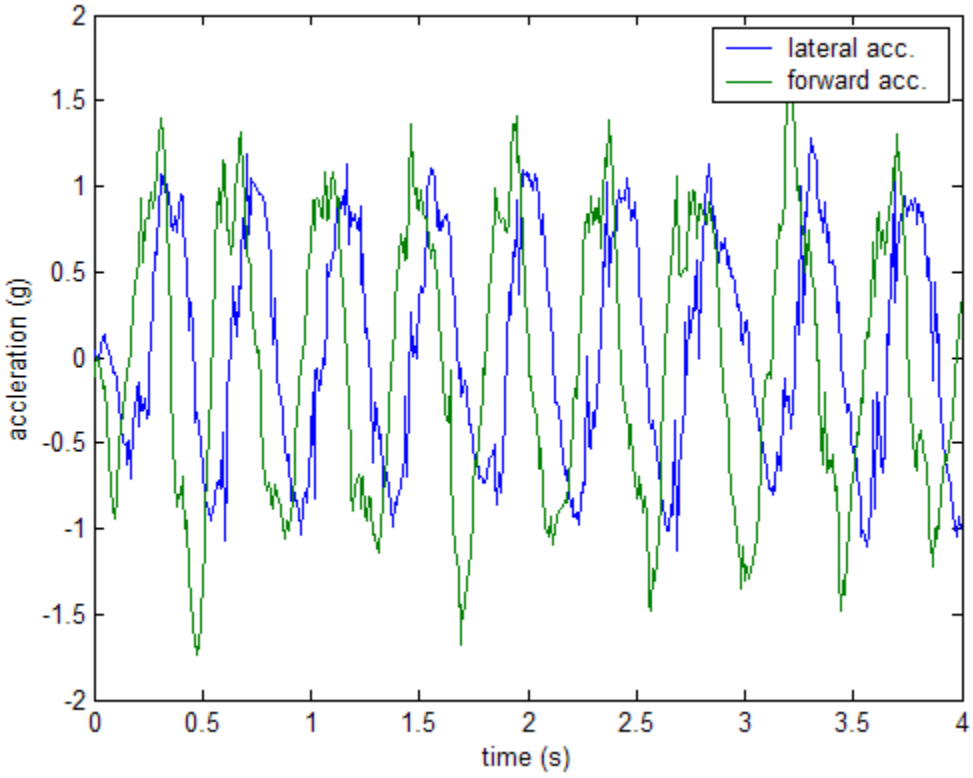

Figure 3.7.5.1. Accelerations produced during the tracing of a CCW circle.

The X-Y plot of this data shown in Figure 3.7.5.2 shows a circle as no motion is ever made solely in one plane of measurement. This ties in to the discussion presented earlier about radial and tangential accelerations. As a circle is much more difficult to hold an exact radius during tracing, there appears to be more noise in the signal, but the general shape is still held.

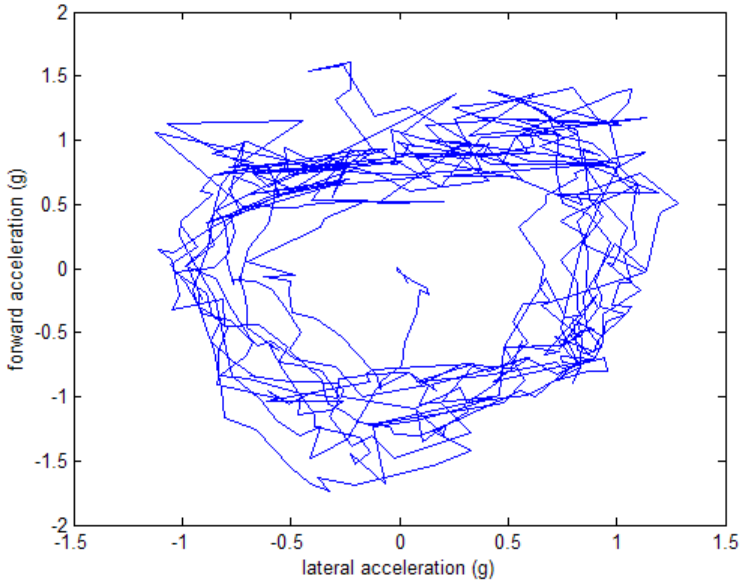

Figure 3.7.5.2. X-Y plot of accelerations produced during the tracing of a CCW circle.

Having completed a number of controlled movements of the device, where the results matched the anticipated output, significant confidence in the measured values is gained. Some of the previously presented work may prove valuable in determining characteristics of motion in future studies. The primary benefit of these tests is to gain an understanding of how the device responds to controlled inputs.

4 Development of LabVIEW Data Acquisition Code

With the acceleration measurement devices constructed, a method for storing the information they measured was needed. An important part of the sensor "system" is the data acquisition component. Among the available software/hardware platforms for reading instrument data, National Instruments' LabVIEW and data acquisition hardware were chosen. This section will outline the requirements for a data acquisition system to interface with the acceleration measurement devices and talk about the design of the code used to collect, store, and save the information.

4.1 Performance Requirements for Data Acquisition

The data acquisition system was intended to ease in testing by having as many controllable variables as possible. Making the interface and operation dynamic, the user could change the data acquisition to suit particular needs for various experiments. Additionally, a portable system was considered important, as it would be needed to conduct tests in the lab as well as other facilities. Finally, the use of currently procured devices was imperative for minimizing the cost of the research.

Having chosen National Instruments (NI) LabVIEW 6.1 as the software platform, data acquisition hardware that could easily be integrated with the software was chosen. Specifically, the NI-DAQCard-6062E was chosen as the main hardware component. This device plugs into a PCMCIA card slot in a laptop computer and easily interfaces with LabVIEW. The primary researcher for this project used their personal laptop for experiments, but any laptop should work. The specifications for this data acquisition card are shown in Table 4.1.1.

Table 4.1.1. Specifications for NI DAQCard-6062E.

Analog Inputs, single ended	16
Analog Inputs, differential	8
Resolution	12 bits
Sampling Rate	500 kS/s
Input Range	±0.05 to ±10 volts

Although this card is an older model, it offers all the required speed and resolution options needed for this research. With four channels containing two dimensions of acceleration data, the sixteen channels available for analog input were more than adequate. This even leaves room if a third channel is ever needed (per limb) or if two devices were to be used on each limb. Being that the frequency response was set to 10 Hz, a sampling rate much over 100 Hz would be considered over-sampling, so only a total of 0.8 kS/s (kilo-samples per second) is needed when 500 kS/s is available. The adjustable range up to ±10 volts is rather large since our max voltage will only be 3.6 volts, but this can be minimized in the software. Specifically, a setting of ±5.0 volts was used because a 0-5 volt option is not available in the software.

The resolution of the card is 12-bits, which is less than the industry standard of 16-bits, but is still adequate. The following equation calculates the least significant bit (LSB) value based on a 12-bit data acquisition and a total range of 10 volts (considering both sides of a ±5.0 volt range):

$$LSB = \frac{10\ volts}{2^{12}\ bits} = 0.0024 \frac{volts}{bit}$$

Knowing this, we can apply the sensitivity (S) of the accelerometer to determine the resolution of the data acquisition system when paired with the measurement device. Assuming a sensitivity of around 200 mV/g (with a power supply of 3.6 volts), the corresponding resolution (R) of acceleration is:

$$R = \frac{LSB}{S} = \frac{2.4\frac{mV}{bit}}{200\frac{mV}{g}} = 0.012\frac{g}{bit}.$$

This resolution of 0.012 g/bit is above the noise floor of 0.008 g as indicated by the data sheet for the ADXL202 [AD]. In practical terms, this means that for every one unit of gravity in acceleration measured, the data acquisition system is capable of saving it in one of 80 bits contained in that one-volt range. This should be more than adequate in that this research does not attempt to record exact values, but rather get approximate acceleration readings at the exact time they occur. In other words, the presence of a spike in acceleration in time is more important than the actual acceleration reached.

Having chosen the data acquisition card, it was important to design the physical interface between the sensors and the computer with the data acquisition card. National Instruments manufactures a product called the BNC-2120, which is a box that has eight male BNC connectors for analog input. This box then attaches to the data acquisition card via a specific cable compatible with the DAQCard-6062E. To connect each individual sensor device to the BNC-2120, cables were constructed from strain gage wire composed of four small-diameter wires (green, black, white, and red). Terminals were made that ended in female BNC connectors to connect the BNC-2120 connector block to each of the eight channels of data from the four sensor units. Figure 4.1.1 illustrates the BNC-2120 connector block with eight wire connectors attached.

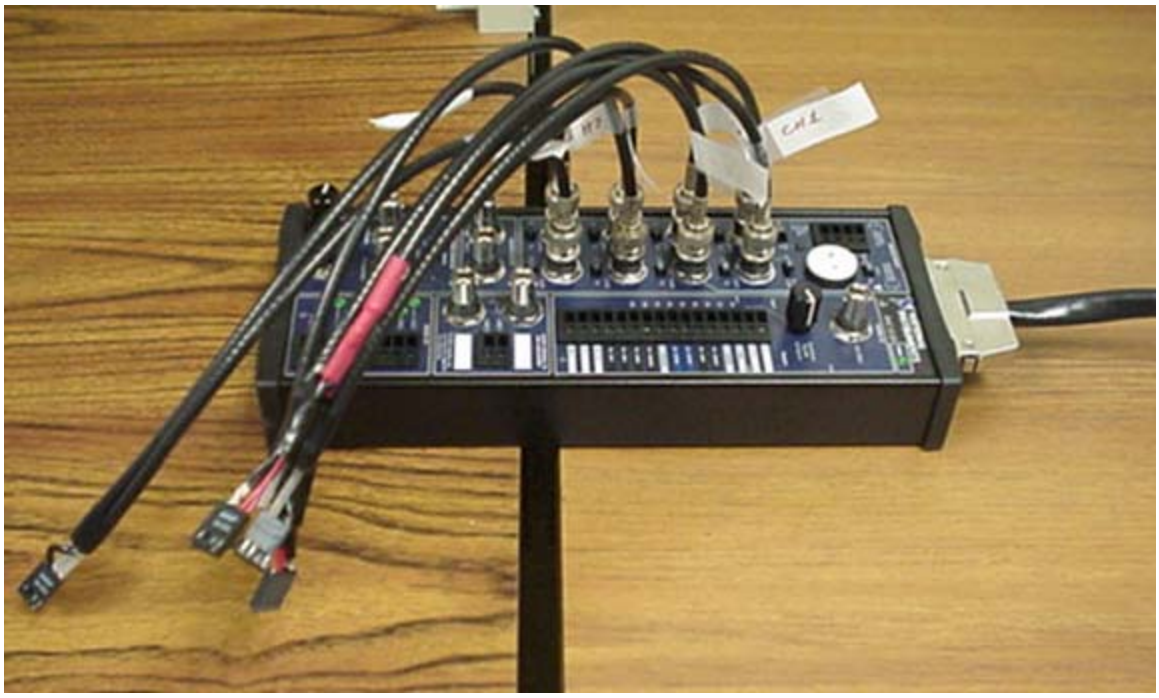

Figure 4.1.1. BNC-2120 connector block with sensor wire adapters, connected to DAQCard.

To ease connection of each individual sensor device to the connector block, long wires were used as described previously. These wires have a 4-pin male terminal on one end and a 4-pin female terminal on the other. Each wire measures approximately 6 feet in length. The female end is intended to mate with the male terminals on each sensor device and the male end of the wire is to connect into the BNC adapters shown in Figure 4.1.1. Figure 4.1.2 show both ends for one wire. As previously mention in describing the pin-outs on the acceleration measurement device circuitry, two adjacent pins transmit the output voltages from the accelerometer and a third separate pin transmits the common ground of the device. The convention of using the outside pin (X_{out}) of the output pair with the green wire on the strain gage wire was kept consistent with all wires produced. The black wire was therefore used to carry the Y_{out} signal and the red wire had the common ground signal.

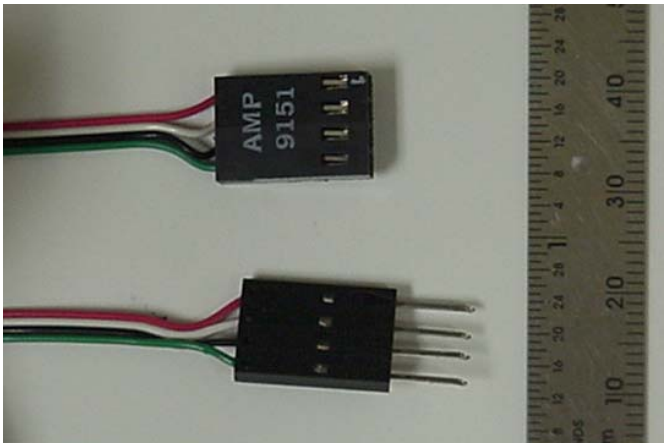

Figure 4.1.2. Wire ends used for connecting signal transmission wire to BNC-2120.

4.2 Front Panel Design and Operator Interface Description

With the eight channels of acceleration data from the four sensor devices connected to the data acquisition card, the next task is to write data acquisition code to set up the recording specifications, save the data, and display the information graphically. Additionally, the code must easily interface with the operator. This section will outline the design of this operator interface. Being that National Instruments' LabVIEW code is written graphically, the programmer typically places all input and output components of the code on what is called the Front Panel. After supplying all the desired interfaces on this screen, the programmer goes to the block diagram, which is where graphical components are wired together, to make the interface work properly.

The following discussion will relate the Figure 4.2.1, where the front panel for this data file is shown. The first component of the front panel is the calibration of the devices. We see a large button labeled "Calibrate," which is to be pressed when all four sensors are placed on flat, steady surface. The next section will describe the reasoning and coding behind this. After calibrating the devices, the sample rate in Hz and sample time in seconds must be input. This determines the size of the file. The last main input buttons on the front panel are "Acquire," "SAVE," and "STOP." Their purposes are self-explanatory.

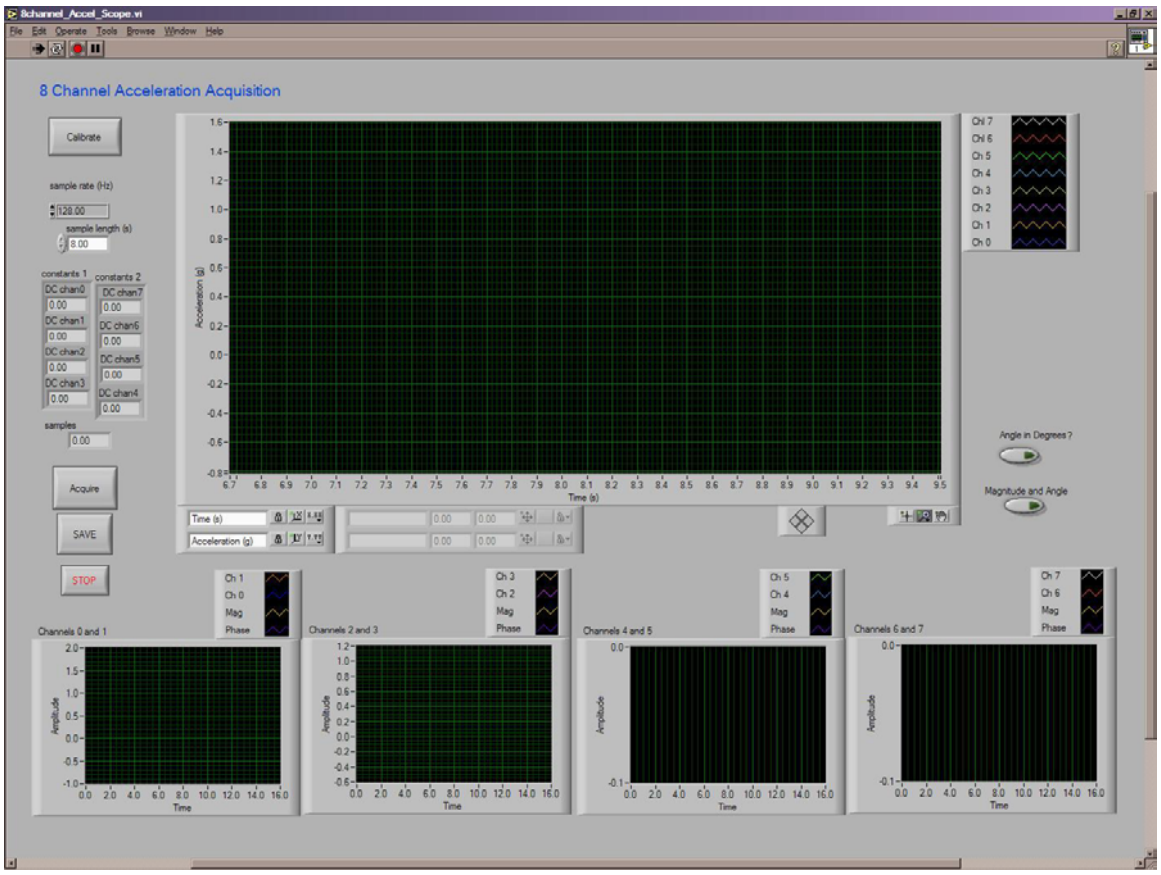

Figure 4.2.1. Front panel of LabVIEW data acquisition software for 8 channels of data.

Having inputted the necessary data for the DAQCard to acquire the information at the given speeds and for the given time, the operator must push "Acquire" and wait for the data to be recorded. Once all the data is in the software, five plots have been placed to show the information. One large plot is a graph of all eight channels of data, which is programmed differently than a chart in LabVIEW. Each of the remaining four graphs represent two channels of data from a single sensor. Colors on the main graph correspond to those in the dual-channel plots. Options exist on the right side of the main graph to also plot the absolute magnitude and angle of application (in degrees or radians) on each of the individual dual-plots.

Once a set of data is recorded that the operator wishes to save, the operator can use the "SAVE" button. A prompt to enter a filename will appear and the data is then saved. The remaining button labeled "STOP" is used to stop the program from running. Once this is pressed, any data remaining on the screen can no longer be saved. Overall, the look and

operation of the front panel for this program are relatively simple to ensure uncomplicated operation.

4.3 Block Diagram Design and Functionality Description

This section will outline the code used to connect the components on the front panel and process data recorded by the DAQCard. If you are unfamiliar with graphical programming, the code is all done with pictures and data travels along lines of different color, depending on the type of data (integer, decimal, string, etc.). Thicker lines indicate arrays and while code was written to operate left to right, the computer executes an operation as soon as all variables needed have been supplied. Smaller pieces of codes called Sub-VIs (VI meaning Virtual Instrument) are integrated into the code. Some Sub-VIs are supplied with the program and the programmer wrote others.

A sequence structure was used in programming the code and each of the four slides for the sequence will be discussed. The four components of the sequence conduct the following operations: calibrate the devices, record data and create a large graph of all accelerations, break up the data into component channels and plot on dual-plots, and finally save the data to a spreadsheet file.

4.3.1 Sequence Code Component for Calibrating Measurement Devices

The first step in the sequence of code written in LabVIEW (labeled 0 by LabVIEW) looks for the button "Calibrate" to be pressed and can be found in Figure 4.3.1.1. Upon selection of this option, the data acquisition system queries all eight channels for one second at 1000 samples/second. During this sampling, the devices are to be placed flat on a stable surface. The sampled data is then run through a Sub-VI called "Calc 4 Mean" that calculates the mean of four inputted data arrays. Two of these Sub-VIs are used on each half of the collected data. This information is then stored in two universal variables called "constants 1" and "constants 2." Calibration will occur when these mean values during static readings are compared to future readings. This calibration assumes that the surface used is parallel

with the surface of the earth and that the mean value represents the zero acceleration reading on all channels. In the event that there are any slight misalignments in the mounting of the accelerometer within the housing, this calibration will negate those affects on the final acceleration value.

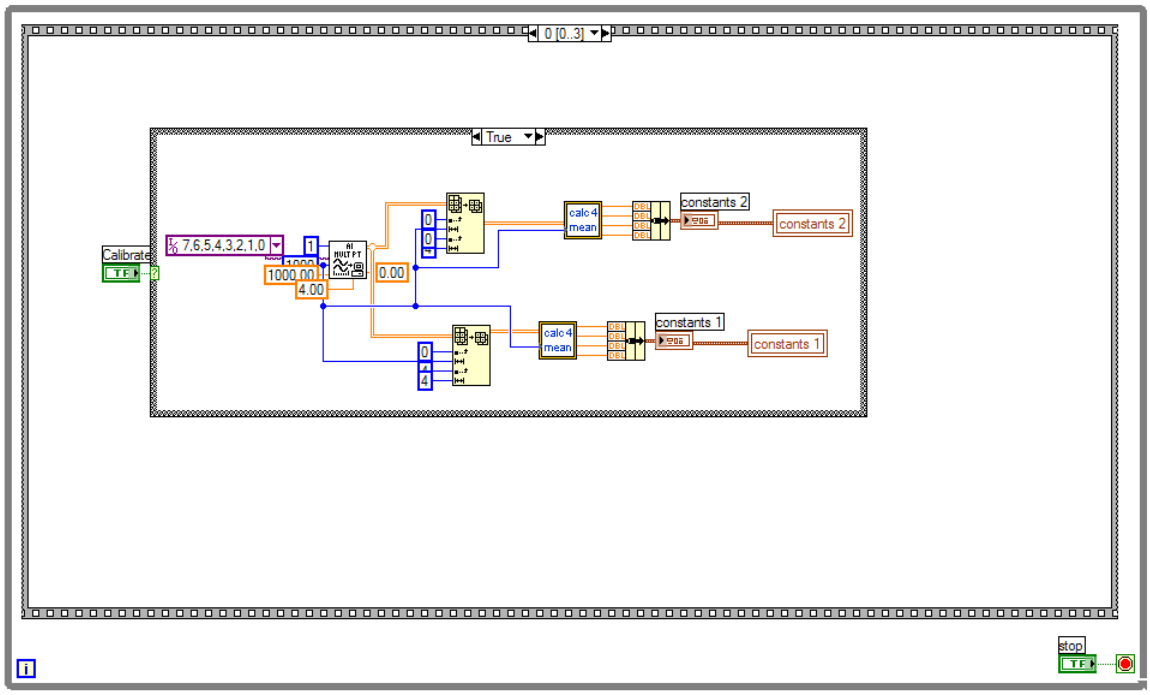

Figure 4.3.1.1. First component of sequence code to calibrate devices.

4.3.2 Sequence Code Component for Acquiring Measurement Device Data

When the "Acquire" button is pushed, the second part of the sequence (numbered 1 by LabVIEW) is activated. This takes the preset data acquisition specifications such as sample rate and time and records channels 0-7 for the time specified on the Front Panel. At the conclusion of this sampling, the data is sent to the calibration Sub-VI code (called "Cal") where the mean values stored in "constants 1" and "constants 2" are utilized in the formulas presented in the discussion of the operation of the ADXL202 earlier in this paper. The results of this calibration are output to an array, where all eight channels are plotted on the main graph of the front panel. This code is shown in Figure 4.3.2.1.

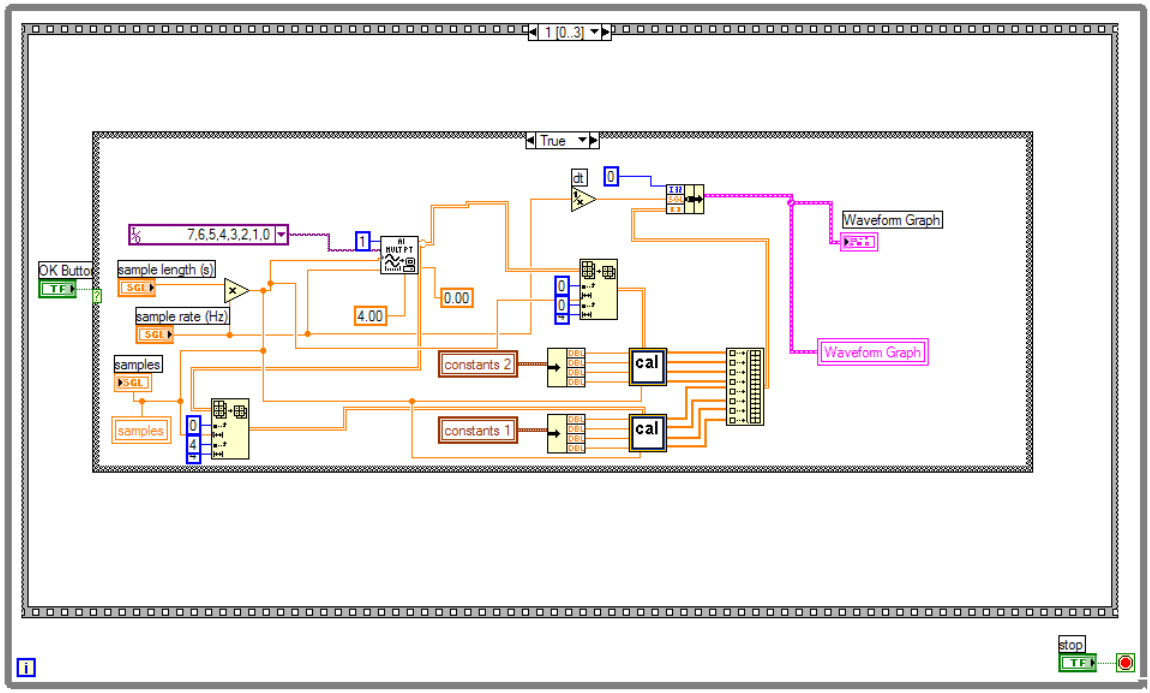

Figure 4.3.2.1. Second component of sequence code to process and plot the data on one graph.

4.3.3 Sequence Code Component for Graphing Dual-Channel Device Data

The third component of the data acquisition sequence (labeled 2 by LabVIEW) is used to separate the individual data arrays from each of the eight channels and plot graphs from each device. The code for this process is shown in Figure 4.3.3.1. In this code, the operator is presented with the option of graphing the data with the total magnitude and angle between acceleration vectors. This option was not necessary for preliminary testing, but may be of interest in future analyses. The operator is also given the option to plot the angle between in radians (from π to $-\pi$) or degrees (from 180° to – 180°). All four data series (two acceleration signals, total magnitude, angle between vectors) are plotted on one of four graphs, one for each limb.

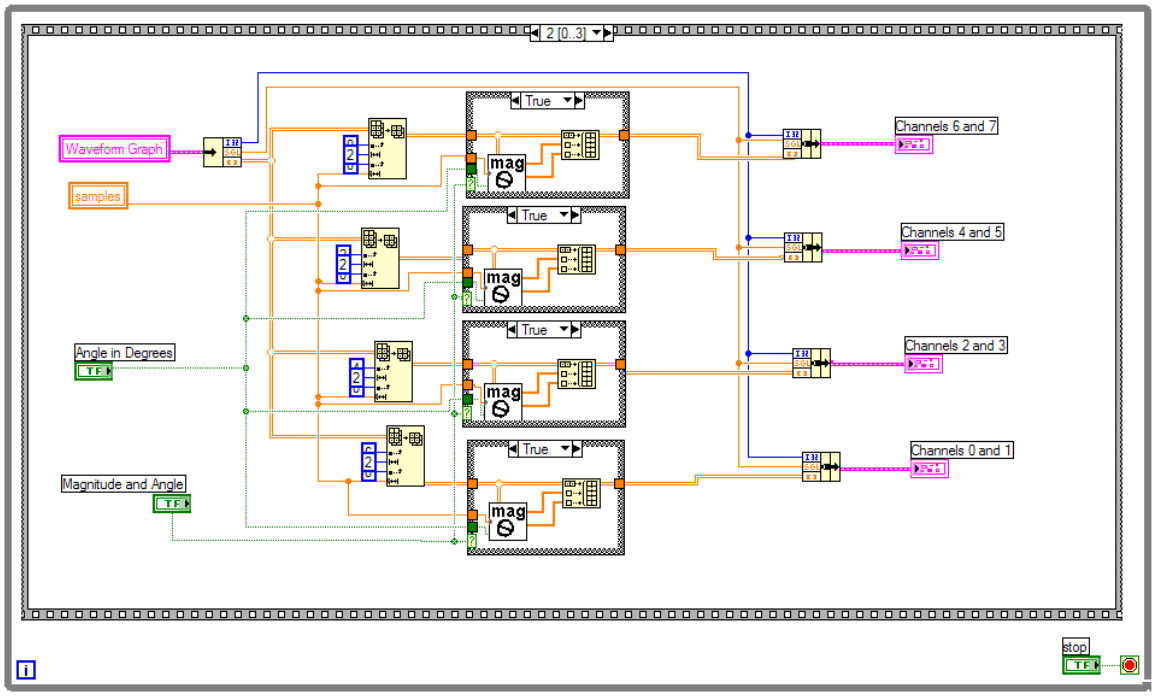

Figure 4.3.3.1. Third component of sequence code to plot dual-channel graphs with magnitude.

This code takes the entire eight-column data set of waveform information from the data acquisition Sub-VI and breaks it into the component pairs of data arrays from each limb. Within each individual pair, a magnitude and phase are calculated over the entire series using the Sub-VI "mag Θ." As previously mentioned, the options of angle units and presence of the additional plots on the graphs are passed from the user inputs. Finally, the output from the magnitude and angle Sub-VI are passed into a cluster of data sent to each individual graph shown on the front panel. On the front panel, each data series' color was matched between the main plot of all eight channels and the dual-channel plots for each limb to ease confusion for the operator. There is no specific designation for each channel to determine which limb the data comes from; this must be determined by the experimenter and noted during testing for future analyses.

4.3.4 Sequence Code Component for Saving Device Data as a Spreadsheet

The final section of the sequence code is used to save the data from all eight channels to a spreadsheet file. Figure 4.3.4.1 illustrates the code for this part of the VI. This loop is activated by a "true" signal passed from the "SAVE" button. When activated, the waveform graph data, containing all eight original acceleration arrays, is transposed and a time array is created corresponding to the individual times that all data points were recorded. This time array is then merged back with the original eight arrays and saved as a text file (*.txt) and the user is prompted for a filename. The result contains nine columns of data, each the same length. This format eases the transition into Matlab and Microsoft Excel for future analyses.

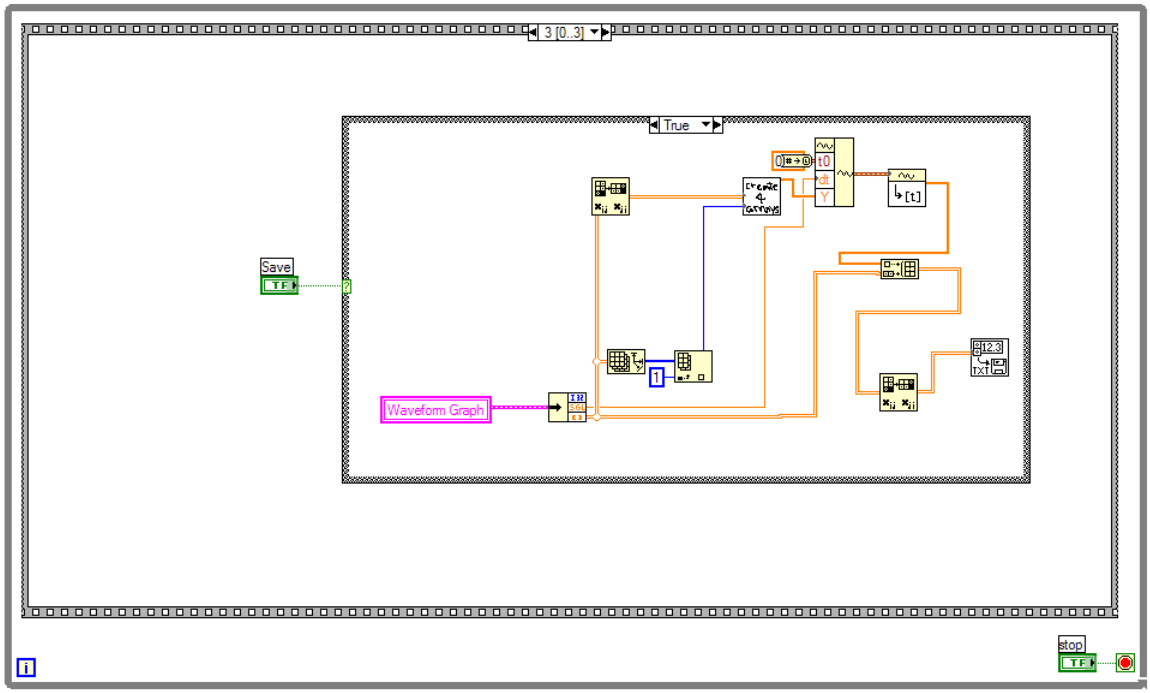

Figure 4.3.4.1. Fourth component of sequence code to save the data as a spreadsheet File.

5 Acquisition of Acceleration Data From Infants

This section will outline how testing was performed, using the acceleration measurement devices, data acquisition software and hardware, and test subjects. A brief discussion of the verification of the measurement device data will be followed by an outline of the Institutional Review Board approval procedure for testing on human subjects. The preparation of the testing lab and equipment will be discussed and then the ideal state for infants during testing will be outlined. A procedure for operating the test equipment and working with test subjects will conclude this section, before an outline of test subject personal information is described.

5.1 Verification of Measurement Device Accuracy and Precision

The design and prototyping have now been discussed, in addition to an explanation of the data acquisition procedure using the LabVIEW code and National Instruments hardware. Before any of the instruments are used, the experimenter must feel confident that the recorded values are truly the accelerations seen by the measurement devices. This section will discuss the procedure and results of some tests done to compare uniformity and accuracy of the acceleration measurement devices when coordinated with the data acquisition system.

5.1.1 Verification of Measurement Device Accuracy Using Integration

While the process of calibrating the devices to eliminate affects of misalignment of the accelerometer chip has been discussed in previous chapters, the values reported from the data acquisition system after the acceleration signals have been processed must be verified. In our lab we don't have any equipment that can produce known dynamic accelerations. Future tests could be done to test the accelerometers alongside a three-dimensional motion

analysis system such as a Vicon. The procedure determined for verifying accurate acceleration measurements was to record accelerations over a known displacement. Using the mathematical technique of integration, the acceleration signal was integrated two times to produce the position data in time, relative to zero-value initial conditions.

The actual test was completed on a smooth, flat surface, to which that the device had been calibrated. From an initial starting position, the device was moved 9 inches in a smooth motion along one of the two measurement axes. The experimenter attempted to complete the motion with only an initial acceleration and an final deceleration. After a few test runs, data was recorded for the motion over a period of about 2 seconds. From this data, the non-zero acceleration data around the movement was spliced from the entire data file in Matlab. The yellow line in Figure 5.1.1.1 shows a plot of this data. Inspection of the acceleration data shows that the acceleration peaked at around 3 units of gravity (g) and dropped to around –2.5 units of gravity before stopping.

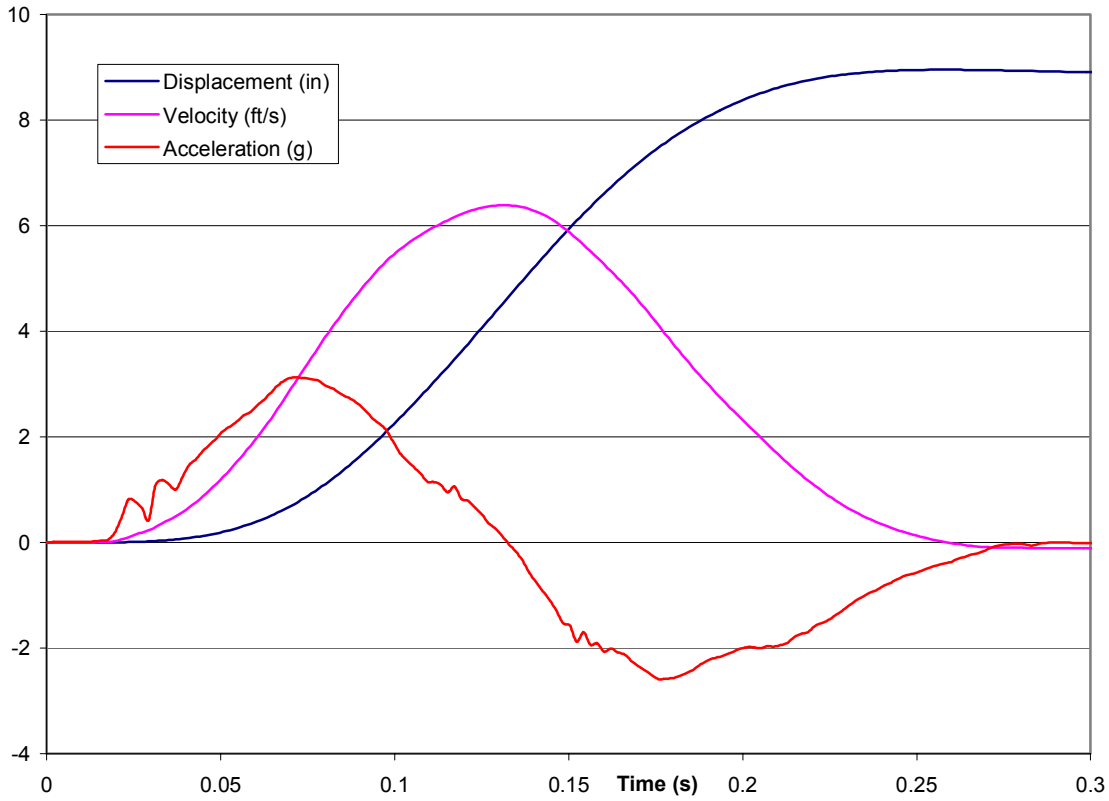

Figure 5.1.1.1. Verification of acceleration measurement accuracy with a known displacement.

Using the technique of integration, the acceleration data was used to create the velocity profile shown in magenta in Figure 5.1.1.1. As would be expected, the velocity starts at zero (as assumed), peaks, and returns to zero. The fact that this integration produced a velocity of zero feet per second after the 0.25 seconds of motion is a positive sign that the instrument is producing accurate data.

To further verify the results, integration was performed on the velocity data to find the position along the line in time. The result is a position plot, shown by the blue line in Figure 5.1.1.1. Clearly, the final position is shown at about 9 inches, so the experimenter can have some confidence in the data produced and processed by the measurement devices and the processing equipment (data acquisition software and hardware).

It is important to understand that this type of linear, one-dimensional motion over a mere 0.25 seconds is much more simplistic than actual three-dimensional motions an infant will make. The point here is to gain confidence in the results that are produced in a controlled setting. As previously discussed, this research does not attempt to collect such accurate three-dimensional data that position of all limbs of an infant could be reproduced in time. The primary objective of such data recording systems is to monitor and record relative peaks in motion that occur. The relative magnitudes and frequencies are of primary interest in this research.

5.1.2 Comparison of Precision Between Different Measurement Devices

The second step in verifying instrument performance was to inspect the precision between two devices. A simple test was conducted where two devices were calibrated to the same surface and then taped together on top each other. Their measurement axes were aligned as closely as possible, but some uncertainty surely exists in that alignment.

While connected, data was recorded as the two devices were physically moved in all directions and rotated in and out of earth's gravitational axis. Plots from both axes of both accelerometers are shown in Figures 5.1.2.1 and 5.1.2.2 over the four seconds of recorded data. In Figure 5.1.2.1 the lateral (Y-axis) direction accelerations are shown for both accelerometer 1 and 2 after being mean-zeroed. A red line is also plotted to indicate the

difference in reading between the two mean-zeroed signals.

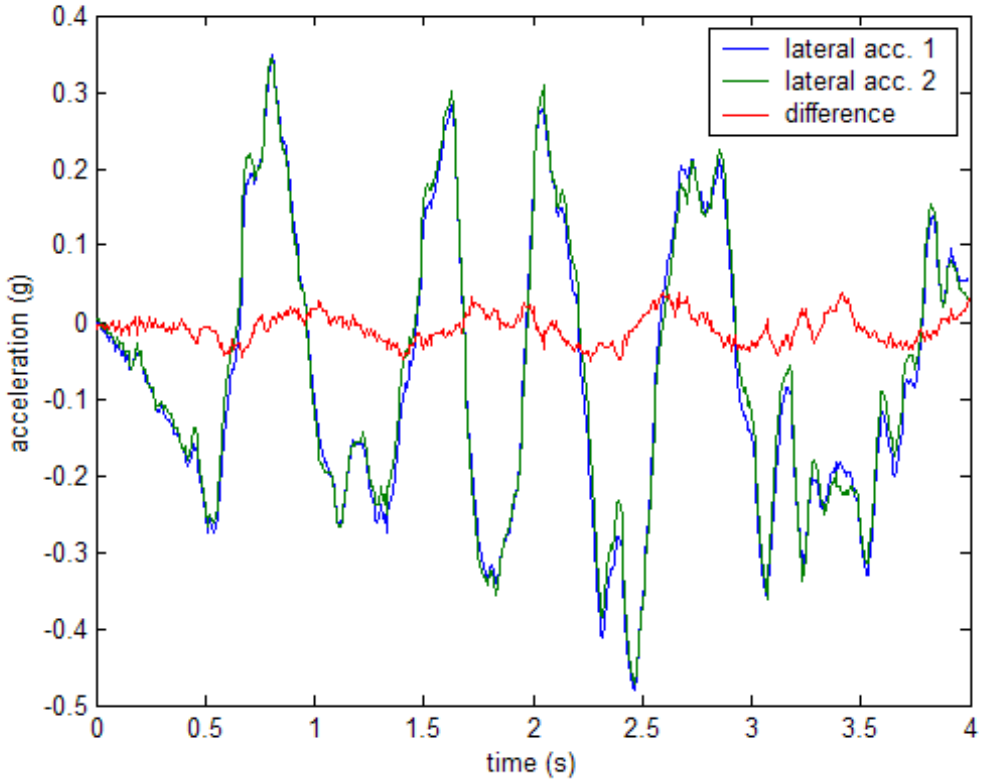

Figure 5.1.2.1. Lateral accelerations and difference measured by connected accelerometers.

Figure 5.1.2.2 shows the same type of plot, but rather for the forward (X-axis) direction, relative to the experimenter. This data has also been mean-zeroed and the red line shows difference between the two signals. Inspection of this plot indicates that the higher points of difference occur when accelerations of larger magnitude were produced. Other versions of these plots were produced comparing the magnitudes recorded by the two devices, in the event that the individual axes were slightly offline, but no difference was seen.

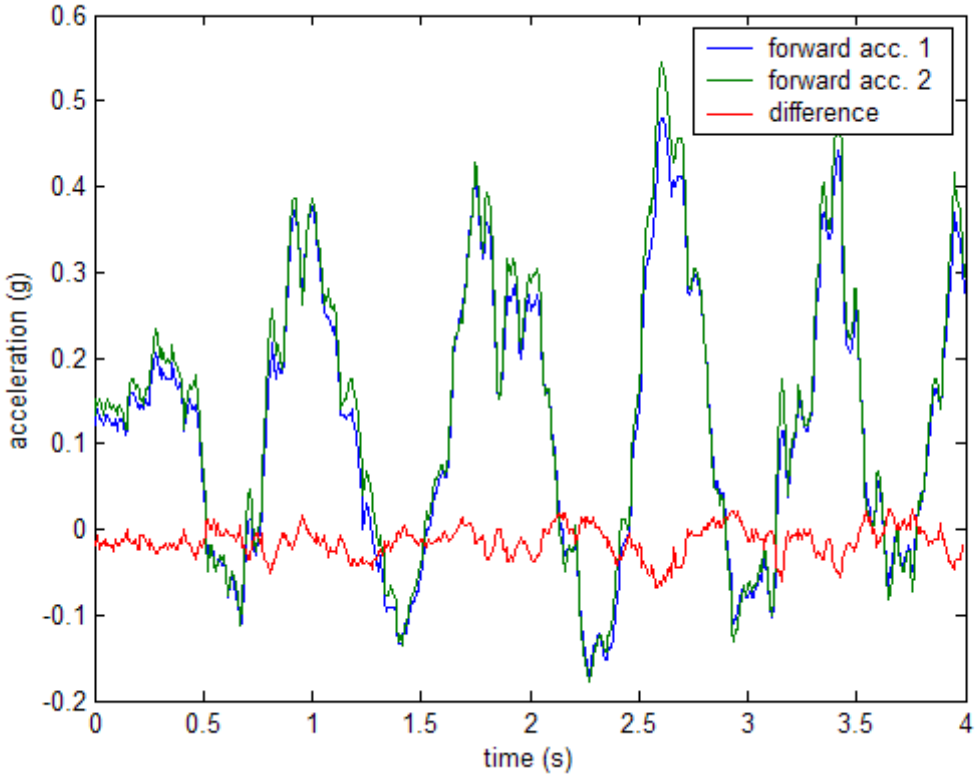

Figure 5.1.2.2. Forward accelerations and difference measured by connected accelerometers.

A final plot was produced comparing the two calculated differences. Figure 5.1.2.3 shows the difference between the recorded accelerations made in the same directions by the two difference devices. The units are a percent difference between them. Inspection illustrates that the maximum absolute difference between the two signals is just over 10 percent. Again, these maximum points appear to occur at high acceleration measurements. As discussed previously, the accuracy at such high points is not as important in this research, but rather a confidence that the device is measuring a relative value at the appropriate time. Visual inspection of Figures 5.1.2.1 and 5.1.2.2 prove that the peak acceleration measurements are recorded simultaneously.

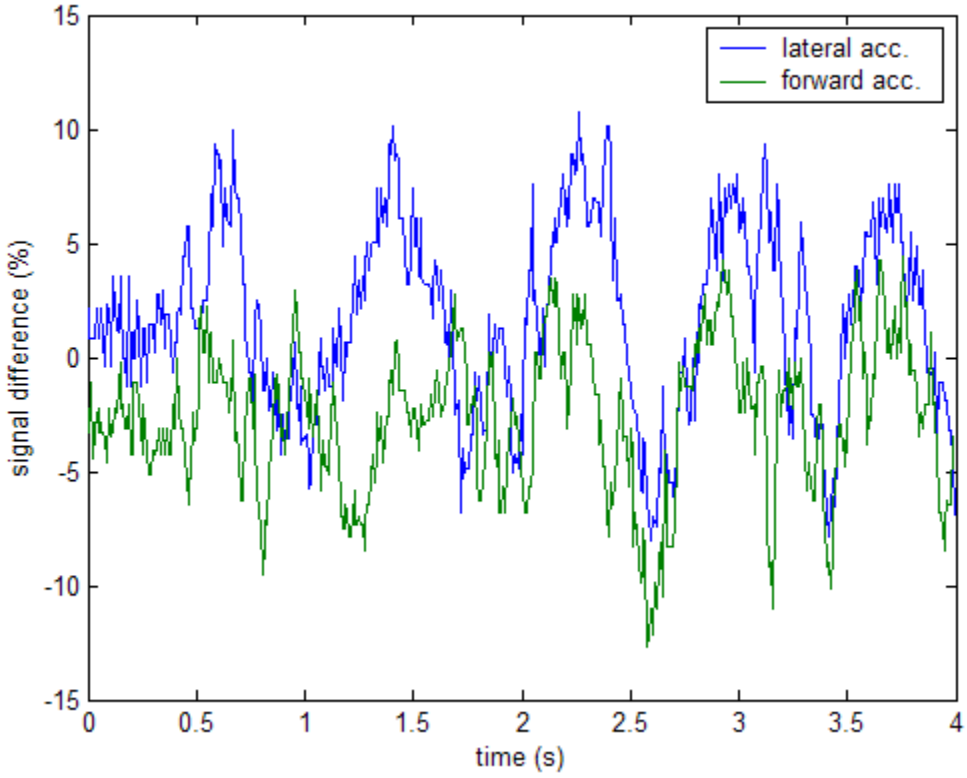

Figure 5.1.2.3. Percent difference measured between connected accelerometers.

Having completed this comparison between signals from the exact same motion, we can feel confident in the ability of different sensors to produce comparable results. There appears to be a maximum error around 10 percent, but as indicated, this is an acceptable error for the purposes of the experiments conducted in this research. Additionally, acceleration data has been used to integrate out the position in time of a measurement device with little error during a controlled test. Confidence is once again built, but full validation of these devices must be completed with a more sophisticated and precise instrument such as a Vicon three-dimensional motion recorder.

5.2 Institutional Review Board Approval for Tests on Human Subjects

Before any testing on human subjects could be conducted on campus, a review by the Institutional Review Board (IRB) was to be completed. Due to the shared test subject

population of 1-3 month old infants, IRB efforts were coordinated with the Infant Perception Lab (IPL) in the Psychology Department at Virginia Tech.

A full IRB approval had already been granted to the IPL for testing on infant human subjects in their lab using skin-mounted electrodes to monitor heart rate. An expedited addition was made to this approval to include the possibility of the test subjects' guardians opting to include their children in these motion studies. Appendix A includes the IRB approval application submitted and approved for this research. Included in this application are test procedures, research intents, and subject surveys and agreements.

5.3 Testing Set-up in Infant Perception Lab

In securing IRB approval and a test subject population, it was important to prove to the guardians of potential human subjects that their infants would not be placed at risk. The test set-up for recording infant GMs with video and the accelerometer devices was designed to minimize the distractions on the infant. As discussed earlier, for true GMs to occur, the infant must be in a relaxed state and not reacting to any outside stimulus, only moving spontaneously. Fostering this state is paramount in recording true GMs with both the video and the acceleration devices.

As for placement of the infant test subject relative to any computer equipment and other stimuli, they were placed outside the view of the infant. Figure 5.3.1 illustrates a mock set-up of the computer relative to a model infant in the Modal Analysis Laboratory. Here we see that the infant is in a supine position with all the computer equipment located above their head. Notice that the computer is about 4 feet above the infant and all wires connecting the accelerometer devices on the infant to the data acquisition system are run perpendicular to the test subject. Enough slack was left in the wires to allow for free motion of the limbs during testing. After running out from the infant, these wires do come back and connect to the data acquisition system.

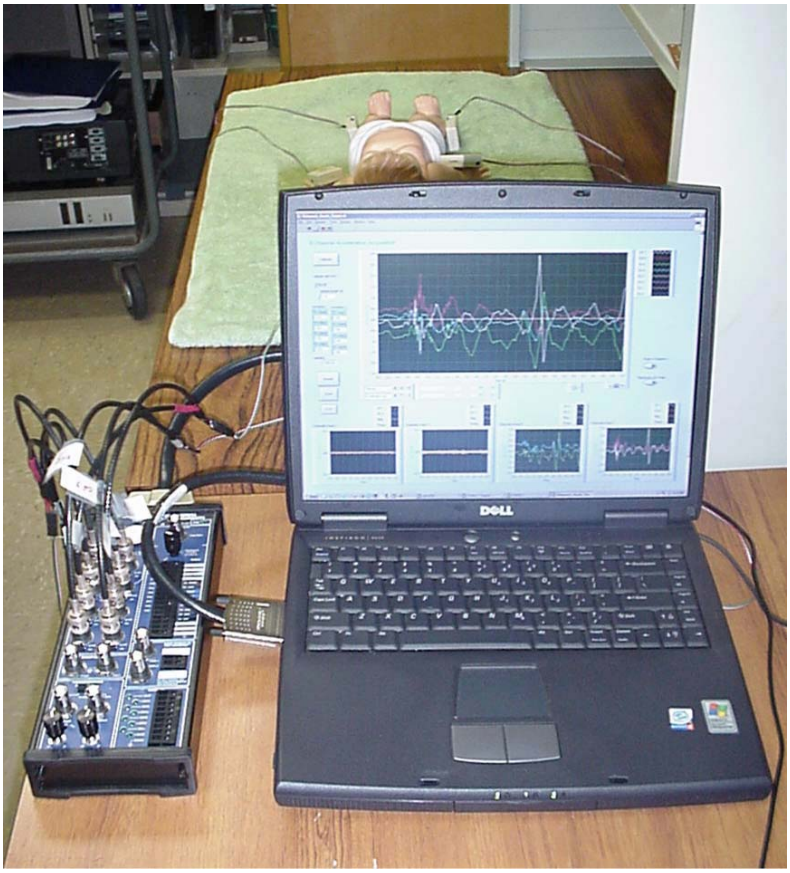

Figure 5.3.1. Mock set-up in Modal Analysis Lab of testing equipment relative to test subject.

Figure 5.3.1 is taken on a table in the Modal Analysis Lab, but in testing conducted in the IPL, testing is to be conducted on a railed table, such as a crib, or on a padded mat on the floor. These precautions are taken to ensure that the infant is not at risk of falling from an elevated position.

Other factors affecting the design of the set-up are external light and noise. It is important that no direct light might be affecting the infant. Examples are sunlight or bright lamps. In addition, external noises that could interrupt the relaxed state of the infant or cause reaction, such as a mother's voice, are considered to be disruptive to GMs. Toys and other objects placed within the reach and field of view of the infant are also not conducive for this testing. It should be noted that infants of this age (1-3 months) have a limited depth perception and cannot make out objects and shapes more than a few yards from them, so the surroundings do not need to be bare.

In preparing the area where the infant is to be tested, it is important that motion not

be constrained. Figure 5.3.2 shows the set-up from the first set of testing with Infant 1. Data from this test has not been presented in this paper due to the obviously constrained nature of the crib he is in. This was a poor set-up and future layouts were done differently, using padded mats on the floor.

Figure 5.3.2. Improper constrained placement of test subject in too small an area.

Finally, the set-up for this testing requires the use of a video camera to record the infant's motions. This camera should also be placed outside of the infant's field of view and placed on a tripod to ensure stable recording. As seen in previous work recoding infant movement, elaborate mirror systems are used to collect multiple angle views of the test subject during experiments. For this research, such involved measures were not taken. Specifically, this work is only to verify that GMs are present and not to diagnose the infants as they most likely from a healthy population. As will be discussed later in this paper, video is solely used to show the motion viewed during recording of acceleration signals. The video is to verify specific patterns characteristic of GMs and to compare with signals during analysis, just for verification purposes.

5.4 Ideal Infant State During Testing

To maximize the comfort of infants and increase the likelihood of motion considered GMs, infants must be a relaxed state during testing. Care must be taken to understand the infant is an individual and the parent becomes a valuable assistant in scheduling an ideal time to test the infant. Many factors must be accounted for relating to personal schedule for eating and sleeping. Tremendous variability exists between infants; therefore the parents are the key to designing an ideal infant state for testing.

It is recommended that an infant should have recently eaten and have taken a nap within the past couple hours. An infant who has not been fed is often cranky and more likely to dwell on their hunger and not relax enough. Recent feeding may also induce a state of sleepiness where the infant may not remain awake enough to move spontaneously, as they are on the verge of falling asleep.

With respect to sleep, infants having just awoken are also often times very cranky due to this change in state. After 30 minutes or so, infants typically calm down and are in a more awake, alert, and calm mode. In some cases, they are accustomed to eating after waking up and this eating may help to calm the infant. If the child has been awake for multiple hours, it is likely that they will begin to get tired and want to fall asleep. For the previously presented reasons, the window about an hour after awaking from a nap and having eaten is ideal to prepare the infant for a calm state to produce GMs.

Another key, already discussed, is the placement of the infant. Whether in a crib or on a padded mat, the infant must be comfortable in a supine position. With limited sensory stimuli, the infant will have four devices attached to their limbs; one per. As shown in Figure 5.4.1, a toy baby (not to scale) has been positioned with the accelerometers in the correct positions with the correct orientation. Note that this picture is of a toy and the eyes of an infant should not be closed as in the picture. This toy measures about 17 inches and is not proportional, while a typical 1-2 month infant will measure about 20-23 inches in length. The ankle accelerometers are oriented to measure the kicking up and out, but not side to side. Wrist accelerometers do not capture accelerations in the plane perpendicular to the back of the hand. From observation, the reaching of hands over the head and sideways kicks were limited in exercise compared to the other two dimensions on each limb.

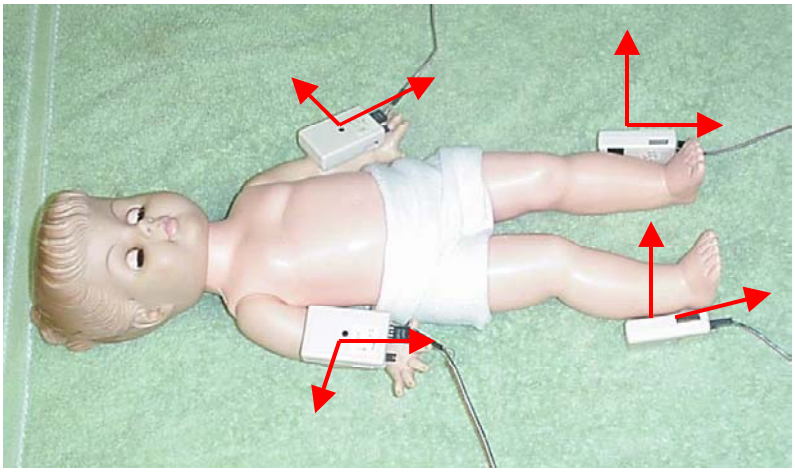

Figure 5.4.1. Model infant with ideal placement of acceleration measurement devices on all limbs.

The figure illustrates a model infant in just a diaper. At the discretion of the parents, any set of clothing that is not restrictive to the infant can be used. In the event that the laboratory is chilly, a jumper is fine. While an infant in just a diaper allows viewing of more skin and muscle tone, the accelerometers are unaffected by the clothing. This assumes that the clothing is not distracting the infant or interfering with the placement and secure attachment of the devices. The relative placement of wires and data acquisition equipment is discussed in a previous section of this chapter.

5.5 Procedure for Acquiring Data in Lab

Once a test subject has been brought to the lab for testing, a brief procedure was followed to prepare the subject and equipment for a test. It is important that all preparations on equipment have already been conducted so that the time an infant stays in a test-ready position is minimized. Additionally, working on devices around the infant may cause them to become uncomfortable because of unknown movements and noises.

To prepare the equipment, the placement of the data acquisition system should be done as described earlier, at the head of the infant's location, a few feet back. Also behind the infant and off to one side, the tripod-mounted video camera should be positioned with a zoom on the infant's position. All measurement devices should be connected to the data acquisition system and new Velcro® bands should be attached. These can be laid out in the

various positions prior to the placement of the infant. The convention of positioning the numbered channels in a clockwise manner around the infant, starting with their left arm, was used. Analysis codes were later programmed to factor this arrangement into the labeling of plots, but this variable should be noted for all experiments.

Calibration of the devices should be conducted well before the infant is to be tested. Prior to this calibration, all jumper terminals on the devices should be independently connected, so that all devices are active. The battery will lose some of its voltage output in the first few minutes after connection, but this will level out after about five minutes. After this waiting period, the calibration can be performed as described in the discussion of the LabVIEW code. All devices should be placed flat with their measurement axes parallel to earth's surface, such that approximate readings of zero units of gravity are measured.

With all the devices turned on and calibrated, the infant can be placed in position for testing. Their state should be previously determined to be adequate for entering a state of spontaneous movements, as described earlier in this chapter. As the infant adjusts to the position, all the acceleration devices should be attached to the proper limb using the Velcro® straps. Testing has found that special light-adhesive tape for skin can be used to further secure the devices to the limbs. Secure attachment ensures minimal additional measured content due to motion of the device on the limb. Any vibration of the device on the limb will appear as noise in the acceleration signal and will mask the important signal from the direct motions of the limbs.

A few moments can be given to the infant after all the devices have been attached. In testing, the infants barely noticed the presence of the devices and were in no way upset by them. Brief contact with the mother may also help to calm and relax the infant. Once this state is reached, the video camera and data acquisition equipment can be activated. The size of data files stored should be manageable. During initial testing, total lengths between 1 and 2 minutes were used. Sample rates of 128 samples per second were chosen because 128 is a power of 2 and would accelerate some types of signal processing. Because this testing is only preliminary with prototypes, these decisions do not have a large impact on the final results.

As files are recorded, it is important to link the start of recording between the data acquisition and the video. For initial testing, finger counts were done in the cameras field of

view as the acceleration data was set to acquire. Future studies would benefit from linking the two technologies to allow synchronized recording with both methods.

During testing, it is important to keep the infant undistracted and in a spontaneous state. As will be discussed in the results of this research, some motion studies conducted required the use of pacifiers and human interaction to calm down the infants, both suppressing GMs. This was not an ideal situation, but to encourage the infant to remain in calm state to enter states of GM motions between interruptions, it was necessary. Again, large-scale surveys of infants in broad experiments cannot allow this interaction, but it was determined to be necessary to get the movement information for this preliminary study.

Finally, when a set of data has been recorded, the information should be saved by the data acquisition code. This is done by hitting the "Save" button, where the user will be prompted to enter a filename. These filenames should reflect the test iteration to ease understanding of the data files during analysis.

At the conclusion of all testing, the measurement devices can be unattached from the infant, and they can be removed from the testing are and returned to their mother. Unplugging the jumpers will turn off all devices and the equipment can be shut down, assuming all information has been saved. Preliminary tests were only conducted over a period of ten to fifteen minutes to minimize the total time each infant spent in the lab that day. Having already been involved in twenty to thirty minutes of testing for the Psychology Department, much more testing was likely to vex the infant further and cause unwanted behavior.

5.6 Test Subject Survey Information

Prior to testing, all subjects were asked a series of questions related to family and birth history. The questionnaire can be found in the IRB approval papers filed with the Psychology Department at Virginia Tech and in Appendix A. The two test subjects used in the trials for this research are detailed in Table 5.6.1. These two infants were located by the IPL in their search for 2-month-old infants for their testing. The test subject numbers are listed on the table for further reference to subject information.

Table 5.6.1. Test subject personal, family, and birth information.

	Infant 1	**Infant 2**
Infant Perception Lab Test Subject #	183	185
sex	male	female
birthday	4/22/03	4/29/03
gestational age at birth (weeks)	38	39
date of testing	7/2/03	6/27/03
postmenstrual age at testing (weeks)	48	48
race	white/Caucasian	white/Caucasian
method of delivery	Cesarean (breech)	vaginal
method of feeding	breast	bottle
mother's age	28	28
time since feeding (minutes)	30	60
time since napping (minutes)	45	120

Important details from Table 5.6.1 are the postmenstrual age of the infant at testing, 48 weeks in both cases. This age is almost ideal for the preliminary testing related to this research because they are strong enough to make gross movements, but do not have the motion capacity for purposeful directed movements until about three months of age. Additionally, the motor control of their bodies has not evolved past a few degrees of freedom, so primarily the large joints (shoulders and hips) are contributing to the motions recorded at the wrists and ankles. The time relative to feeding and napping is also listed, which can relate to how calm the infant was at the time of testing. During testing, periods of calm, spontaneous motions were noted and sections of video and data were used only when deemed as a GM by a trained physician [Peck]. As listed, Infant 1 was male and Infant 2 was female and both were white/Caucasian and born to 28 year-old mothers.

An important fact to note is that Infant 1 was born breech and a Cesarean was performed due to the feet-first nature of the birth. It has been suggested that this may point to different leg motions than with non-breech infants. During these experiments, much more kicking was seen from Infant 1, compared to the other test subject, but no motions were determined to indicate any dysfunction; only that the legs were very active. Such facts will be important to note and follow in future studies that compare populations or an infant over time.

6 Analysis of Acceleration Data

This section will explain what happens with data from the acceleration measurement devices once it has been recorded and stored using the data acquisition set-up in LabVIEW. This includes the transfer of data into Matlab for analysis and the use of various algorithms developed to produce graphical analyses of the data. Such analyses include spectrograms and Fourier transforms of windowed data in the frequency domain to look for frequency components, as well as cross-correlations of multiple limb data to look for interlimb coordination. These analyses will be briefly discussed, but to this point in the research, they have not been studied to determine optimum characteristics for viewing of important visual aspects. A final section of this chapter will review sections of video footage taken from test subjects and detail findings from the data and the analysis presented in this chapter.

6.1 Transfer of Data to Matlab

After acquiring data using LabVIEW and associated hardware, post processing was performed in Matlab. Other programs such as Microsoft Excel were used to create some graphics, but Matlab was primarily used. Programs such as LabVIEW are capable of post-processing and live data processing as it is acquired, but the experimenters have more experience with signal processing with Matlab code.

The data has been saved in spreadsheet-file format with nine columns of data, one of time and eight channels of acceleration information. Once again, the processed acceleration values were saved, not the base voltage value measured by the accelerometer. This information is easily imported into Matlab 6.1 using the "Import Data" option. Having imported the information in, it was imperative to organize it into clearly labeled individual data arrays. A Matlab code (Appendix B) was written to take a two-dimensional array of data from the spreadsheet and split it into individual arrays. In the same program, all the data files were plotted on one set of graphs in four subplots as seen in Figure 6.1.1. This code also calculates and plots the absolute magnitude of the total acceleration vector.

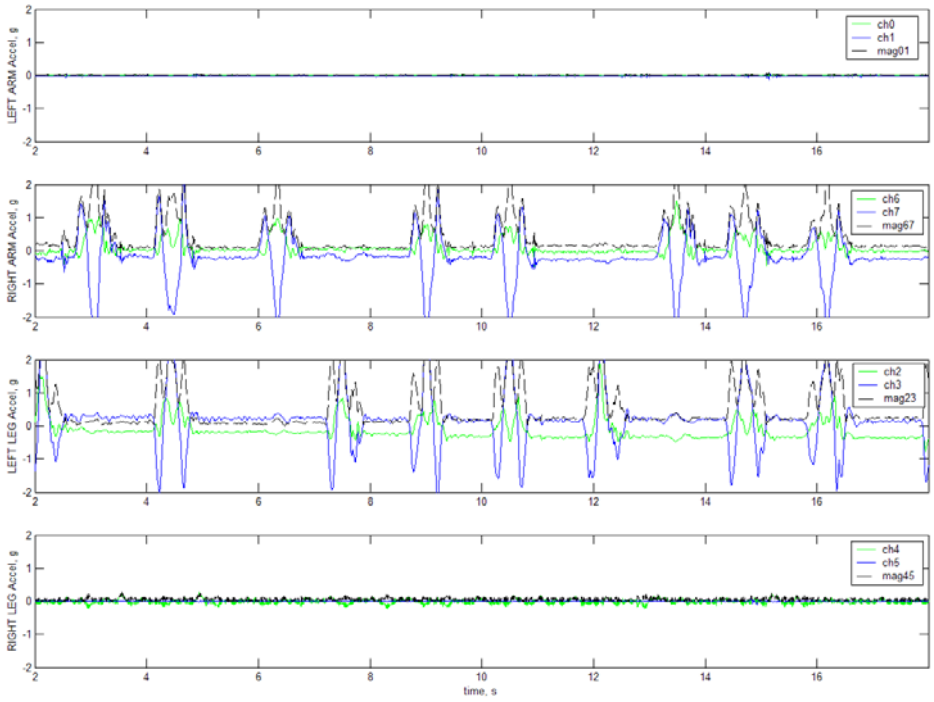

Figure 6.1.1. Sample plot of 8 channels of data after importing the spreadsheet file into Matlab.

As previously discussed, a standard arrangement of the measurement devices on the test subject was used throughout testing. Because of this consistency, the Matlab code was written to assume that channels 0 and 1 were form the left arm, channels 2 and 3 from the left leg, and so on, clockwise around the infant.

At the conclusion of this code, the user is able to access the data from all eight channels by the variable names "Ch0" through "Ch7," while time is stored in "t." One reason for the choice of data samples around 1 to 2 minutes in length was to minimize difficulty reading a set of data plots. As you can see from the 16 total seconds of data in Figure 6.1.1, 120 seconds would become too compressed on a page for viewing. During prototyping and initial testing, this is an important consideration.

6.2 Fourier Transforms and Spectrograms to View Frequency Components

In signal processing of engineering data, looking at the frequency content is often an important way to view underlying actions within a set of data. In many cases, this hidden component could be a vibration at a constant frequency over the duration of the experiment or during key moments. For this research, motions are constantly changing and therefore hidden frequencies may not be as noticeable. Nonetheless, frequency content was studied in the sample data to see what type of results could be extracted.

6.2.1 Explanation of Fourier Transforms and Their Use

During the design of the electronics for the device, the frequency response was limited to below 10 Hz by the capacitors chosen. This was done to help limit the noise in the measurements. An additional result is that frequencies above about 6 Hz are attenuated so that their magnitudes are only a fraction of what was truly happening at the measurement point. It was assumed that this cutoff is a safe limit because high-frequency human vibrations are not expected to exceed that limit; at least in this research.

Taking the recorded data, a Fourier Transform can be conducted on a set of data to transfer the information from the time domain to the frequency domain. In this transformation, the components of the original signal are represented by powers of the signal at progressive frequencies. The derivation of how a Fourier Transform works is relatively difficult to explain, but is based on the premise that the resulting power spectrum across the frequency domain can be used to recreate the original signal in time. To return to the time domain, each coefficient in the frequency domain is applied to a sine or cosine wave at the corresponding frequency, then all waves are summed to reach the original signal.

What is important to understand here is that high magnitudes at a specific frequency indicate a high amount of original signal content at that frequency, signaling an underlying frequency component. This can indicate an unseen disturbance or problem with the signal source. An example is the natural shakes an adult produces when their hand is outstretched

from their body and free. A survey was done of a few graduate students in the Modal Analysis Lab, and in simply holding their hand out while an acceleration measurement device was attached, signals indicated frequency components from 2 to 4 Hz. This is simply the natural shakes that these individuals in their hands, which may be important to monitor in at-risk infants.

6.2.2 Affects of Sampling on Frequency Extraction and Fourier Transforms

In preparing to conduct a Fourier Transform (FFT for fast-Fourier Transform) on data to look for frequency content, it is important to plan for the type of information an analyst is searching for. Specifically, in data acquisition, factors such as sample rate and length of sample dictate limitations on the results a Fourier Transform can produce.

As mentioned much earlier in this paper, for a frequency to be resolved from source data, at least 10 data points per oscillation or revolution are required to have a clear FFT result. The minimum is considered to be 2 to 2.56 data points per oscillation to ensure there is no bias due to the Nyquist frequency, but this is a minimum. Therefore, with a resolution down to 6 to 10 Hz, just to get enough data to resolve those frequencies clearly in a FFT, 60 to 100 samples per second must be taken. As this number rises, the final data file size increases, which slows the analysis process.

A second problem is resolving frequencies under 1 Hz. These oscillations that take over one second to occur are difficult to resolve in these human movements just be cause of the dynamic nature of the acceleration measurements and their short burst length. When only 2 seconds of acceleration information is recorded from a burst of motion, the lowest frequency that could conceivably be resolved is 0.5 Hz. While minutes of data a typically stored, this limitation becomes difficult during the process of windowing data, which will be discussed later in this section.

6.2.3 Use of Windows in Analyzing Data for Frequency Content

A technique used during most signal processing analyses of data is to apply a window to the data being analyzed. Because only a section of data is viewed during processing, there appears to be an abrupt beginning and end to the data. To help negate any affects of these abrupt ends of data, the ends are manipulated such that the data appears to pan in and only the center of information is emphasized. By multiplying a known window shape over a series of data, this can be accomplished. One popular window is called a Hann Window (also known as a Hanning Window) and the general shape is shown in Figure 6.2.3.1.

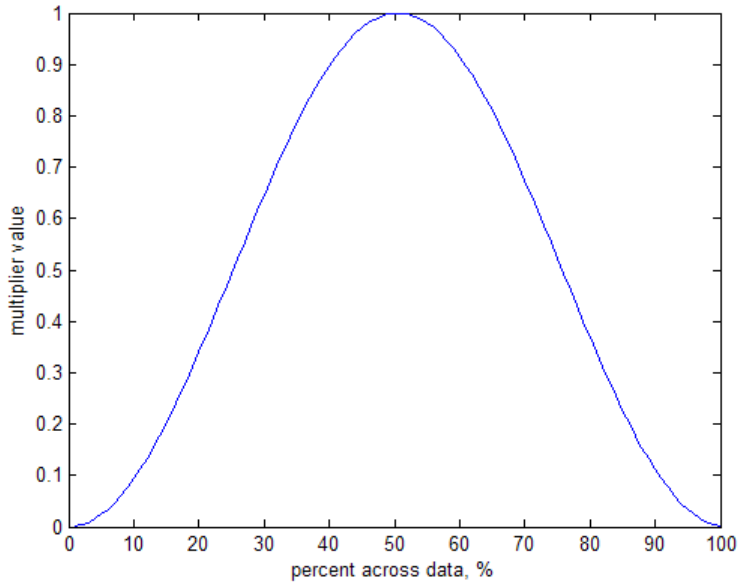

Figure 6.2.3.1. Shape of a Hann Window multipliers across the data.

The primary benefit of windows in analyzing frequency content is that low frequency noise is reduced because the ends are attenuated. Figure 6.2.3.2 shows 6 seconds of original acceleration data and the result of applying a Hann Window. Inspection reveals that in the center of the time series, the original data and windowed data match up very closely. At the edges, it is clear that the window has minimized the overall affect of the original signal. Given this, it is often wise to choose a window size twice as large as the important data so that key parts are not attenuated too much. This consideration should be based on the

lowest resolvable frequency to be investigated. Another window option could also be used, but a Hann Window is very popular in engineering applications.

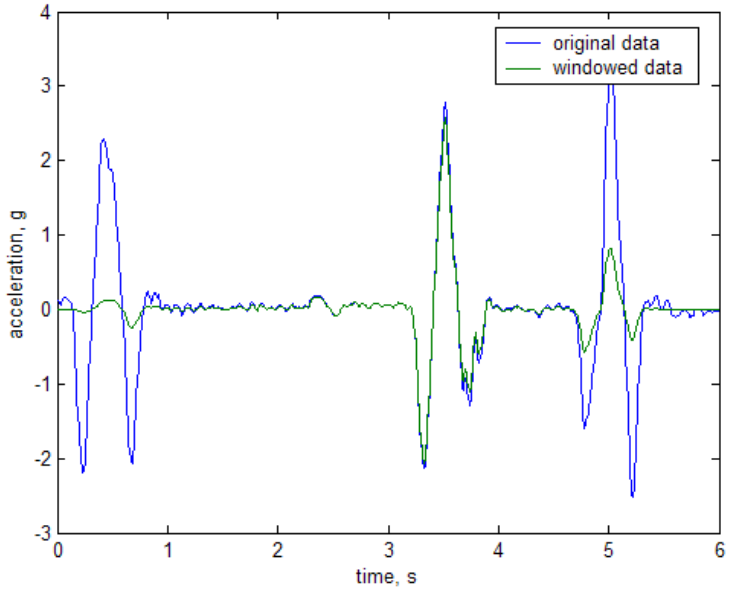

Figure 6.2.3.2. Affect of applying a Hann Window on sample acceleration data.

6.2.4 Results from Spectrogram Application on Acceleration Data

A spectrogram is a series of FFTs conducted on a sliding window in time. The result is a three-dimensional plot where the horizontal axis is the original time values of data from the series, while the vertical axis is the frequency axis. The third dimension can be plotted in the z-dimension, or simply denote the magnitude of the frequency content by the color used.

With regards to the sliding window in time, the analyst has a lot of freedom to determine a number of variables conducting the analysis. First, the analyst must choose the size of the window. Second, the amount of overlap between windows much be chosen, along with the type of window to be used, as previously discussed. Figure 6.2.4.1 illustrates some of these decisions on some sample data. In this figure, 6 seconds of data are shown, with red and green boxes overlaid on the data. The red boxes illustrate 2-second wide windows that are offset by one second each. The green boxes illustrate 1.5-second wide

windows offset by one second each. While the amplitude of the boxes is not related to how they windowing is done, we can see how the window affects the analysis in time.

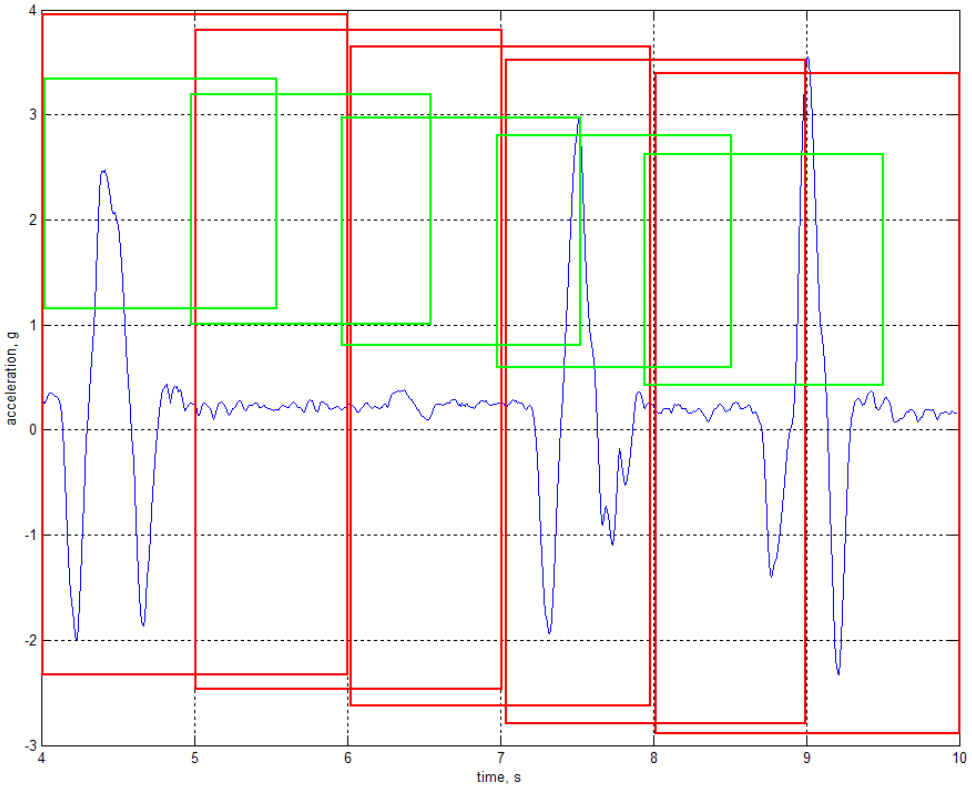

Figure 6.2.4.1. Illustration of windows applied to acceleration data for a spectrogram.

Looking at the window placement horizontally, we can see that the final red window ends exactly at the end of the 6 seconds of data. On the other hand, the green window does not conclude at an edge because a final window would not have enough data to fill it. An important consideration is to utilize window widths that will effectively use all the data. Secondly, there are only 5 red windows over 6 seconds of data. Due to the 1 second offset, the last second of data cannot have its own window applied to it. This results in an effective loss of time when a spectrogram is produced.

Once the characteristics related to window size and shifting have been determined, a spectrogram can be produced. As mentioned, at each beginning time for a window, the FFT magnitudes over the vertical frequency axis are plotted as color intensities (blue to red in the following case). A spectrogram was produced from the 20 seconds of data previously

presented in Figure 6.1.1 and is shown in Figure 6.2.4.2. Looking back at the original data, we can see that the left arm and right leg were motionless during testing, so this explains their uniform appearance in the spectrogram. In contrast, the spectrograms from the right arm and left leg are much more differentiated. In the Matlab spectrograms, frequency is plotted up to the Nyquist value (64 Hz for the 128 Hz sampling rate), which tends to bunch the valuable data at the lower sections of the spectrograms. This can obviously be done differently in future analyses.

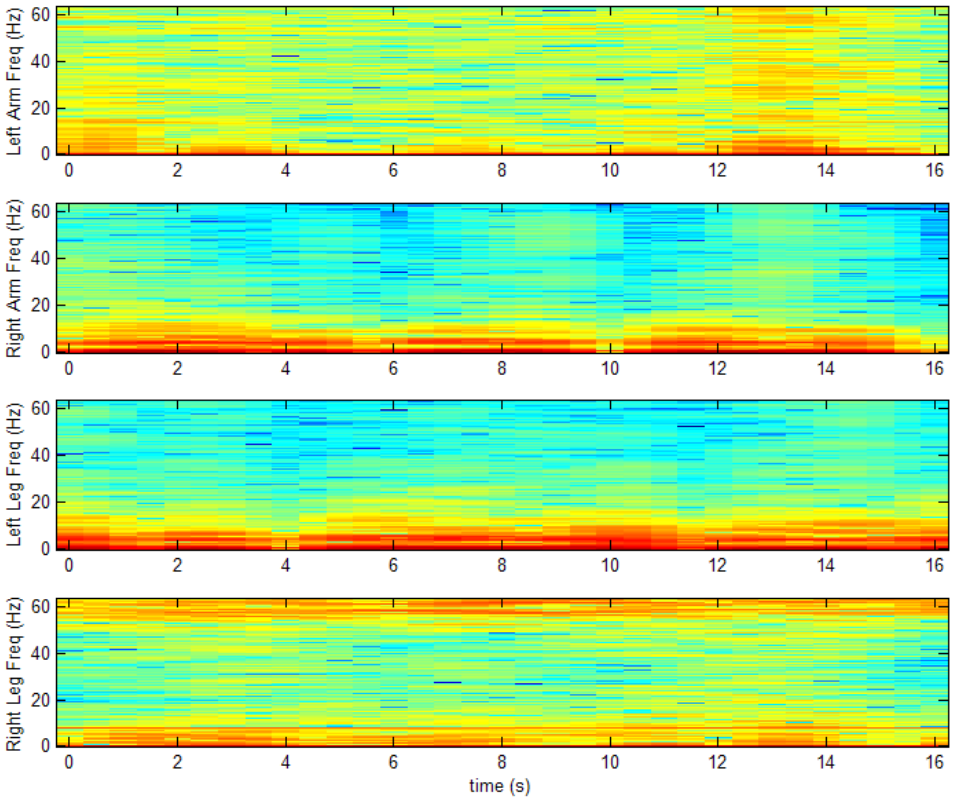

Figure 6.2.4.2. Spectrograms from sample acceleration seen in Figure 6.1.1.

Reviewing the spectrograms above, we can see the impact of some of the analyst's decisions. First, we see that only 16 seconds of data is plotted, from the original 20 seconds. This indicates that a window width of 4 seconds was used in this analysis. As previously discussed, this should be adequate to determine frequencies as low as about 0.5 Hz.

Secondly, the width of data lines at each window's data indicates a slide of about 0.5, or 64 data points. While this can be adjusted, it is unlikely that minimizing the slide will produce anything more than finer detail in the graphics while vastly increasing the analysis time required by the computer.

Overall, we can see a number of problems with the spectrograms in Figure 6.2.4.2. First, the frequency axis is too large and extends to frequencies that cannot be measured with the designed acceleration measurement devices (max frequency of 6-10 Hz). Second, the resolution in the lower, important frequencies is minimal, making it very hard to distinguish differences between different windows. Finally, the intensity of the frequency magnitudes in the spectrograms is blurred and offers no valuable information between time windows or between limbs. As currently conducted, the spectrogram does not appear to offer any substantial benefits in analysis. This does not mean that frequency content is invaluable and should not be studied in human motion, rather this method appears unproductive and a new method should be developed.

6.3 Cross-correlation Viewed with a Sliding Window

Before the multi-dimensional cross-correlation technique used in the analysis of this research is discussed, a brief introduction to correlation and its uses will be discussed. From there, the multi-dimensional option and associated code will be described. Finally, a description of interpreting the multi-dimensional analysis technique will be given.

6.3.1 Introduction to the Basics of Cross-Correlations and Their Uses

A common method for analyzing the relation between two different signals is to calculate the cross-correlation between them. This signal processing technique utilizes the same windowing as previously described, but rather than simply running an FFT on the window, the correlation compares that window to another window from a different signal. These two windows are slid across each other. What results at each window comparison is a coefficient representing how well the two signals match up when shifted that amount. Most often this

technique is simply used once on a pair of entire data files. At points of high correlation values, the signals are very similar.

When discussing correlation, the term lag is used to describe the shifting of the two data signals. When the two signals being compared are aligned perfectly in the time domain they were recorded at, there is said to be zero lag. As one signal is shifted in time either backward or forwards, their respective starting points are lagged; this distance is called the lag and can be positive or negative depending on which signal is your reference.

Figure 6.3.1.1 shows the absolute acceleration vector magnitude after being mean-zeroed for motion recorded by the right arm and left leg sensors (during operational experiments not on humans). It is clear from these two signals that over the course of their 20 seconds of recording, each produced three distinct motions that included three acceleration components. It turns out that just by visually inspecting these plots, we can tell that the first two motions from both sensors were coordinated and occurred at the exact same time. Their final motions seem similar in magnitude, but occurred at different times.

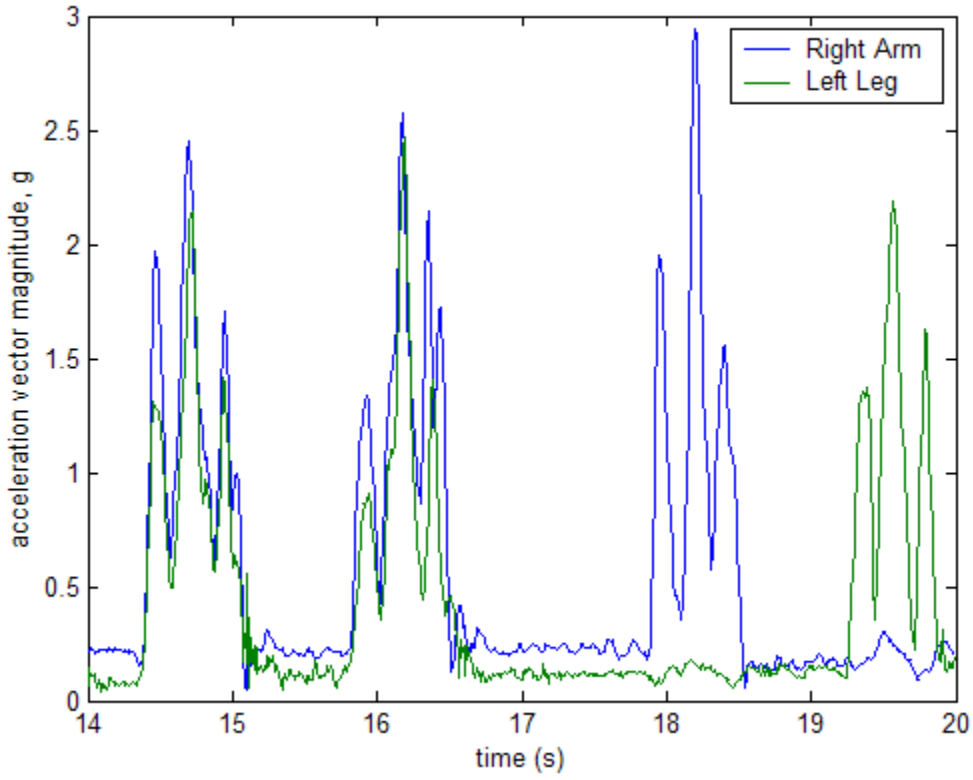

Figure 6.3.1.1. Absolute acceleration vector magnitudes for two sensors.

As described above, a biased cross-correlation we performed on the two signals in Matlab. Biased simply means that the coefficients were scaled by the inverse of the total number of data points and is an option in the Matlab function, "xcorr." Figure 6.3.1.2 illustrates the resulting cross-correlation of the two signals.

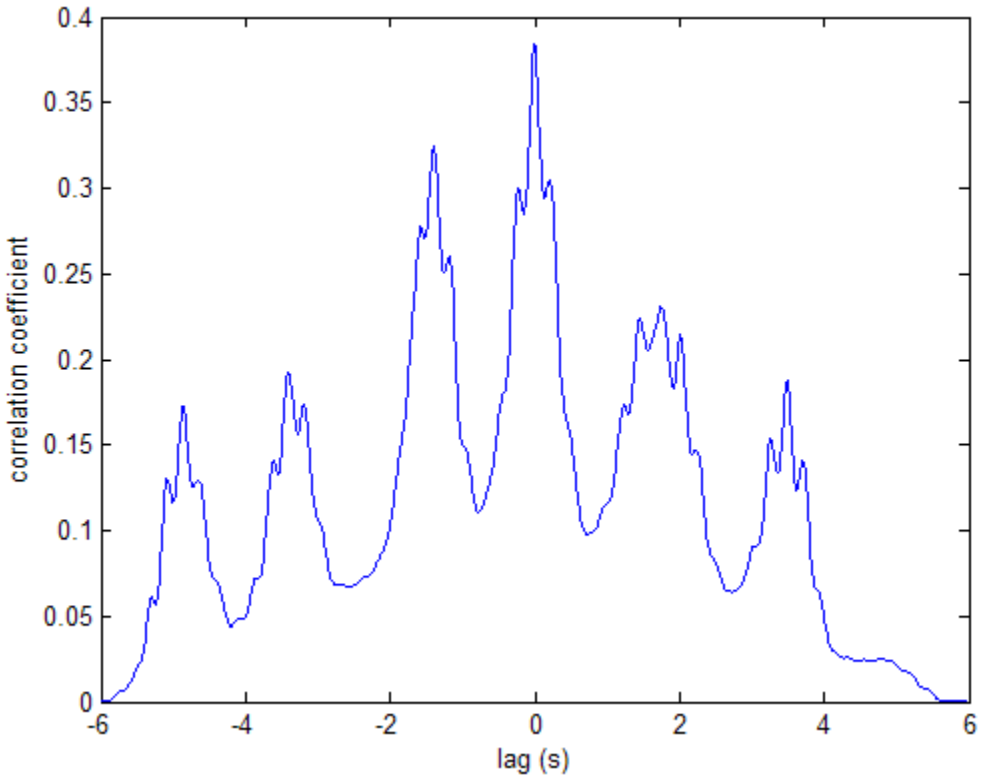

Figure 6.3.1.2. Cross-correlation of right arm and left leg data as shown in Figure 6.3.1.1.

Looking at this plot, we see the x-axis is labeled as the lag axis, where zero is located in the middle. Clearly the maximum correlation is at zero lag because two of the three accelerations match up the best in time. We see the second peak at –1.5 seconds lag because as the left leg (green line) is moved back in time 1.5 seconds, two motions again pair up, creating another high correlation. When the left leg data is at a lag of 2 seconds, we see another high correlation, but this is lower than the other two peaks because this shift only pairs up for about one and a half of a motion. This peak is much broader though because there is a longer time in lag that the two signals pair up well.

What we learn from this previous discussion is that the high correlations are

produced when two signals are well paired. We would expect to see a correlation of up to 1.0 when the two signals are exact. Looking back, it would be hard to get exactly paired signals when they are composed of a number of individual bursts of motion, as opposed to constant motion. For this reason, it is thought that sliding a smaller window (possibly containing only a few bursts of motion) over an entire data set may help in the analysis.

6.3.2 Introduction to Multi-Dimensional Cross-Correlations in Time

As discussed previously, and recommended, the cross-correlation plot was used as the primary component in creating a multi-dimensional spectrogram-style intensity plot. Plots of this nature are not industry standard, but will be shown to offer insight into the analysis of coordinated human motion. The added dimension of these plots comes from cycling the signal section being correlated as the time is moved through. The benefit of this is that smaller time sections can be used rather than the entire time signal; so small bursts and groups of bursts can be used in the correlation.

Figure 6.3.2.1 shows the same original two sections of right arm and left leg signal as used earlier in this chapter. Atop these signals are different color lines outlining the spans of windows used in computing different slices of cross-correlation. Original signal sections from one plot are indicated within the span shown with thicker, darker lines. The thinner, lighter lines of similar color represent positions at which the original sections are cross-correlated with the other entire signal. As discussed previously, there are analysis design aspects the analyst must determine before conducting this processing. First, the window size must be determined. In Figure 6.3.2.1, this window size has been set to 2 seconds, just about enough to contain two consecutive bursts of acceleration data. Second, the overlap must be considered. Here we see an overlap of 1 second (128 data points). This is most likely not enough an overlap for real analyses, but for the purposes of explanation, this is easier to display.

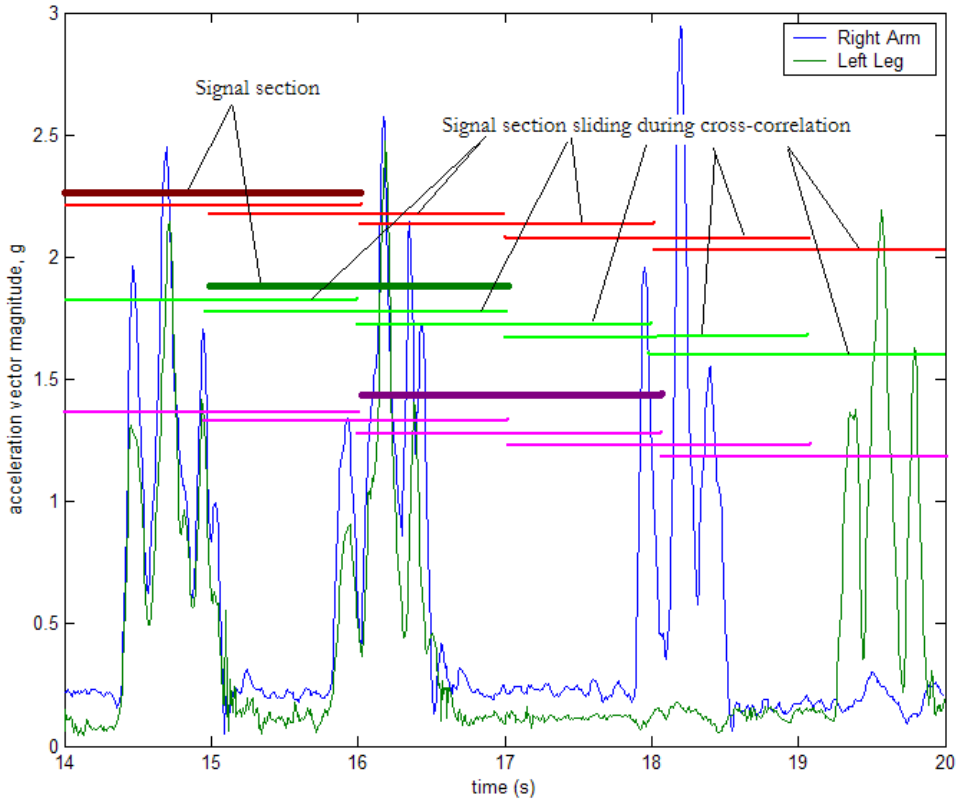

Figure 6.3.2.1. Example of windowed signal sections during cross-correlations.

Inspection of the edges of the time signal with the sections in Figure 6.3.2.1 shows a similar problem as faced with individual cross-correlations; there are sections where correlations cannot occur due to the end of the data. The result is that depending on window size, there will be less overall information.

Just as in the spectrogram, the vertical axis, of the final graphic, represents the x-axis of the base component (cross-correlation plots). The z-axis (intensity of the plot) is the y-axis (correlation coefficient) from the base component. The added dimension is the x-axis of the new plot that represents the time through the original signal. An example is shown in Figure 6.3.2.2 between the left leg and right arm data from above. Notice the red oval surrounding one vertical slice, which is from the cross-correlation of a window of data based at the time indicated on the horizontal axis. Viewing the intensity, we see that on the line of zero lag, there exist five distinct points in time where there is clear correlation, and likely coordinated movements.

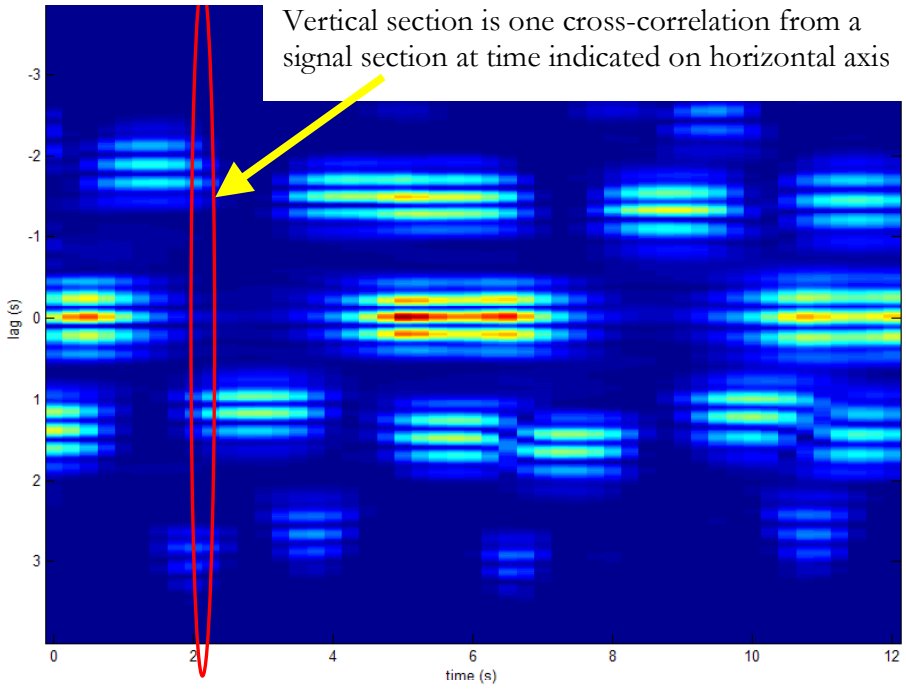

Figure 6.3.2.2. Multi-dimensional cross-correlation of sample data from right arm and left leg.

Inspection of the limits on the time axis and lag axis show an 8 second difference compared to the original 20 seconds of data. As previously discussed, there are difficulties having two windows to overlap at both ends of the signal. As shown on the lag axis, there are 4 seconds of lag data in both directions. This is essentially subtracted from both the beginning and end of the multi-dimensional cross-correlation. Obviously this affect is minimized, as the window width is made smaller.

6.4 Results of Analysis of Sample Video Footage From Infants

Having explained all the prerequisites to preliminary infant testing, from test set-up to data transfer and analysis, two brief infant motion studies were completed on two-month old infants. These studies required coordination with the Infant Perception Lab (IPL) in the Psychology Department at Virginia Tech, as they were conducting a study on infants in the same age range as needed for this research. Information about the two infants tested can be

found in Table 5.6.1. Institutional Review Board approval had been granted for the research (see Appendix A) and all necessary parental consent forms were completed.

6.4.1 Recorded Motion and Analysis from Infant 2

Infant 2 was a 2 month-old female at the time of testing. Procedures were conducted in the IPL facilities, on a padded mat on the floor to minimize constrained motion due to the limited size of cribs available. A 30-second video and screen shot from this testing is shown in Video 6.4.1.1 (video6411.mpg). In this frame, we can see a graduate student from the IPL kneeling at the base of the infant and the feet of the mother on the infant's right-hand side. To maintain the infant's clam demeanor, this presence was required. After acquiring the video and corresponding data, Dr. Dawn H. Peck reviewed the footage (from a much larger sample) and commented on sections of video that resembled characteristic GM motions [Peck]. It should be noted that Dr. Peck was not evaluating the neurological function of the infants, per Prechtl's method [Prechtl, 1997], but rather making general comments about sections of video footage containing quality GMs, based on her experience in the field.

Video 6.4.1.1. Infant 2, 30-second video sample (see video file **video6411.mpg**).

Following the data collection and video review, the 30-second sample shown in

Figure 6.4.1.1 was synchronized with data taken at the same time. That data is shown graphically in Figure 6.4.1.1, with all four limbs data separated and labeled accordingly. As discussed previously in this chapter, Figure 6.4.1.1 shows not only the individual measured axes of acceleration on each limb, but also the mean-zeroed magnitude used in computing spectrograms and multi-dimensional correlations.

Within the data, key motions from the corresponding video are going to be discussed. For both the data and the video file, the time is synchronized, beginning at 0 seconds, although this simply represents a clip from a much larger pair of video and data files. Also note the nearly constant measurements that are made with values of positive or negative one unit of gravity. These represent times when the measurement device's axis had been rotated into the axis of earth's gravity and was not moving. Using mean-zeroing techniques will later negate this affect. In future analyses, this rotation information could become distinguishable and valuable to understanding GMs from a broader perspective.

In general, looking at the data, the infant's legs were much less active than the arms. Specifically, the left arm was more active than the right during this sample. Comparing the time of occurrence between the two signals, we see two distinct coordinated movements of the arms at 10 and 26 seconds. In the case at 10 seconds, the right arm briefly rotates (seen in the mean value shift) before moving at the same time, at the same rate, as the left arm. This total movement is easily seen in the video just after a few second pause in all motion at 10 seconds into the file.

In the case at 26 seconds, nearly identical amplitudes of acceleration between the two arms are seen. This motion also appears to occur about 1.5 seconds after a coordinated movement between the two legs. In viewing the video footage, at 24 seconds we see the paired leg kick, immediately followed by coordinated arm movements of similar amplitude. This will be pointed out further in later figures related to coordination.

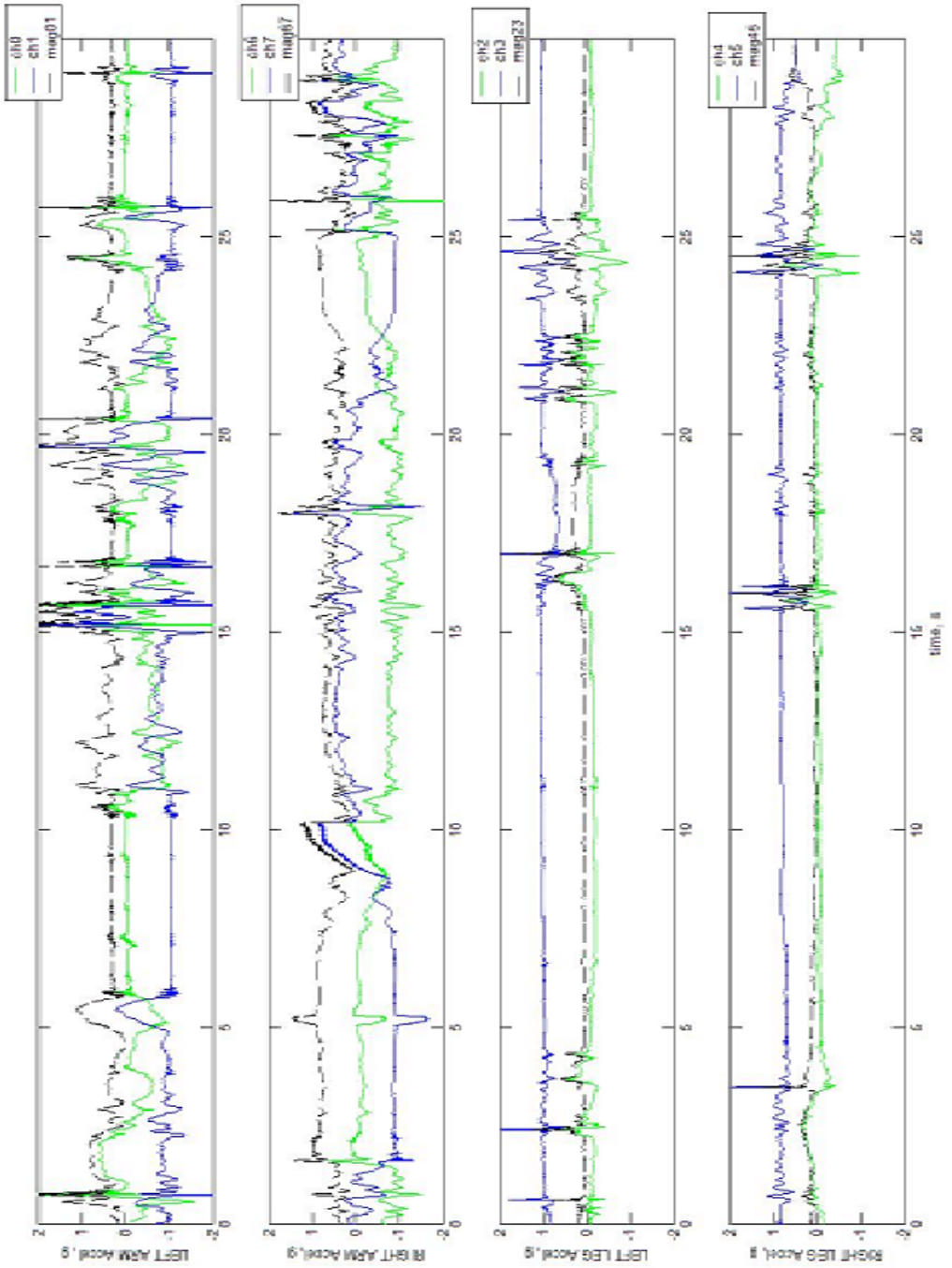

Figure 6.4.1.1. Synchronized acceleration data from four limbs of Infant 2 (see Video 6.4.1.1).

Simply looking at the amplitudes of the acceleration signals over the 30-second time period, there are distinctly different types of amplitudes. While there are a number of peaks of about 1.0 units of gravity, there also exist a number of higher amplitudes, up to 2.0 units of gravity. There appears to an equal distribution of both. Comparing the two types of peaks, there appears to be a difference in their width. The peaks of less magnitude seem to be spread out over a larger amount of time, while higher acceleration peaks tend to occur over much less time. From this, it can be inferred that similar amounts of power have been exerted on the limb, possibly to move it the same distance, based on the range of motion. Relating back to the integration discussion from an earlier chapter, less acceleration over a longer time is capable of traversing the same distance as a higher acceleration over a short period of time. Reviewing the video footage, it is clear that there are two distinctly different types of movement: quick, hard bursts of energy and slower, easier motions. What is visually interpreted as different physical motions appears in the data a distinctly different types of signals based on amplitude and length of application time.

The first analysis completed on the 30-second data sample from Infant 2 was a series of spectrograms on the acceleration data from the four limbs. Again, this computes the frequency content of a sliding window on the magnitude of mean zeroed data. Although previous discussions of this process of analyses have deemed it insufficient in many respects for determining important characteristics of human movement, it was conducted nonetheless.

Figure 6.4.1.2 illustrates the four spectrograms from the 30-seconds of acceleration data previously shown in this subsection. Observation quickly reveals that the top two plots (arm data) contain much more frequency content than the spectrograms of the legs. Review of the video footage also revealed this difference in quantity of motion. Additionally, wide, intense frequency content areas around periods of gross movement are seen. This was seen in the higher peaks in the acceleration data, but it is once again easy to spot in these plots. Overall though, these plots are inefficient at describing much in detail about the plots. As discussed in the description of this code, the frequency scaling (vertical axis) is unable to distinguish the lower, more important frequencies. The intensity is also inefficient in comparing various plots, as smaller amplitudes do not appear much different in the spectrogram. These scaling issues may require recoding in future iterations of analyses.

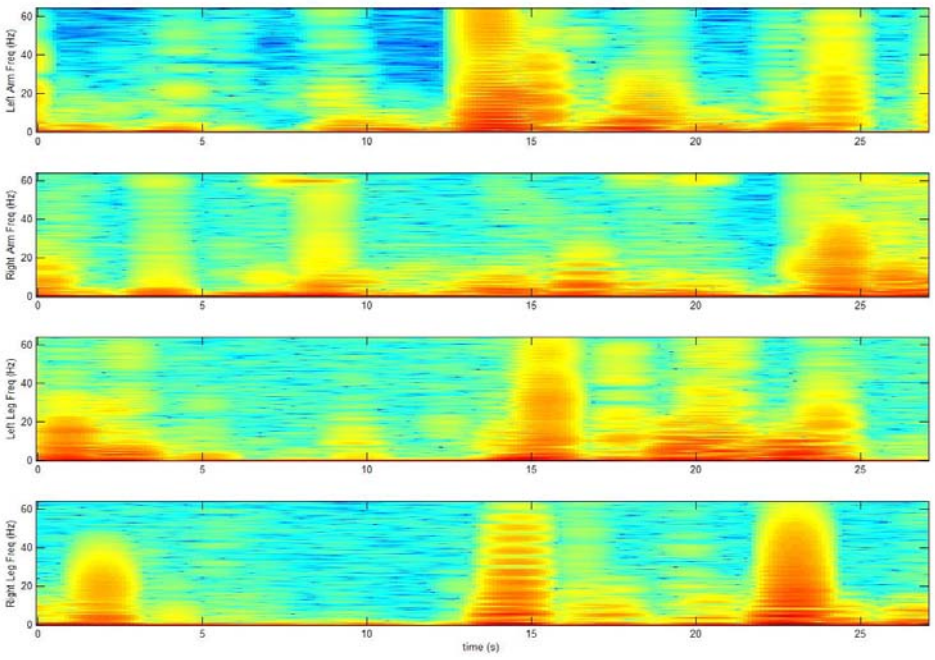

Figure 6.4.1.2. Spectrograms of 30-second acceleration data sample from Infant 2.

A second, more productive analysis on the data was performed to investigate the coordinated movements between limbs. As discussed in previous parts of this chapter, the method of cross-correlating a sliding window on multiple axes was used. The plots are shown in the following figures. In each case, there is some indication of coordinated movement, as shown by the red intensity spots on the plots. It should be noted that only the correlation plots between adjacent limbs (four total plots) have been shown, because the other two relations do not appear to contain any valuable information. Remember too that time indications are relative to the start of the window used in sliding correlation. As an example, on the time axis, the point at 0 seconds actually represents information from the 0- to 3-second window used in correlation (assuming a 3-second window is used).

Figure 6.4.1.3 shows a cross-correlation between the two arms of Infant 2 over the 30-second data sample. In this plot we can see specific points of high coordination at approximately 0, 10, and 19 seconds, as indicated by the red points. In each case, we can refer back to Figure 6.4.1.1 and Video 6.4.1.1 to see that there are in fact motions occurring at approximately that time in both limbs. The figure also shows some of these points at

vertical positions on the lag axis, indicating a slight lag between the motions, which is somewhat noticeable in the data plots and video.

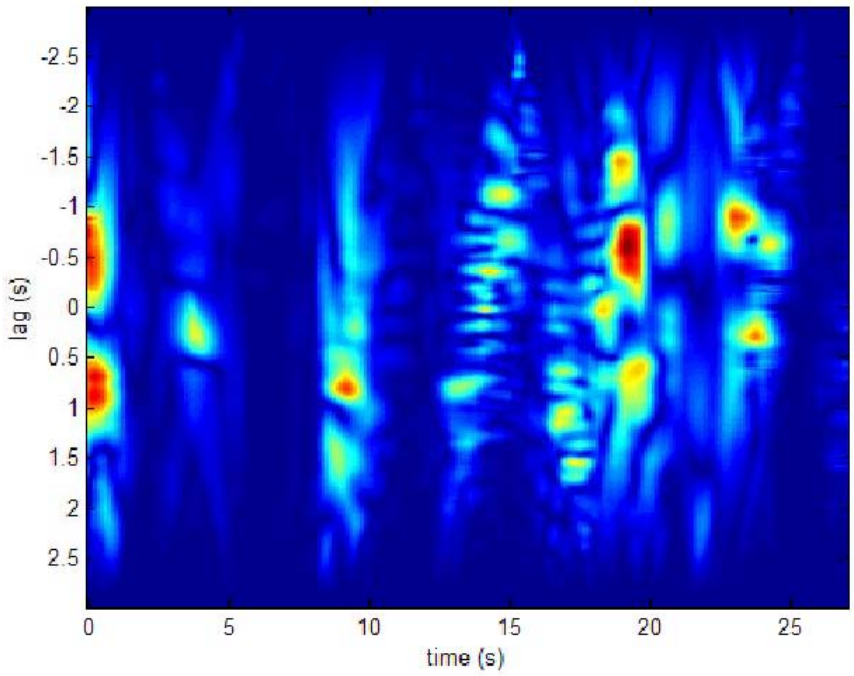

Figure 6.4.1.3. Multi-dimensional correlation between the left and right arms of Infant 2.

In comparing the leg data from Infant 2, as shown in the correlation plot of Figure 6.4.1.4, there is little evident coordinated movement. The one point of high intensity appears approximately 24 seconds into the file. Looking back at Figure 6.4.1.1, we see a distinct motion of both legs at about 24 seconds. The graphical representation in Figure 6.4.1.4 does an excellent job of pointing these paired motions out to the analyst. Of almost equal importance is the fact that no other coordinated movements are noted in the correlation plot, which is clear from manual inspection of the data and video from Infant 2. It is the vast area of blue that points out the uncoordinated nature of the two limbs. This does not however indicate any dysfunction, simply that no other motions were paired. It has already been stated that very little motion occurred in the legs of Infant 2 during this period.

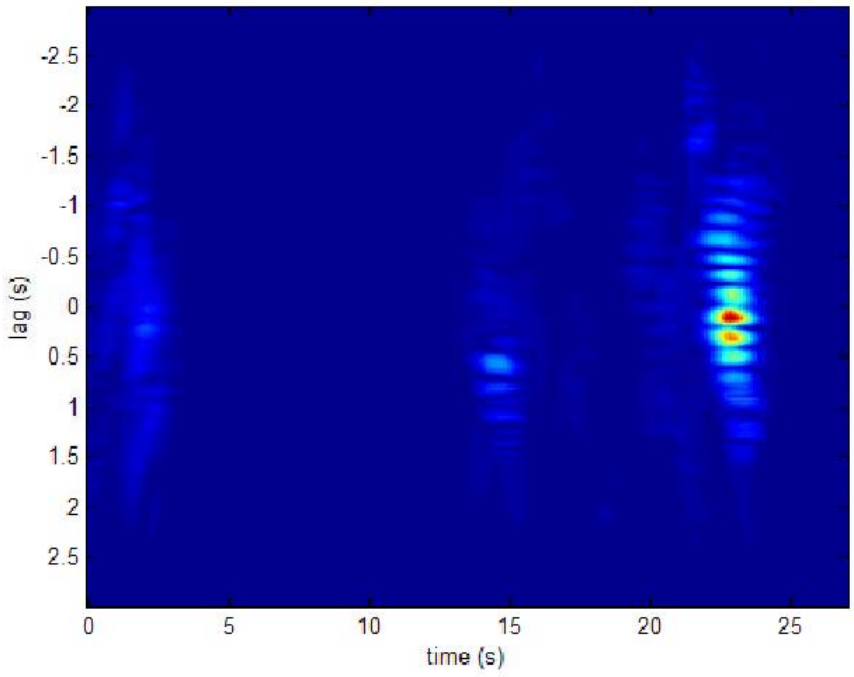

Figure 6.4.1.4. Multi-dimensional correlation between the left and right legs of Infant 2.

Again, we see very little coordinated motion between the left side limbs of Infant 2, as indicated in Figure 6.4.1.5. This correlation has one primary point of high correlation at about 14 seconds into the file, but at a lag of approximately 1 second. Comparing this to Figure 4.6.1.1, we see motion occurring in the left arm from 14 to 17 seconds and in the left leg at about 16 seconds. Taking into account the offset in time due to the 3-second window, this lag makes sense as the arm is leading the leg.

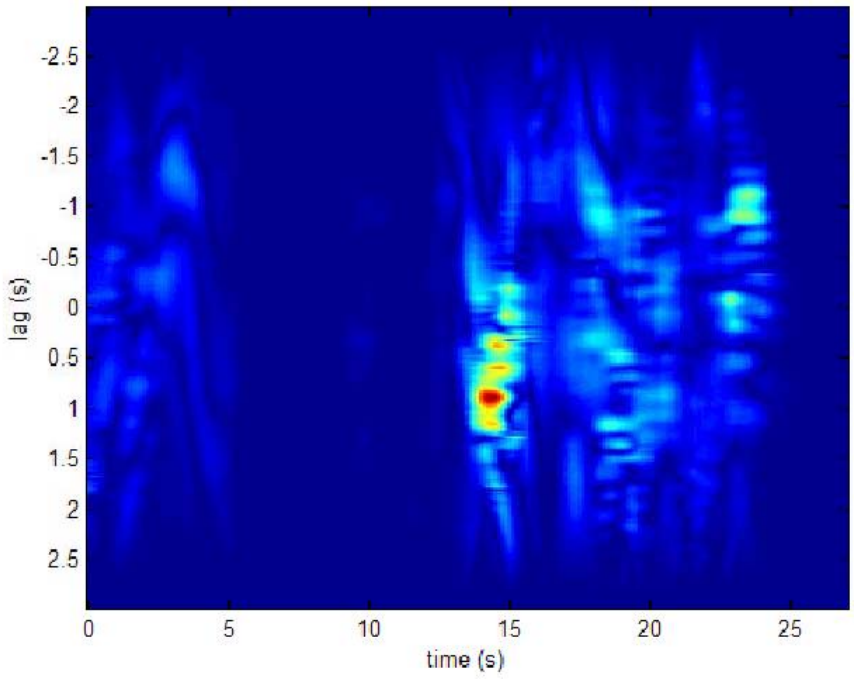

Figure 6.4.1.5. Multi-dimensional correlation between the left arm and left leg of Infant 2.

As in the last figure, we see another strong lag on the infant's right-hand side limbs. Figure 6.4.1.6 shows the correlation plot between the right arm and right leg. Here, there is a clear high correlation at a negative lag of 1 second at a point approximately 24 seconds into the data file. Again comparing this to the data file in Figure 6.4.1.1, we see two motions occurring in these limbs at about this time. The difference here is that the leg is leading the arm, so a negative lag appears in the correlation plot. This is in contrast to the lag discussed on the left side of the infant's body in Figure 6.4.1.5. In Figure 6.4.1.6 we do see an increase in other areas of increased correlation at various times and of different lags. These correlations are of a smaller magnitude than the previously discussed motions, but do occur at similar times to the correlations between other limbs. This could be due to recorded movements on adjacent limbs from motion on other limbs, or could be related in some other form to be determined through further study.

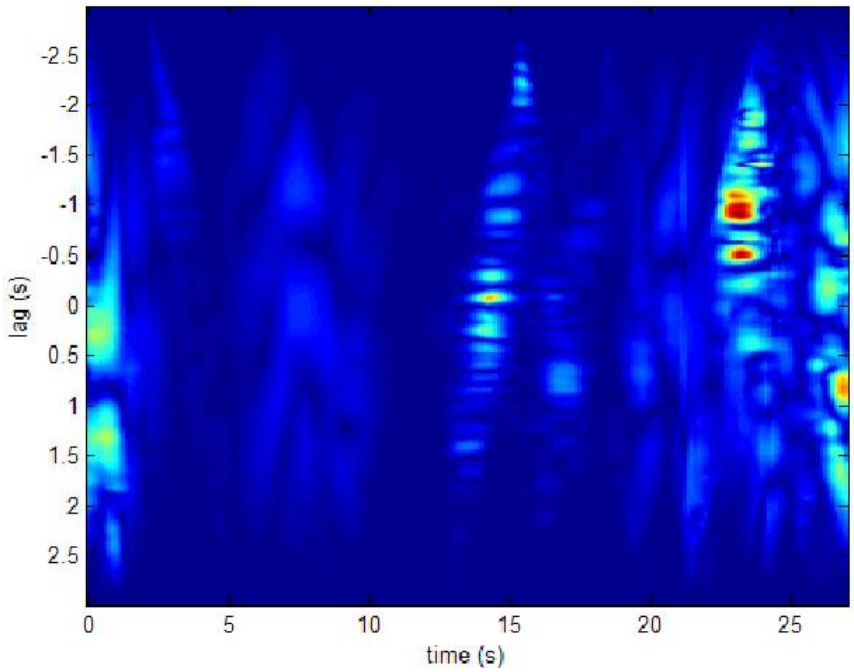

Figure 6.4.1.6. Multi-dimensional correlation between the right arm and right leg of Infant 2.

Although Infant 2 did not exhibit vast amounts of leg movement, what has been shown in the pervious series of correlation plots is a clear comparison between the correlation plots and the recorded data and video footage. Simply by looking at a colored graphic of data, analysts can clearly see where movements occurred simultaneously on different limbs, or even lagging each other by a few seconds. This technique obviously is only just budding, but could serve to be valuable with further research on various motions.

6.4.2 Recorded Motion and Analysis from Infant 1

A second series of 30 seconds of acceleration data from Infant 1 (male) was analyzed just as that of Infant 2. This disparity in presentation order is due to two factors: this testing of Infant 1 occurred after that of Infant 2, and the video footage of Infant 1 was not reviewed by Dr. Dawn Peck, as the data for Infant 2 was. Because of these reasons, there is less confidence in the presence of GMs in the data files from Infant 1, but the data does represent recorded motion using the acceleration measurement devices on an infant in the 2-

month range.

At the time of testing, Infant 1 was exactly 2-months old. A series of data from Infant 1 had previously been recorded seven days earlier, but was later determined to be mostly unrepresentative of GMs due to the constrained nature of the crib the infant was placed in. Following that problem, future tests were conducted on a padded mat on the floor to allow more freedom of movement.

Dr. Peck did mention that Infant 1 did demonstrate a number of purposeful movements, such as bringing his thumb to his mouth in her initial review of the data taken a week earlier while in a crib [Peck]. It was also noted that Infant 1 had very active leg movements. The mother mentioned that he was born breech, but this is not in any way linked to neurological dysfunction, just the physical orientation of the infant in the womb at the time of birth. Having tested Infant 1 after an additional week of maturation after Dr. Peck's general review of the motion patterns, it is likely that some motions are getting into more mature GMs and are in fact purposeful. For the purpose of general infant movement measurement, this does not affect the recorded data, but should be noted.

The aforementioned 30-second data file is shown in Video 6.4.2.1 (video6421.mpg). This file was recorded at the home of the infant with all the equipment from the IPL, including the digital video recorder, acceleration measurement devices, and data acquisition hardware.

Video 6.4.2.1. Infant 1, 30-second video sample (see file **video6421.mpg**).

Within the video, there are a few things to note. First, the knees and hand on the left side of the frame are those of the graduate teaching assistant from the IPL. A pacifier is also seen to the left of the infant. During some of the testing, the graduate student would interact with the infant to calm him down and sometimes use the pacifier. During this section of data, there was no interaction and the infant was not actively seeking the pacifier, although he was crying during part of the recording. Crying does however disrupt GM motion as stated by Hadders-Algra: "GMs during crying are abrupt, jerky, and tremulous… GMs during crying should be excluded from the analysis [Hadders-Algra, 1999]." For the purposes of this research, recording infant motion in general, these movements during crying were included in these sample analyses.

The data files transferred from the data acquisition software into Matlab have been displayed in Figure 6.4.2.1. Once again, the individual axes measurements are presented alongside the magnitude computed from the mean-zeroed data. In this data set, there was a malfunction with Channel 0 data, so only one axis from the left arm is available during analysis.

In reviewing the video file (Video 6.4.2.1) and comparing it to the data file, there are some obvious differences in the motion characteristics of Infant 1 compared to Infant 2 in the previous analysis. Primarily there exists far more leg movement in the data files from Infant 1. Included in this leg movement is more hip and trunk movement, essentially accelerating the two attached limbs. As mentioned, this type of movement is more advanced and requires more strength than simple movements of the limbs. Infant 1 was noted to have much more muscular development and was more aware of his body than Infant 2. This is a sign that he may be maturing out of the GM phase.

Secondly, we see a stagnant period of motion from about 10 to 22 seconds with only a few small motions in single limbs during this span. The infant is clearly much calmer during this period. Finally, the last 8 seconds include a number of motions occurring at the same time over multiple limbs of the infant. These motions are quite strong and quick, which is evident in the data signals. In contrast to Infant 2 (Figure 6.4.1.1), Infant 1 seems to exhibit much quicker motions as seen by the short amount of time during each burst of acceleration. This is not indicative of any dysfunction, but is a noticeable difference both in reviewing the video footage and studying the measured acceleration data.

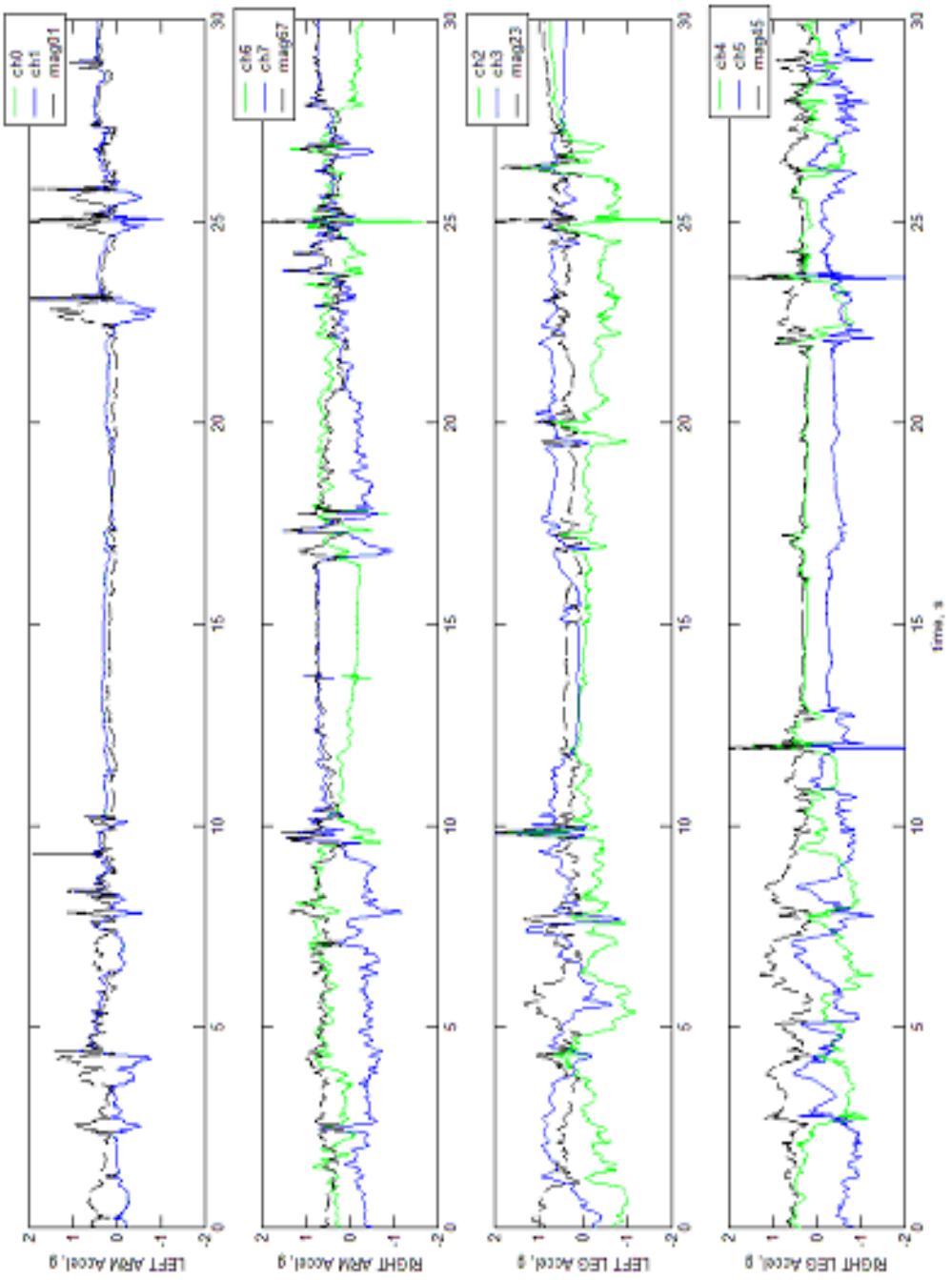

Figure 6.4.2.1. Synchronized acceleration data from four limbs of Infant 1 (see Video 6.4.2.1).

A spectrogram of each limb's data was created using the methods previously described. These spectrograms are shown in Figure 6.4.2.2 and once again fail to show much important information. The scale and intensity on the plot do not accentuate the lower frequencies and there appears to be no difference in the visual interpretation of the figure, while there are clear differences in looking at the data and video. Another complication is that there exists a significant amount of frequency content throughout the entire time span of the data, when viewing of the data disproves this. Clearly there is much work to be done on this data analysis method.

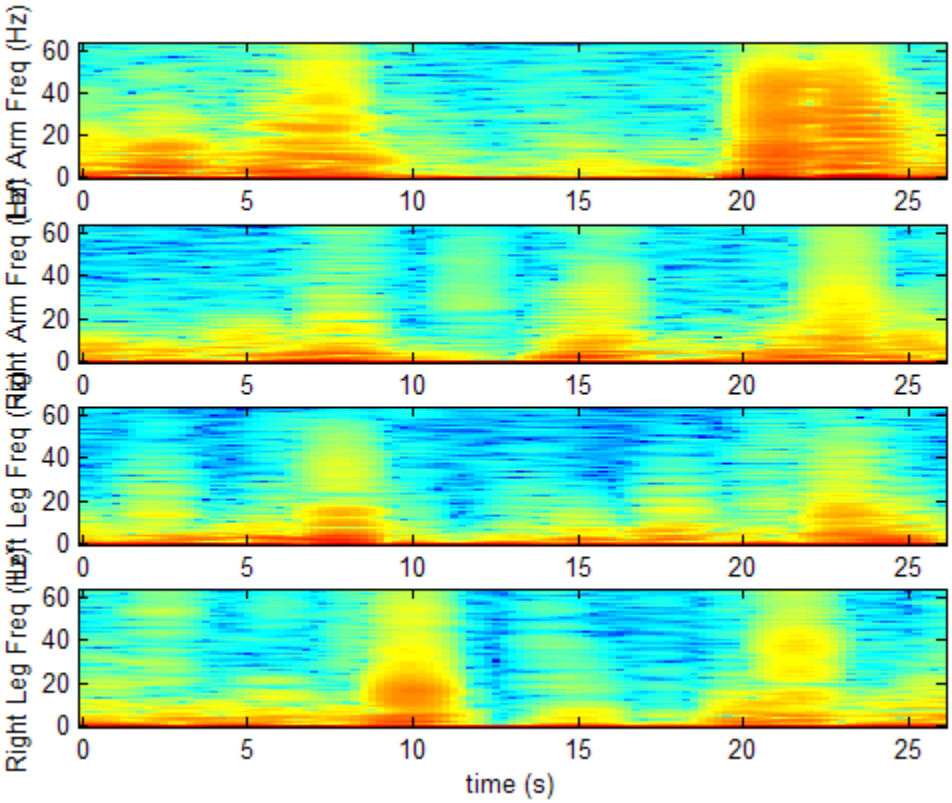

Figure 6.4.2.2. Spectrograms of 30-second acceleration data sample from Infant 1.

In contrast, the correlation plots comparing different acceleration signals tends to show much more important information. Figure 6.4.2.3 shows the coordination between the two arms of the infant. As previously mentioned, there was little motion in the arms, but

the figure finds almost simultaneous motion in the two arms at a time of about 22 seconds into the file. The dark red point in Figure 6.4.2.3 indicates this. It should be noted that these analysis plots were conducted with a window width of 4 seconds as opposed to the 3-second window used in the previous analysis. The purpose of this difference is to illustrate the change on the graphics to the audience. Comparing the two, there is little difference outside of resolution. The edges on the lag axis do tend to be sparser since the window is wider and correlation is lower with increased time.

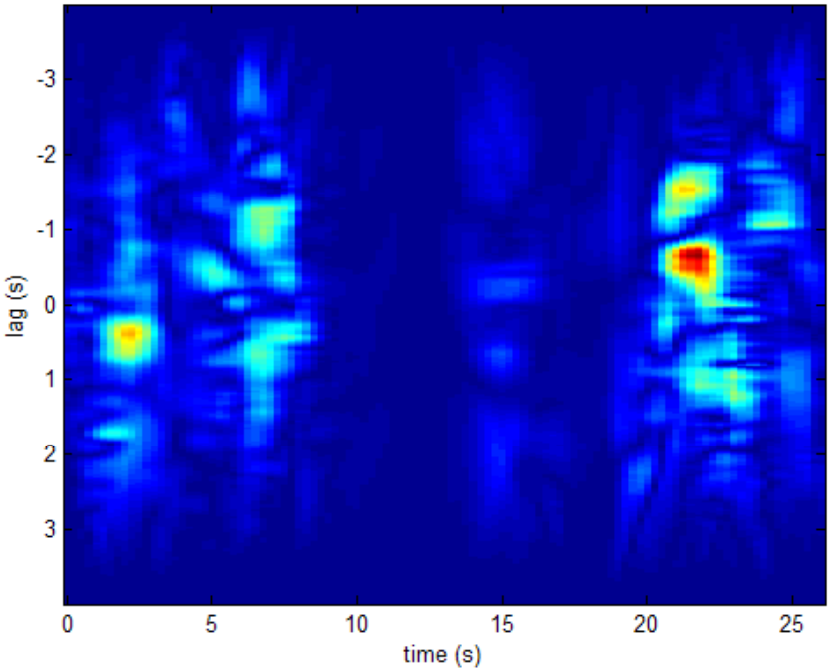

Figure 6.4.2.3. Multi-dimensional correlation between the left and right arms of Infant 1.

In correlating the leg motions, as shown in Figure 6.4.2.4, there appears to be much more action. The first 10 seconds are very well correlated as shown with the large number of yellow areas, indicating paired motions over the legs. As seen in Video 6.4.2.1, the first 10 seconds of footage show rotating and lifting of the hips, thus changing the base acceleration of the legs. Atop these accelerations due to rotation, there is kick data that appears in the correlation as red areas. In general, there appears to be more data across the zero-lag axis as there are so many motions that can be paired.

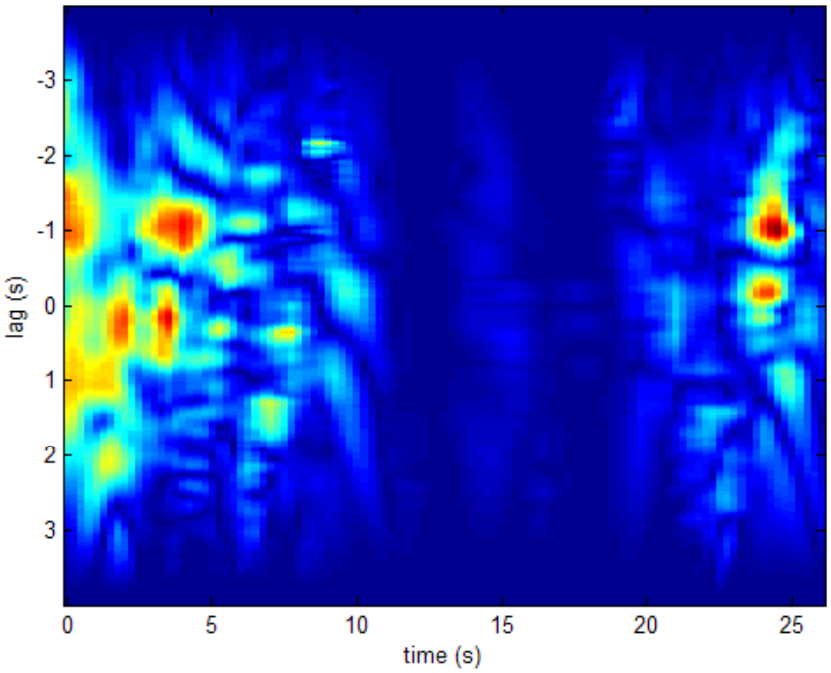

Figure 6.4.2.4. Multi-dimensional correlation between the left and right legs of Infant 1.

Further inspection of Figure 6.4.2.4 shows a number of blue/yellow areas equally spaced tracking in a straight line around the 5-second point. The slope here is about –1 seconds lag per 1 second time. It is hypothesized that these equally spaced points are due to the constant frequency at which accelerations are recorded during some back and forth motions. Because a back and forth motion on two limbs may be at a constant, equal frequency, sliding the signals across each other during correlation will result in multiple points in lag where they correlated well, at each spaces. It is thought that this is the case here.

On a final note, the 24-second point shows another time when the right leg is leading the left leg and producing a negative lag. This is quite clear in Figure 6.4.2.1 and is similar to the analysis of Figure 6.4.1.6. Again, there is no link to say that one leg is in fact leading another leg, either muscularly or neurologically, but the physical motion produced shows this. Further studies are in order to determine how often this occurs in both normal and abnormally neurologically developed infants' movements

Figure 6.4.2.5 correlates the left-hand side of Infant 1's body movements. Here

there is really only one clear correlated movement occurring at about 3 seconds in time. Comparison with Figure 6.4.2.1 shows that indeed there is a coordinated movement at this time in the data, but it is not quite as clear as shown in the correlation figure. There appears to be quite a bit of noise around the beginning and end of the correlation data, which could be due to the rotation of the hips during recording. Longer studies with more data are needed to evaluate the interference from such gross body movements during testing.

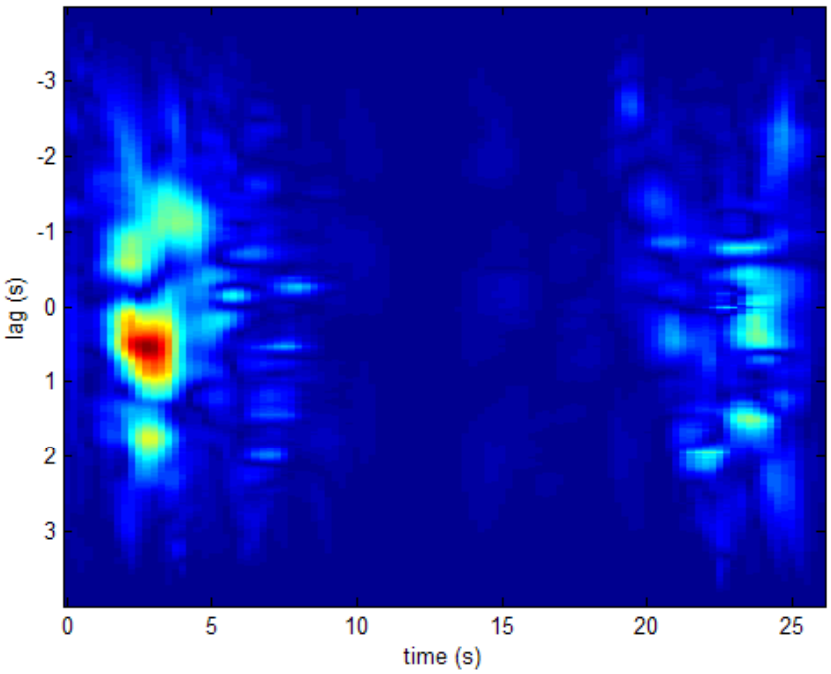

Figure 6.4.2.5. Multi-dimensional correlation between the left arm and left leg of Infant 1.

The forth correlation plot of the infant's right-hand side (right arm and right leg) is shown in Figure 6.4.2.6. Again, a large amount of noise is seen in the first and last 10 seconds of data during the gross body movements. The very high correlation indicated with the dark red point at about 8 seconds and 0 seconds lag is also seen in the data, but not as prominently as one would expect from the graphic. There could be noise issues once again, or this could be indicating something difficult to spot in the data. A more in depth analysis has not been conducted on such high-correlation occurrences.

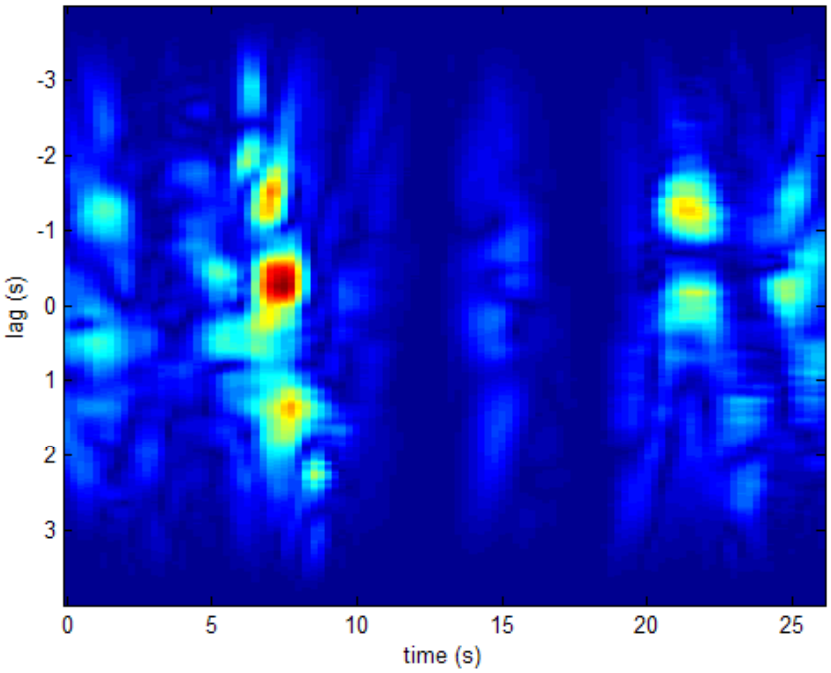

Figure 6.4.2.6. Multi-dimensional correlation between the right arm and right leg of Infant 1.

Although cross-body correlations were not completed during the analysis of Infant 2's 30-second data sample, they have been done for Infant 1 due to the increase in overall movement across the entire body. This data is shown in Figures 6.4.2.7 and 6.4.2.8 where the left arm is correlated with the right leg and the right arm with the left leg, respectively. In both plots we see much more information than was present in similar plots for Infant 2 (although not shown). In simply visually comparing the plots of Figure 6.4.2.1, we can see similar motions at the 23-point between the left arm and right leg as indicated in the correlation. Some of the other high-correlation points are more difficult to figure out.

The data for the right arm and left leg appears to pair up well at about 10 seconds and 25 seconds, but Figure 6.4.2.8 does not seem to indicate such matching. There is no explanation for this, but there could be problems in simply comparing signals across the body. Once again there is much to study in future tests.

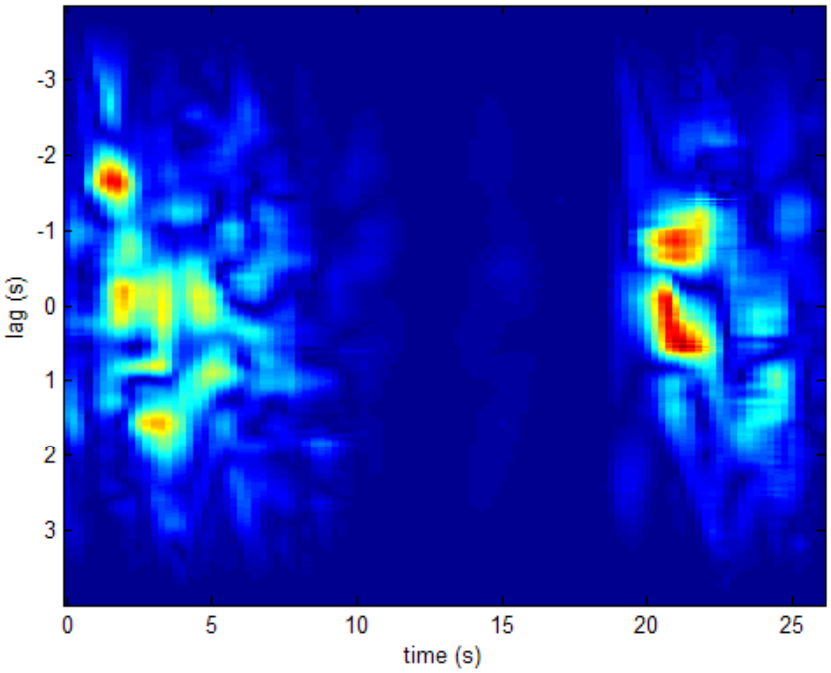

Figure 6.4.2.7. Multi-dimensional correlation between the left arm and right leg of Infant 1.

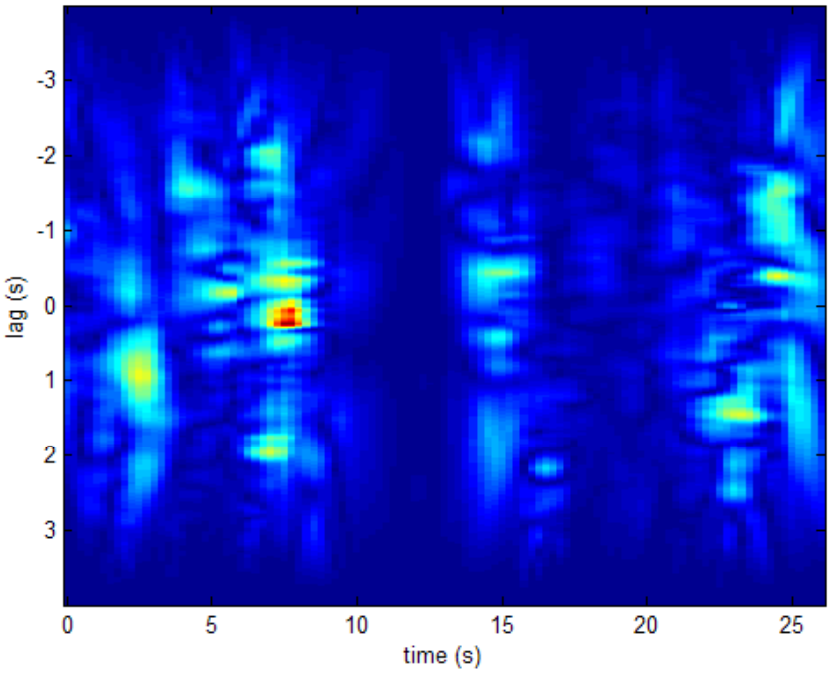

Figure 6.4.2.8. Multi-dimensional correlation between the right arm and left leg of Infant 1.

6.4.3 Comments on Analyses of Data and Video from Both Infants

Having now viewed footage and data plots from two 30-second sections of infant GMs, there are a few comments that can be made about the process. First, it is quite clear that the data files stored are very well synchronized with the video footage and are representative of the actual motion that occurs, both in period and amplitude.

In conducting the two types of analyses described in this chapter on the two data sections, a number of comments can be made. The present method of frequency inspection with spectrograms does not appear to hone in on important information. A number of changes need to be made to this analysis process, but low frequency information during period of motion and rest remain of interest in this research. On the other hand, the method of conducting multi-dimensional cross-correlations between the mean-zeroed magnitude data from two limbs does easily indicate coordinated movements quite clearly. This method of visual interpretation of seconds or minutes of data is much faster and more repeatable than reviewing video footage. Iterations on the procedure are obviously required to maximize the efficiency of this review, but that requires much more testing on a larger subject population.

Overall, it has been shown that the miniature acceleration measurement devices can be prototyped relatively easily and inexpensively, enabling the accurate monitoring of movement information from human infants. Various analyses have been conducted on the recorded data producing mixed results, but in general there appear to be a number of opportunities to expand and improve such techniques. This paper will conclude by discussing a number of these improvements required in the future for this research to prosper.

7 Conclusions and Future Work

This paper has presented the entire engineering process involved in this research project thus far. From the initial concept and motivation, through design and calibration of measurement equipment, and finishing with collection and analyses of movement data from human infant subjects. The goal of creating a new method to capture and review movement from infants has been accomplished, but remains unpolished. While the year of work spent on this project has been well spent exploring the feasibility of using the methods presented here, there remains quite a bit of work to evolve this technique into a useable form for the medical and engineering communities.

7.1 Conclusions from Current Work

This section will briefly review the principle conclusions that have been made from the preliminary work presented in this paper. These conclusions include the measurement of acceleration data during human movement as well as methods for analyzing data to characterize the data from an overall perspective. Finally, the possible benefits of this research to the diagnosis of cerebral palsy and other neurological dysfunctions will be discussed.

7.1.1 Recording Accelerations from Limbs as a Means to Record Movement

This paper has clearly shown video footage of human infant movement (GMs, specifically) synchronized with recorded acceleration data from the measurement devices attached to the infant's four limbs. Simply reviewing both sets of information obviously indicates that the acceleration data is indicative of the motion seen on video. Calibration of the devices has also shown very little inter-sensor variability. Using integration techniques on the acceleration data, position data was extracted from a preliminary test in one-dimension,

proving instrument accuracy.

Initial concerns relating to multiple degrees of freedom (joints) controlling the limbs, and therefore final measured movement at the sensors have diminished. As discussed in the beginning of this report, the limited muscle control of infants at an age of 2 months was seen in the sample videos. Only the larger, gross muscle movements of the shoulder, hips, and knees were evident. Additionally, the assumptions relating to which two axes to measure acceleration from appear to be valid. Motion was primarily limited to those axes oriented with the sensor axes. In general, the measured accelerations represent the movement very well and are recorded much more easily.

7.1.2 Investigating Coordinated Movements using Cross-correlation

As one method to analyze the recorded acceleration data, creating multi-dimensional cross-correlations between data sets from two limbs, has proven to distinguish coordinated movements from uncoordinated movements. This method even goes so far as to estimate paired movements of limbs that may lag each other time, something that may prove valuable in future testing on neurologically impaired subjects.

The intensity plots shown throughout the chapter pertaining to analyses clearly indicate points in time where two limbs made a movement at the same time. These plots can be quickly reviewed to determine such points, where as video footage must be reviewed a number of times and it is much more difficult for a video analyst to pay attention to all four limbs at the same time. In the cross-correlation plots, each set of limbs can easily be compared without worry of being overburdened during review due to excessive information presented at once, as in live video review.

This method requires refinement, but has made the process of pattern recognition more graphical. The color interpretation of the plots is much easier on an analyst than the previous method of video review. Future iterations of this analysis process will only improve the overall efficacy of this method.

7.1.3 Investigating Underlying Frequency Components using Fourier Transforms

Previous discussions of the use of spectrograms to investigate frequency content of infant movement have not been extremely productive in creating graphics containing easily distinguished characteristics. The scaling remains as the primary limitation in this difficulty, but as discussed in this paper, the data acquisition settings play a role in this. In general, the burst nature of movement data also plays a role in minimizing the efficiency of spectrogram interpretation.

Future work could be done to determine methods for possibly monitoring the frequency just in bursts of data or during data from periods of minimal movement. Within just these sections of data there is likely to be an underlying frequency that humans may not be able to perceive during video review due to the high speed. It is assumed that frequencies above about 6 Hz are not expected from human vibrations, even smaller tremors during rest. Much more work must be done to investigate the variables controlled during the analysis procedure such as sample rate and window size to get proper scaling and zooming on features of interest. The possible benefits from frequency investigation remain an important part of this research, despite the poor performance of current analysis methods.

7.1.4 Overall Benefit of Research to Cerebral Palsy Diagnosis Techniques

As discussed in the background information on the diagnosis of cerebral palsy and the disorder in general, there are many ways to incorporate a more universal method for quantifying infant movements. It is known that studying GMs can accurately predict the outcome of neurological diagnoses, but this requires a significant amount of time by a trained physician. The Gestalt nature of these diagnoses also makes inter-institutional comparison difficult. The presented method has proven to create data files representative of the human movement seen during similar types of video monitoring and analysis.

Remaining is a long process of improving the quantification and analysis procedures using broad spectrums of human subjects to hone the techniques. The end result is a technique that could easily augment current procedures and add a valuable tool to the

neurological physician's bag. Past methods of diagnosis have not been able to track tests results over a long period of time and often require review. With this method, new analysis algorithms could be applied to old data months after the information is initially recorded, adding an entirely new dynamic dimension to the analysis process. Referring back the clinical classifications of GM analysis over time, histories could now be tracked with multiple results of data analysis at different testing points rather than a simple single-letter qualitative classification.

In general, the three components of diagnosis can be improved with this method: (1) easier, more reproducible data acquisition of physical quantities, (2) storage, analysis, and reanalysis of more data and information than before, lacking the imprecision due to various Gestalt perceptions of analysts, and (3) more a more graphical, faster method to review data without looking through repetitive video footage.

7.2 Future Work

While this present work on this project has proven valuable results, it is the hope of the author that this work will continue. This section will present a number of improvements considered paramount to the success of future iterations of this design and process. These include improvements to the physical devices and data transmission techniques, as well as improved methods of analysis of resulting data. As recommended throughout this research, a comprehensive study on many infants with varying degrees of neurological dysfunction must be surveyed with the equipment to investigate the validity of this method as a whole for the intended purpose.

7.2.1 Improved Data Acquisition and Transmission

This research as accomplished quite a bit using mere prototypes constructed from sampled manufacturer parts. The technology available is constantly evolving and requires review, but a monetary investment into instruments would benefit the overall project. First, a smaller overall circuit design and housing would minimize the impact on the infant. While the GMs

did not appear to be constrained during this testing, printed circuit board could greatly reduce the overall size and weight of the device.

A second method of improving data acquisition would be for the integration of wireless technology for transmission of data to the acquisition hardware. Current technologies involving infrared data transmission and bluetooth protocol could be easily implemented alongside the current circuit components, but would require more expertise in programming of such protocols in micro-controllers than was available to the primary researcher on this project. In either method of data transmission, a master transceiver connected to the base data acquisition station (LabVIEW enabled laptop computer) communicates with slave devices that communicate queried information back to the master.

Current software programmed in National Instrument's LabVIEW has been adequate for recording the necessary information at the required speeds, but could stand to be updated by a more adequate programmer. The software used for this work was coded in LabVIEW 6.1, but the new LabVIEW 7.0 has recently been released and offers a number of data acquisition improvements over old code that could help this project. Within the code it would be helpful to make a seamless acquisition and viewing option so that streaming data could be viewed during acquisition. It would also be helpful to allow constant data acquisition that does not require the operator to choose the length of data to sample. Using the code available in LabVIEW 6.1, this was not accomplished with even data spacing and simultaneous sampling from multiple channels.

7.2.2 Improved Analysis Procedures

As discussed throughout this paper, the analyses procedures for investigating cross-correlation and frequency content using spectrograms have shown some valuable information, but require refinement. Specifically, a more versatile method for zooming in and improving resolution on plots would be helpful. The analysis variables such as window size and overlap must also be investigated more closely when broader studies are conducted on multiple test subjects. In doing this, methods for accentuating valuable information in the data could be revealed.

Although not attempted in this work due to the short data samples, surveys of burst frequency and strength could be helpful in quantifying the motor activity of an infant. Over just 30 seconds of data it is hard to get accurate averages on the number of times an infant's movements exceed certain limits on acceleration or how many times this is done. With more data stored and analyzed form multiple infants, a survey of such data qualities could be conducted.

With the release of improved data acquisition software in LabVIEW 7.0, there may be new methods to complete some forms of analyses online, during testing. Results could then be tracked during acquisition and lead the operator to some early conclusions of an analyst. This had not been possible with past codes because of the stop and go nature of acquisition, requiring completion of all measurement before the data could be accessed.

7.2.3 Comprehensive Study of Infant General Movements with Accelerometers

Unavailable during this testing was a broad infant population on which to test the devices and record data. Future studies will rely on surveys of much larger populations across a larger spectrum of ages during GM motion and quality of neurological development. This was difficult to accomplish during research because of the lack of adequate relationships with medical facilities and neonatal intensive care units (NICU). The cooperation of the Infant Perception Laboratory though, was crucial to the results and analyses already accomplished.

Upon attaining such cooperation, a calibration study of the device measurement should also be conducted. Using a known method for collecting movement data, such as a Vicon three-dimensional position device used in gait labs, alongside the prototype devices, samples from the same movement should be collected. Just as position was found through integration of collected acceleration data, the position data recorded can be differentiated to determine the acceleration during recorded motion. A comparison of these two sets of acceleration data is crucial in validating the accuracy of the measurement devices built. Again, their exact measurement is not necessarily required for adequate understanding of gross GMs, but a high level of confidence in their results could be gained from such a

comparison to already proven methods.

As has been attempted during the first year of this project, sponsorship of this research by a larger institution affiliated with cerebral palsy diagnosis and care will necessitate the attainment of patient populations. Approval for this type of new research on infants with possible dysfunctions requires more time and coordination with affiliated groups than was available during this initial work. Dr. Dawn H. Peck has been very helpful in describing the needs of the medical community from a physician's perspective. Dr. Andre Muelenaer has participated equally in adding to the knowledge base of integration with a NICU, such as the one associated with the Carilion Biomedical Institute in Roanoke, Virginia. Future associations are imperative for successful integration with the medical community.

A source of funding for this work would also help in attaining a larger patient population, as well as better equipment and instruments. A grant was submitted to the United Cerebral Palsy Research Foundation [UCP, 2002] in March of 2003. Other possibilities for funding lie with the National Institute of Health's National Institute of Neurological Disorders [NINDS] and Stroke and the American Academy for Cerebral Palsy and Developmental Medicine [AACPDM].

7.3 Final Comments on the State of Research

As outlined throughout this paper, a significant amount of research has been conducted to determine a method to suit the need of quantifying infant movements. What has been presented is a new method, unique in its direct measurement of a force-related physical quantity (acceleration) that has been paired with visual video footage per the current qualitative clinical method of diagnosis. Data from the acceleration measurement devices has been used in various types of analyses, investigating overall movement, coordination between limbs, and frequency content. There have been both positive and inconclusive results, but a foundation for further iterations has been laid.

It is the feeling of the author that this work has a long way to go, but represents a method of great promise to the medical community. Never before have such miniature electronics been utilized to acquire movement data, something important to understand in both well and dysfunctional infants. While damage to the brain can be monitored using

various imaging technologies, the impact that this damage has on the motor function of infants and adults has not been adequately studied due to difficulties in comparing quantified movement information across multiple institutions. Here lies a method that gives precise and comparable results, which are easily used by a technician requiring minimal training. Had the opportunities for improvement of diagnosis and understanding of neurological dysfunctions such as cerebral palsy not been so great, the author and principle researcher would not have invested so much time and effort in this process. Extending this work further only opens more doors to aid in the good of those persons affected by disorders such as cerebral palsy.

Appendix A: Institutional Review Board Application for Tests on Humans

Using Accelerometers to Quantify Infant General Movements

Robin P. Cooper, Alfred L. Wicks, Mark S. Conover

BACKGROUND AND RATIONALE

For decades, neurologists have been interested in the general movements (GMs) of infants because certain characteristics can indicate neurological dysfunctions. Motions over the entire body that show fluency, variation, and complexity characterize normal GMs. These movements change as an infant ages, giving way to more fidgety movements that are smaller and more complex, occurring irregularly over the entire body. Fidgety movements (occurring at two months post-term) lack fluidity, complexity, and variation in the presence of neurological dysfunction. It has been found that analysis of these movements is an accurate predictor of neurological dysfunction – cerebral palsy, in particular.

Recent advancements in the field of micro electro-mechanical systems (MEMS) give scientists more opportunities to make physical measurements without intruding on the system being measured. For example, acceleration can now be measured using a small chip manufactured by Analog Devices that measures 5 mm x 5 mm x 2 mm. Using such a device, measurements of acceleration, which is directly related to force, can be made from the limbs of infants. Due to the spontaneity of GMs, these small devices can be placed within wristwatch-type housings and eliminate complicated and intrusive equipment used in present quantitative measurement studies of infant movement. It is believed that use of such measurement tools will allow physicians to get data from an infant's GMs that can later be used in the diagnosis of neurological dysfunction. During this study, acceleration data from GMs will be recorded only to provide researchers data synched with video footage for research on signal processing techniques to investigate coordination between limbs.

METHOD

Participants. This study will involve a group of 1-2-month-old infants (n=6). The infants will be recruited from a group of infants pre-arranged by Dr. Cooper for a study with prior IRB approval.

Apparatus. Infants will be placed on a padded and railed table in a supine position. To increase spontaneity and decrease external stimuli, distractions will be placed outside of the infant's field of view. The experimenter will be at the head of the table with a laptop computer for data acquisition. Other experimenters and parents can also be located at the head of the table, but out of the infant's sight. Wristwatch-type devices, measuring 1 in. x 1.25 in. x 0.38 in. and attached with a new Velcro strap, will be placed on the wrists and ankles of the infants. Each device weighs 25 grams, or about 2/3 of an ounce. Each device contains a small circuit with an ADXL202 two-dimensional accelerometer, a few small capacitors, a resistor, and a coin-shaped 3.6V battery. The devices are each connected to a central data acquisition system (laptop computer and BNC-connector box) with light strain-gage wire (composed of four smaller wires). These wires will be lightly taped to the infant's hands and feet (using light medical tape) to secure the wire's position as it is routed out the side of the table railing and back to the data acquisition system. A digital video camera will record parts of the session where infants GMs are very active.

Procedure. The study will be conducted at the Infant Perception Laboratory in the Department of Psychology at Virginia Polytechnic Institute and State University. Upon arrival, the parent(s) will be asked to sign two informed consent forms (one that they keep), and a Family Information Sheet (Appendices A and B). This is also a time period for the parents to ask any questions that they may have and to ensure that the infant is in a quiet, awake state. After the infant has complete the primary testing of Dr. Cooper and the infant is believed to be in an alert and calm state, the infant will be placed in a supine position on the railed table and allowed to relax. The parent may stay with the infant as the acceleration devices are prepared and placed on the infant.

The experimenter will then place the four acceleration measurement devices on the wrists and ankles of the infant. At this point, they will not be wired to the data acquisition system. The devices placed on the wrists will be oriented on the top of the wrist, where a watch is normally worn. The devices on the ankle will be placed on the outside of the ankle,

above the anklebone. All Velcro straps will be unused material and will be fastened only tight enough to ensure no vibration of the device during motion. No "hook" side of the Velcro will come in contact with the infants skin. Once all the acceleration devices are placed securely on the infant, the strain gage wire connecting the devices to the data acquisition system will be connected between the measurement device and data acquisition system.

The experimenter and all other persons present for testing will sit at the head of the table and limit any other possible distractions from the room; including excessive light, noise, etc. Once the infant is lying calmly, without distractions, the data acquisition system will be triggered to begin recording. Initial estimates are that five minutes of data will be stored from each infant. During the recording phase, the conditions promoting spontaneity will be maintained. Additionally, a digital video recorder may be used to record some of the motion patterns of the infant for latter comparison with acceleration signals and validation of coordinated movements seen in recorded signals.

RISK/BENEFIT ANALYSIS

There are minimal risks associated with this study. There are no tangible benefits for participation. The scientific benefit is that the results will contribute to the understanding of quantified infant general movements. The acceleration data from infant general movements may be valuable in future methods of diagnosing cerebral palsy. Data collected during this study will be used by the experimenters to determine signal characteristics indicative of coordinated movement.

CONFIDENTIALITY/ANONYMITY

Each participant in this study will receive a randomly assigned number. All of the data gathered will be associated with that number and will have no connection with the participant's or parent's names. Informed consent forms will be kept separate from the infant data files. This session number will appear on the videotape of the infant, on their coding sheet, family information sheet, and summary data sheet.

Application - Appendix A

VIRGINIA POLYTECHNIC INSTITUTE AND STATE UNIVERSITY

Informed Consent for Participants of Investigative Projects

Title of Project: Using Accelerometers to Quantify Infant General Movements

Principle Investigators: Dr. Robin P. Cooper
Dr. Alfred L. Wicks
Mark S. Conover (graduate assistant)

I. Purpose of Research Project

You and your infant are invited to participate in our study of quantifying infant general movements using miniature accelerometers. The purpose is to attempt to use quantified data from human movement to detect signal patterns indicative of coordinated movement.

II. Procedure

Your infant will be tested for approximately 5 minutes, provided that he/she is awake, alert, and quiet. He/she may wear a comfortable jumper during the procedure. You will help keep your infant calm and relaxed on a padded table with railings as 4 wristwatch-type devices are secured to his/her wrists and ankles by a trained research assistant. These devices weigh 25 grams (about 2/3 of an ounce) and will be secured with a new strip of Velcro. Once the acceleration measurement devices are secured to your infant, small gage wire will be connected from the devices to a central data acquisition system, located at the head of the table, out of your infant's field of view. The devices and wires will in no way constrain the motion of your infant.

Once the data acquisition system is set and your infant is in a supine position, data

will begin being collected. The general movements of your infant are natural, spontaneous motions that occur over the entire body and are present in all infants up until about 58 weeks post-menstrual age. To ensure the spontaneous nature of these movements, distractions must be minimized. This includes distractions such as excessive light, noise, and external objects. During the recording, all individuals (mother and researchers) will need to remain at the head of the table and out of your infant's line of sight. During the data acquisition, the miniature accelerometers in the wristwatch devices will detect the acceleration throughout movement. To help our understanding of these movement signals in the future, video footage may be recorded from some of the testing. This will be done from the head of the table, so as not to take the infant's attention.

Finally, when 5 minutes of data have been collected, or your infant is unable to remain in a calm enough state to produce usable data (i.e. not producing general movements) the test will conclude. The wires will be detached from the measurement devices and then the Velcro will be undone to detach the devices from your infant. The study will be complete at this point.

III. Benefits of this study

Your baby's participation in this study benefits the field of infant motor function analysis. Specifically, this study will help us understand the measurement of infant general movements as well as signal processing to describe coordination.

IV. Extent of Anonymity and Confidentiality

All of the information gathered in this study will be kept confidential and the results will not be released without your parental consent. The information that your baby provides will be identified by session number only, not a name. Your informed consent will be kept separate from your infant's information. The results of this study may be presented at scientific meetings, and/or published in a scientific journal. If you would like, you will be sent a summary of this work when the project is completed. All tapes will be destroyed 3 years after the completion of this study.

V. Freedom to withdraw

You have the right to terminate your involvement in this project at any time and for any reason, if you so choose.

VI. Approval of research

This project has been approved by the Human Subjects Committee of the Department of Psychology and the Institutional Review Board of Virginia Tech.

VII. Subject's permission

I have read and understand the informed consent and conditions of this project. I have been given the opportunity to ask further questions about this procedure and I understand I have the right to end this session for any reason if I so choose. If I have any questions regarding this research and its conduct, I should contact one of the persons named below. Given these procedures and conditions, I have permission to Dr. Cooper, Dr. Wicks, their graduate and undergraduate students, and their co-workers to use their video recording and acceleration data of my infant in their research.

Dr. Robin P. Cooper, Principle Investigator	231-5938
Dr. Alfred L. Wicks, Engineering Advisor	231-4323
Mark Conover, Graduate Assistant	231-1271
Dr. David Harrison, Chair, Human Subjects Committee	231-4422
David M. Moore, DVM, Assistant Vice Provost for Research Compliance	231-4991

Signature of Parent:_____

Date:_____

Witness:_____

Application - Appendix B

FAMILY INFORMATION SHEET

Please fill out the following information:

1. Mother's age at infant's birth _____
   Father's age at infant's birth _____

2. Type of delivery: vaginal _____ c-section _____

3. Type of feeding: breast _____ bottle _____ both _____

4. Number of brothers and sisters:
   Brothers _____ Ages _____
   Sisters _____ Ages _____

5. Parents' highest level of education

	Mother	**Father**
Less than 7th grade	_____	_____
Junior High School	_____	_____
Some High School	_____	_____
High School Graduate	_____	_____
College Graduate	_____	_____
Graduate Degree	_____	_____

6. Number of people living in household _____

7. Mother's occupation _____
   Father's occupation _____

8. Mother's Race _____
   Father's Race _____

Appendix B: Matlab Code for Creating and Plotting Single Data Arrays

```
s=size(data);   %calc size of incoming data matrix
n=s(1,2)-1;     %take the number of columns and subtract 1, this is the number of channels sampled
t=data(:,1);    %the first column is the time array

ch0=data(:,9);   %assuming there are always channels in pairs, ch0 and ch1 are assigned
ch1=data(:,8);   %0 is used due to LabView standard for labeling the first component
mag01=sqrt((ch0.*ch0)+(ch1.*ch1)); %calculates magnitude of the left arm data
if n>2
   ch2=data(:,7);
   ch3=data(:,6);
   mag23=sqrt((ch2.*ch2)+(ch3.*ch3));
   if n>4
      ch4=data(:,5);
      ch5=data(:,4);
      mag45=sqrt((ch4.*ch4)+(ch5.*ch5));
      if n>6
         ch6=data(:,3);
         ch7=data(:,2);
         mag67=sqrt((ch6.*ch6)+(ch7.*ch7));
      end
   end
end

figure      %the following makes one plot with four subplots of each limb's data
if n==8
   subplot(2,2,1), plot(ch1,ch0), ylabel('acceleration, g'), xlabel('acceleration, g'), title('LEFT ARM')
   subplot(2,2,4), plot(ch7,ch6), ylabel('acceleration, g'), xlabel('acceleration, g'), title('RIGHT ARM')
   subplot(2,2,2), plot(ch3,ch2), ylabel('acceleration, g'), xlabel('acceleration, g'), title('LEFT LEG')
   subplot(2,2,3), plot(ch5,ch4), ylabel('acceleration, g'), xlabel('acceleration, g'), title('RIGHT LEG')
end
```

Appendix C: Matlab Code for Plotting Spectrograms for Acceleration Data

```
data=input('Variable Name for Matrix Data?   ');
ti=input('Start Time (s)');
tf=input('Finish Time (s)');
to=input('Offset Time (s)');
Fs=128;

s=size(data);    %calc size of incoming data matrix
n=s(1,2)-1;   %this is the number of channels sampled
t=data(:,1);     %the first column is the time array
Ti=ti*Fs+1;
Tf=tf*Fs;
if tf>max(t)
    Tf=length(t);
end
d=data(Ti:Tf,:);
t=d(:,1)-to;
ch0=d(:,9);
ch1=d(:,8);
ch00=ch0-mean(ch0);
ch01=ch1-mean(ch1);
mag01=sqrt((ch0.*ch0)+(ch1.*ch1));
mag001=sqrt((ch00.*ch00)+(ch01.*ch01));
   ch2=d(:,7);
   ch3=d(:,6);
   ch02=ch2-mean(ch2);
   ch03=ch3-mean(ch3);
   mag23=sqrt((ch2.*ch2)+(ch3.*ch3));
   mag023=sqrt((ch02.*ch02)+(ch03.*ch03));
      ch4=d(:,5);
      ch5=d(:,4);
      ch04=ch4-mean(ch4);
      ch05=ch5-mean(ch5);
      mag45=sqrt((ch4.*ch4)+(ch5.*ch5));
      mag045=sqrt((ch04.*ch04)+(ch05.*ch05));
         ch6=d(:,3);
         ch7=d(:,2);
         ch06=ch6-mean(ch6);
         ch07=ch7-mean(ch7);
         mag67=sqrt((ch6.*ch6)+(ch7.*ch7));
         mag067=sqrt((ch06.*ch06)+(ch07.*ch07));

W=input('Window size (s)')*Fs;
Sl=input('Slide size (data points)');
maxfreq=input('Max freq to plot to (Hz)?  ');

figure  %this will plot a 4x1 matrix of spectrograms as detailed
subplot(411), specgram(mag001,W,Fs,[],W-Sl), ylabel('Left Arm Freq (Hz)'), xlabel(' ')
subplot(412), specgram(mag067,W,Fs,[],W-Sl), ylabel('Right Arm Freq (Hz)'), xlabel(' ')
subplot(413), specgram(mag023,W,Fs,[],W-Sl), ylabel('Left Leg Freq (Hz)'), xlabel(' ')
subplot(414), specgram(mag045,W,Fs,[],W-Sl), ylabel('Right Leg Freq (Hz)'), xlabel ('time (s)')
```

Appendix D: Matlab Code for Creating Multi-Dimensional Cross-Correlations

```
data=input('Variable Name for Matrix Data?   ');  %Get data file name to analyze
ti=input('Start Time (s)');     %starting time to begin analysis
tf=input('Finish Time (s)');    %finish time to end analysis
to=input('Offset Time (s)');    %how much offset should be displayed on the plot
Fs=128;    %a sampling rate of 128Hz is assumed

s=size(data);    %calc size of incoming data matrix
n=s(1,2)-1;   %take the number of columns and subtract 1, this is the number of channels sampled
t=data(:,1);     %the first column is the time array
Ti=ti*Fs+1;    %calculate initial time index
Tf=tf*Fs;      %calculate final time index
if tf>max(t)   %in case file is shorter than indicated by finish time input
    Tf=length(t);
end
d=data(Ti:Tf,:);  %extract data to be analyzed from entire data file
t=d(:,1)-to;  %time data
ch0=d(:,9);   %ch0 data array
ch1=d(:,8);
ch00=ch0-mean(ch0);   %mean-zeroed ch0 data
ch01=ch1-mean(ch1);
mag01=sqrt((ch0.*ch0)+(ch1.*ch1));    %magnitude of Ch0 and Ch1 vector pairs
mag001=sqrt((ch00.*ch00)+(ch01.*ch01));  %magnitude of mean-zeroed data
   ch2=d(:,7);
   ch3=d(:,6);
   ch02=ch2-mean(ch2);
   ch03=ch3-mean(ch3);
   mag23=sqrt((ch2.*ch2)+(ch3.*ch3));
   mag023=sqrt((ch02.*ch02)+(ch03.*ch03));
      ch4=d(:,5);
      ch5=d(:,4);
      ch04=ch4-mean(ch4);
      ch05=ch5-mean(ch5);
      mag45=sqrt((ch4.*ch4)+(ch5.*ch5));
      mag045=sqrt((ch04.*ch04)+(ch05.*ch05));
         ch6=d(:,3);
         ch7=d(:,2);
         ch06=ch6-mean(ch6);
         ch07=ch7-mean(ch7);
         mag67=sqrt((ch6.*ch6)+(ch7.*ch7));
         mag067=sqrt((ch06.*ch06)+(ch07.*ch07));

W=input('Window size (s)')*Fs;  %length of window used for analysis
Sl=input('Slide size (data points)');   %how far to slide window along
maxfreq=input('Max freq to plot to (Hz)?  ');   %max to plot
n=Tf-Ti+1;
N=floor((n-W)/Sl)+1;
f=Fs*(1:maxfreq*W/Fs)/W;
tlag=(0:N-1)*Sl/Fs;  %adjust time due to less data from sliding

corlag=(W-(1:W*2-1))/Fs;

win=triang(W);   %triangular window used

%the following loop applies the window to mean zeroed data and performs all
%the cross correlations.
for j=1:N
    st=1+(j-1)*Sl;
    fn=st+W-1;
    mzch01=(ch1(st:fn)-mean(ch1(st:fn)))+i.*(ch0(st:fn)-mean(ch0(st:fn)));
    mzch23=(ch3(st:fn)-mean(ch3(st:fn)))+i.*(ch2(st:fn)-mean(ch2(st:fn)));
    mzch45=(ch5(st:fn)-mean(ch5(st:fn)))+i.*(ch4(st:fn)-mean(ch4(st:fn)));
    mzch67=(ch7(st:fn)-mean(ch7(st:fn)))+i.*(ch6(st:fn)-mean(ch6(st:fn)));

    la(1:W,j)=win.*mzch01;
    ra(1:W,j)=win.*mzch67;
    ll(1:W,j)=win.*mzch23;
    rl(1:W,j)=win.*mzch45;
    ralacorr(1:2*W-1,j)=abs(xcorr(ra(:,j),la(:,j),'unbiased'));
    rarlcorr(1:2*W-1,j)=abs(xcorr(ra(:,j),rl(:,j),'unbiased'));
    lallcorr(1:2*W-1,j)=abs(xcorr(la(:,j),ll(:,j),'unbiased'));
    rlllcorr(1:2*W-1,j)=abs(xcorr(rl(:,j),ll(:,j),'unbiased'));
    larlcorr(1:2*W-1,j)=abs(xcorr(la(:,j),rl(:,j),'unbiased'));
    rallcorr(1:2*W-1,j)=abs(xcorr(ra(:,j),ll(:,j),'unbiased'));
end

figure  %to plot all four main correlations
subplot(332), imagesc(tlag,corlag,ralacorr)
subplot(334), imagesc(tlag,corlag,rarlcorr)
subplot(336), imagesc(tlag,corlag,lallcorr)
subplot(338), imagesc(tlag,corlag,rlllcorr)
```

Glossary

cerebral palsy (CP) – A disorder usually caused by brain damage occurring at or before birth and marked by muscular impairment. Often accompanied by poor coordination, it sometimes involves speech and learning difficulties. (cerebral - of or relating to the brain or cerebrum., palsy - complete or partial muscle paralysis, often accompanied by loss of sensation and uncontrollable body movements or tremors.) [dictionary.com]

Fast Fourier Transform (FFT) – An efficient mathematical technique to decompose a time signal into sinusoidal components in the frequency domain. [Smith, 1997]

general movement (GM) – Movements in infants showing a large variability involving limbs, head and trunk, arising early during fetal life and extending until voluntary motor activity takes over around four months of age. [Hadders-Algra and Prechtl, 1992]

Gestalt perception principles - The perceptual principles that allow people to group visually similar objects into entities, or groups. [Thórisson, 1994]

motility – Ability to move spontaneously and independently. [dictionary.com]

Nyquist frequency – Half of the sampling frequency, which is the highest frequency that is recoverable from an FFT. [Smith, 1997]

postmenstrual age – Age of an infant relative to the menstruation cycle before pregnancy. [dictionary.com]

transceiver – A transmitter and receiver housed together in a single unit and having some circuits in common, often for portable or mobile use. [dictionary.com]

References

AACPDM, "AACPDM Web Site," http://www.aacpdm.org/home.html.

AD, "Analog Devices iMEMS Accelerometers," http://www.analog.com.

Bos, A.F., et al. "Spontaneous Motility in Preterm, Small-for-gestational Age Infants. I. Qualitative Aspects," *Early Human Development*, vol. 50, (1997), pp. 115-129.

BrownDog, "Brown Dog 8-pin DIP to TO-99 Adapter," http://www.brndog.com.

Crossbow, "Crossbow Accelerometer Products," http://www.xbow.com/Products/Accelerometers.htm.

Dictionary.com, http://www.dictionary.com.

Einspieler, C., Prechtl, H.F.R., Ferrari, F., Cioni, G., Bos, A.F. "The Qualitative Assessment of General Movements in Preterm, Term and Young Infants – Review of the Methodology," *Early Human Development*, vol. 50, (1997), pp. 47-60.

Hadders-Algra, M. and Prechtl, H.F.R. "Developmental Course of General Movements in Early Infancy. I. Descriptive Analysis of Change in Form." *Early Human Development*, (1992), pp. 201-213.

Hadders-Algra, M. "Quality of General Movements in Infancy Related to Neurological Dysfunction, ADHD, and Aggressive Behaviour," *Developmental Medicine and Child Neurology*, vol. 41, (1999), pp, 381-391.

Hadders-Algra, M. "Quality of General Movements Video Tape," Developmental Neurology, University Hospital Groningen, the Netherlands (2002).

Harris, S.R. and Heriza, C.B. "Measuring Infant Movement – Clinical and Technological Assessment Techniques," *Physical Therapy*, vol. 67, no. 12, (December 1987), pp. 1877-1880.

Harris, S.R. "Movement Analysis – An Aid to Early Diagnosis of Cerebral Palsy," *Physical Therapy*, vol. 71, (1991), pp. 215-221.

Heriza, C. B. "Implications of a Dynamical Systems Approach to Understanding Infant Kicking Behavior," *Physical Therapy,* vol. 71, (1991), pp. 222-235.

Kistler, "Kistler Internationl AG," http://www.kistler.com/web/kistler_portal.nsf/urlnames/kistler_frameset?OpenDocument&CTY=US&Lang=en.

MEMSIC, "MEMSICS Dual Axis Thermal Accelerometer Solutions," http://www.memsic.com.

Miller, J. and Roid, G. "Sequence Comparison Methodology for the Analysis of Movement Patterns in Infants and Toddlers With and Without Motor Delays," *The American Journal of Occupational Therapy*, vol. 47, (April 1993), pp. 339-347.

National Institute of Neurological Disorder and Stroke (NINDS), "Cerebral Palsy: Hope Through Research," http://www.ninds.nih.gov/health_and_medical/pubs/cerebral_palsyhtr.htm.

Peck, D.H., email "Video Feedback," (July 3, 2003).

Piek, J.P. "A Quantitative Analysis of Spontaneous Kicking in Two-month-old Infants," *Human Movement Science*, vol. 15, (1996), pp. 707-726.

Piek, J.P. "Is a Qualitative Approach Useful in the Comparison of Spontaneous Movements in Fullterm and Preterm Infants?" *Human Movement Science*, vol. 20, (2001), pp. 717-736.

Prechtl, H.F.R. "State of the Art of a New Functional Assessment of the Young Nervous System. An Early Predictor of Cerebral Palsy," *Early Human Development*, vol. 50, (1997), pp. 1-11.

Robertson, S. "Oscillation and Complexity in Early Infant Behavior," *Child Development*, vol. 64, (1993), pp. 1022-1035.

Smith, S.W. "The Scientist and Engineers Guide to Digital Signal Processing," (1997), http://www.DSPguide.com.

Star Micronics, "Star Micronics – USA," http://www.starmicronics.com.

Tadiran, "Tadiran TL-5186," http://www.tadiranbat.com/specs6/tl_5186.htm.

Thelen, E. and Fisher, D., "The Organization of Spontaneous Leg Movements in Newborn Infants," *Journal of Motor Behavior*, vol. 15, no. 4, (1983), pp. 353-377.

Thórisson, K.R. "Simulated Perceptual Grouping: An Application to Human-Computer Interaction," Proceedings of the Sixteenth Annual Conference of the Cognitive Science Society, (Atlanta, Georgia, August 13-16, 1994), pp. 876-881.

United Cerebral Palsy Research and Education Foundation (UCP), "Diagnosis of Cerebral Palsy – A Research Status Report," (2002), http://www.ucpa.org/ucp_generaldoc.cfm/1/4/11654/11654-11654/3968.

Vicon, "Vicon Movement Systems Home Page," http://www.vicon.com.

Vita

Mark S. Conover

The author, Mark Stuart Conover, was born in Alexandria, Virginia on January 23, 1978 and has resided in Great Falls, Virginia since the age of 1. He graduated in June 1996 from the Thomas Jefferson High School for Science and Technology in Alexandria before beginning his undergraduate study at Virginia Tech in Mechanical Engineering (the only University he applied to).

After co-oping in the Lycra® division of E.I. DuPont de Nemours and Company in Waynesboro, Virginia during his junior year, he received his Bachelor's Degree in Mechanical Engineering in May 2001 from Virginia Tech, graduating Summa Cum Laude and as a Commonwealth Scholar. During the following summer and fall, Mr. Conover interned in Hannover, Germany for Continental AG in the Air-Spring Fatigue Lab thanks to a program supported by the International Association for the Exchange of Students for Technical Experience (IAESTE).

He then began the pursuit of a Master's Degree in Mechanical Engineering at Virginia Tech in January 2002 and was introduced to this research project by Dr. A. L. Wicks in August 2002. During his seven years at Virginia Tech, Mr. Conover is proud of his extracurricular accomplishments as a member of the Virginia Tech Triathlon Team, a campus tour guide with the Hokie Ambassadors, and as a charter member and active alumni of the Delta Sigma Phi Fraternity.

After receiving his Master's Degree, Mr. Conover is eager to effectively use his engineering skills while striving to uphold Virginia Tech's motto, "Ut Prosim" (Latin for "That I May Serve"), in both his life and career.